Fakultät für Medizin

Hymenoptera venom allergy: venom proteomes and patient transcriptomes

Johannes Gunter Parzival Grosch

Vollständiger Abdruck der von der

Fakultät für Medizin

der Technischen Universität München zur Erlangung des akademischen Grades eines Doktors der Naturwissenschaften genehmigten Dissertation.

Vorsitzender: Prof. Dr. Marc Schmidt-Supprian

Prüfer der Dissertation:

1. Priv.-Doz. Dr. Simon Blank
2. Prof. Dr. Michael Sattler

Die Dissertation wurde am 10.03.2022 bei der Technischen Universität München eingereicht und durch die Fakultät für Medizin am 12.07.2022 angenommen.

ZENTRUM ALLERGIE UND UMWELT

TECHNISCHE UNIVERSITÄT MÜNCHEN

Hymenoptera venom allergy: venom proteomes and patient transcriptomes

Hymenopterengiftallergie:

Giftproteome und Patiententranskriptome

Dissertation zur Erlangung des Doktorgrades

(Dr. rer. nat.)

Johannes Gunter Parzival Grosch

Für meine Eltern und Großeltern.

An expert is a person who has found out by his own painful experience all the mistakes that one can make in a very narrow field.

- Niels Bohr

Abstract

Allergies to Hymenoptera venoms are life-threatening diseases. The only curative approach is venom immunotherapy. To ensure the best treatment, comprehensive component-resolved diagnostics (CRD) are often required. The prerequisite for molecular *in vitro* diagnostics for allergies is knowledge of the composition of the allergen source. Especially when allergies to the venoms of closely related Hymenoptera are present, unambiguous diagnostics can only be achieved using marker allergens. In the course of this work, the protein components of the venoms of the Vespoidea species *Polistes dominula*, *Vespula vulgaris*, and *Vespula germanica* were described by mass spectrometry, possible allergens were identified, and species-dependent differences were elucidated. *P. dominula* venom (PDV) contains 100 protein families, compared to 157 for *Vespula* spp. venoms (YJV). Eleven secreted proteins were found in PDV and 33 in YJV. As no promising species-specific proteins were identified, the future establishment of new marker allergens for CRD to discriminate between PDV and YJV allergy is

unlikely. In addition to unambiguous diagnostics, patients beginning venom immunotherapy may benefit from predictive markers for successful therapy that are raised in a minimally invasive and low-risk manner. To identify new candidates, time-dependent differences in gene expression of patients during the first weeks of venom immunotherapy were identified based on the transcriptome of peripheral blood mononuclear cells. Single-cell RNA sequencing was used to describe transcriptional changes in T cells, B cells, monocytes, macrophages, and dendritic cells. Differentially expressed genes were identified, pathway, and trajectory, as well as gene set enrichment analyses, were performed. In the course of this, a T cell state unknown in the context of venom immunotherapy was described, which is characterized by an interferon-response gene cassette. For example, the genes MX1, MX2, OAS1, and OAS3, which fulfill antiviral functions, were differentially expressed. In addition, promising time-dependently regulated genes were identified in all cell populations considered, providing the field of predictive transcriptome markers in the context of venom immunotherapy with new leads for further studies. Furthermore, a tag-based carrier system for the identification of Ves v 5-specific B cells was developed and tested in flow cytometry and a single cell RNA sequencing platform.

This work lays further foundations for improving diagnosis and therapy of wasp venom allergy by elucidating venom composition and monitoring transcriptional changes in immune cells during the up-dosing phase.

Abstract – DE

Allergien gegen Hymenopterengifte sind potentiell lebensbedrohliche Erkrankungen. Der einzige kurative Ansatz ist die Giftimmuntherapie. Um die bestmögliche Behandlung zu garantieren, ist oftmals eine umfassende komponentenaufgelöste Diagnostik nötig. Die Voraussetzung für molekulare *in vitro* Diagnostik für Allergien ist das Wissen über die Zusammensetzung der Allergenquelle. Gerade wenn Allergien gegen die Gifte von eng verwandten Hymenopteren vorliegen, ist eine zweifelsfreie Diagnostik meist nur über Markerallergene zu erreichen. Im Zuge dieser Arbeit wurden die Protein-Bestandteile der Gifte der Vespoidea Spezies *Polistes dominula*, *Vespula vulgaris* und *Vespula germanica* mittels Massenspektrometrie beschrieben, mögliche Allergene identifiziert und spezies-abhängige Unterschiede herausgearbeitet. *P. dominula* Gift (PDV) enthält 100 verschiedene Proteinfamilien, während es bei den *Vespula* spp. Giften (YJV) 157 sind. In PDV wurden elf, in YJV 33 sekretierte Proteine gefunden. Da keine vielversprechenden, spezies-spezifische Proteine identifiziert wurden, ist die zukünftige Etablierung von neuen Markerallergenen für die komponentenaufgelöste Diagnostik zur Diskriminierung zwischen PDV- und YJV-Allergie unwahrscheinlich. Neben einer eindeutigen Diagnostik profitieren Patienten, welche eine Giftimmuntherapie beginnen, von prädiktiven, minimalinvasiv und risikoarm erhobenen, Markern für erfolgreiche Therapie. Um hierfür neue Kandidaten zu identifizieren, wurden, basierend auf dem Transkriptom von mononuk-

leären Zellen des peripheren Blutes, zeitabhängige Unterschiede in der Genexpression von Patienten während der ersten Wochen einer Giftimmuntherapie herausgearbeitet. Durch Einzelzell-RNA-Sequenzierung wurden transkriptionelle, therapieabhängige Veränderungen in T Zellen, B Zellen, Monozyten, Makrophagen und Dendritischen Zellen beschrieben. Es wurden Zellpopulationen quantifiziert, differentiell exprimierte Gene identifiziert sowie Pathway-, Trajektorie- und Gene Set Enrichment Analysen durchgeführt. Im Zuge dessen wurde ein im Kontext der Giftimmuntherapie unbekannter T Zellzustand beschrieben, welcher sich durch eine Interferon-response Genkassette auszeichnet. Differentiell exprimiert waren hier unter anderem die Gene MX1, MX2, OAS1 und OAS3, welche antivirale Funktionen erfüllen. Darüber hinaus wurden vielversprechende, zeitabhängig regulierte Gene in allen betrachteten Zellpopulationen identifiziert, welche dem Feld der prädiktiven Transkriptom-Marker im Bereich der Giftimmuntherapien neue Anhaltspunkte für weitere Studien liefert. Des Weiteren wurde ein tag-basiertes Carrier-System zur Identifizierung von Ves v 5-spezifischen B Zellen entwickelt und in der Durchflusszytometrie sowie einer Einzelzell-RNA-Sequenzierungsplattform getestet.

Diese Arbeit legt weitere Grundsteine zur Verbesserung von Diagnostik und Therapie von Wespengiftallergien durch die Aufklärung von Giftzusammensetzung und dem Monitoring transkriptioneller Veränderungen in Immunzellen während der Aufdosierungsphase.

Acknowledgments

This work would not have been possible without the help of various people. First of all, I would like to thank Benjamin Schnautz and Johanna Grosch, who were indispensable helpers in and around the lab. Of course, my thanks also go to my supervisors, Simon Blank and Michael Sattler, who always critically reviewed my work. The most valuable ideas were stimulated by Alexander Heldner, Sonja Heine, and Michael Dittmar through regular discussions and advice. In addition, I would like to thank all cooperation partners as well as all people who gave me tips on the fly. Last but not least, I must of course thank Carsten Schmidt-Weber, who made the work possible in the first place.

I would also like to thank my family and friends who supported me in difficult times.

Preliminary Remarks

Parts of the work were subject to peer review and previously published in *Toxins*. Sentences, small passages or whole paragraphs from the published articles may be adopted verbatim without being highlighted/cited separately.

Grosch et al. Shedding Light on the Venom Proteomes of the Allergy-Relevant Hymenoptera *Polistes dominula* (European Paper Wasp) and *Vespula spp.* (Yellow Jacket). Toxins. 2020 May 14;12(5):323.
https://www.mdpi.com/2072-6651/12/5/323
https://doi.org/10.3390/toxins12050323

Grosch et al. Characterization of New Allergens from the Venom of the European Paper Wasp *Polistes dominula*. Toxins. 2021 Aug 10;13(8):559.
https://www.mdpi.com/2072-6651/13/8/559
https://doi.org/10.3390/toxins13080559

Abbreviations

AIT	*antigen-specific immunotherapy*
APC	*antigen presenting cell*
BCR	*B cell receptor*
CAP	*cysteine-rich secretory proteins, antigen 5, and pathogenetic 1 proteins*
CD	*cluster of differentiation*
CDR	*complementarity determining region*
CRD	*component-resolved diagnostics*
CV	*column volume*
DC	*dendritic cell*
DEG	*differentially expressed gene*
DPP IV	*dipeptidyl peptidases IV*
GO	*gene ontology*
GSEA	*gene set enrichment analysis*
HBV	*honey bee venom*
H-chain	*heavy chain*
Ig	*immunoglobulin*
IL	*interleukin*
ILC2	*type 2 innate lymphoid cell*
L-chain	*light chain*
LC	*liquid chromatography*
M/M	*monocytes / macrophages*
M-PBS	*milk-PBS*
mAb	*monoclonal antibody*
MHC	*major histocompatibility complex*
MS	*mass spectrometry*
NC	*nitrocellulose*
PBMC	*peripheral blood mononuclear cell*

PCR	*polymerase chain reaction*
PDV	*P. dominula venom*
PLA1	*phospholipase A1*
PLA2	*phospholipase A2*
PLELL	*protein lethal (2) essential for life-like*
rcf	*relative centrifugal force*
RT	*room temperature*
scFv	*short chain fragment variable*
SHM	*somatic hypermutation*
SNR	*signal-to-noise ratio*
T_{Akt}	*activated T cells*
T_{CM}	*central memory T cells*
TCR	*T cell receptor*
T_{EM}	*effector memory T cells*
T_{EMRA}	*effector memory T cells re-expressing CD45RA*
TLR	*toll-like receptor*
T_N	*naïve T cell*
$T_{N\text{-}IFN}$	*naïve - interferon response T cells*
UMI	*unique molecular identifier*
VAMP	*venom associated molecular pattern*
VEGF C	*vascular endothelial growth factor C*
VDJ	*variable, diversity, joining*
VIT	*venom immunotherapy*
YJV	*Yellow jacket venom*

Contents

1. Introduction

1.1. Venom allergy - basics and pathophysiology

Allergies, pathological reactions of the body to harmless (environmental) antigens, are a relevant and global problem. The different allergy phenotypes, such as food, inhalation, drug, and venom allergies differ primarily in the type of allergen exposure. While the uptake and processing of allergens in food and inhalation allergies happens via mucous membranes, stings under real conditions occur in different regions of the body and by different insects. Therefore, exposure, unlike with food and drug allergens, can only be reduced, not avoided.

A sting and the associated initial exposure to the venom is followed by the sensitization phase, the priming of the immune system to allergens. The venom is injected into the victim by the stinging insect and allergens, which are part of the venom along with other toxic components, are taken up at the site of the sting and presented to specialized cells of the immune system [1]. After

the antigen uptake, antigen-presenting cells (APC) transport allergens to the nearest lymph node and present processed allergen fragments of about 12-25 amino acid length on majory histocompatibility complex (MHC) II molecules [2–4]. $CD4^+$ T cells with allergen-specific T cell receptors (TCR) bind the MHC-II - epitope complex and, costimulated by the corresponding cytokine environment, differentiate into T_h2 cells [5]. The pre-existing microenvironment is initiated by interleukin (IL) 33 and driven by type 2 innate lymphoid cells (ILC2). After stimulation with IL25 and IL33, ILC2s produce pro-allergic cytokines, such as IL13, and support the shift towards T_h2 response [6, 7]. T_h2 cells contribute to the cytokine environment by the additional production of IL4, IL5 and IL13 and, therefore, trigger class switch in B cells to immunoglobulin (Ig) G1 and IgE producers [8–10].

Allergen-specific IgE is causally responsible for the symptomatology of an allergic reaction. The IgE binds the allergen and cross-links FcϵRI on the surface of mast cells and basophils [11]. Triggered by this stimulus, a variety of low molecular weight substances are released, such as cytokines, chemokines, lipid mediators, enzymes and histamine [12], which together cause the symptoms of the IgE-mediated type 1 hypersensitivity reaction.

General allergic symptoms comprise, but are not limited to, sneezing, itchy, runny nose, itchy, watery eyes, rashes, swelling, pain, stomach cramps, and vomiting. A more severe consequence of an allergic reaction is systemic anaphylaxis,

where symptoms such as hypotension, vasodilatation, bronchoconstriction or hypoxia threaten a patient's life [13]. In the case of venom allergy, three clinical manifestations are distinguished: local, large local (a swelling exceeding 10 cm in diameter) or systemic reactions [14, 15].

1.2. Immunoglobulins - from B cells to antibodies

1.2.1. Cellular stages of B cell development and activation

Immunoglobulins are probably the most efficient weapon the body has to bind and neutralize foreign antigens from viruses, bacteria, fungi, or helminths. Due to their high variability in the antigen binding site (paratope regions), they can recognize virtually all epitopes. However, this efficiency comes at a high price, the risk of the body overreacting to harmless antigens - as is happening in allergy - or recognizing the body's own (protein) structures and the resulting autoimmune diseases. Accordingly, the life of a B cell is characterized by selection and control of B cell receptor (BCR) specificity.

The life cycle of a B cell begins in the bone marrow, where hematopoietic stem cells are first transformed into pro- and then pre-B cells [16–18]. These two precursor cell types are characterized by intracellular μ heavy chain, which in combination with surrogate light chains forms the pre-B cell receptor. This receptor performs a variety of tasks, such as positive and negative selection, but

also ensures proliferation and cell survival [19]. The last developmental step in the bone marrow is reached when B cells express full IgM on their surface, the so-called immature stage. They now leave the bone marrow - from here on they are referred to as transitional B cells - and migrate to the spleen. Until they enter the spleen, they are T1, and thereafter T2 B cells [20]. Here the further fate of the B cells is decided: either they differentiate to follicular (IgD and CD23 high, IgM low) or to marginal zone B cells (IgD and CD23 low, IgM high). While the former respond more to T cell-dependent activation, the latter tend to T cell-independent activation. Follicular and marginal zone B cells are considered mature (naïve) B cells [21–23]. In the context of allergy, B cell activation that is dependent on T cells has more relevance: antigens are presented to B cells, which bind them with the BCR, take them over (through receptor-mediated endocytosis), and internalize them. After degradation of the antigen, it is bound on MHC-II molecules and made available at the cell surface for binding of the corresponding TCR. The T_h cell thus activated provides the necessary cytokine milieu and expresses CD40L at the surface. The B cell requires CD40L as a costimulant for proliferation, class switch, and somatic hypermutation. Only when all B cell stimulatory effects come together, i.e. antigen presentation by APCs, costimulation by CD40L, and the appropriate cytokine milieu, follicular B cells become activated (Figure 1.1). At this point, the B cell is at a cross: differentiate into short-lived antibody-producing plasmablasts, into long-lived

antibody-producing plasma cells, or long-lived memory B cells [24–27].

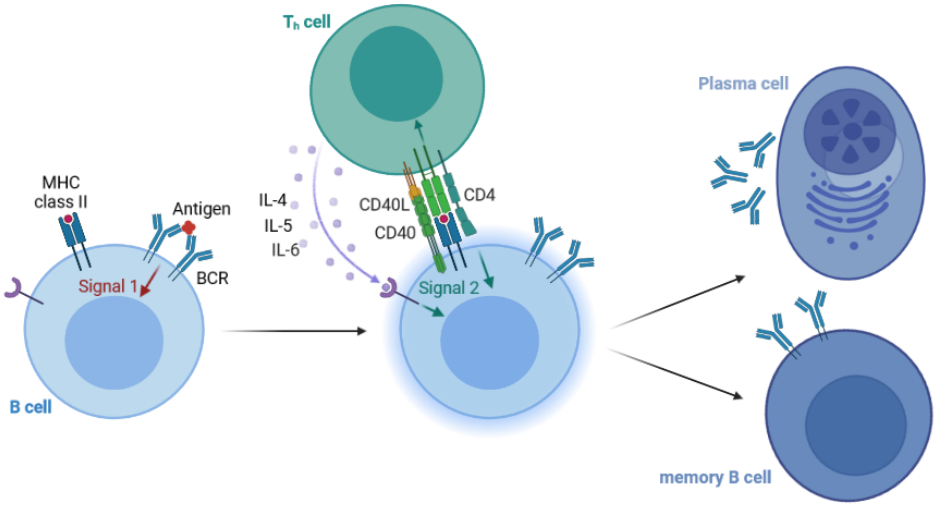

Figure 1.1.: Activation and differentiation of B cells to plasma cells or long-lived memory B cells. After the up-take of an antigen via B cell receptor (signal 1) and presentation on MHC-II, a T_h cell with corresponding CD4 is recruited. The costimulation happens through CD40-CD40L binding and the release of costimulatory cytokines (signal 2). The collective signals lead to the activation of the naïve B cell and initiate the differentiation into memory B cells or antibody-producing plasmablasts and plasma cells. Adapted from "Thymus-dependent Antigens Induce T-dependent B Cell Responses", by BioRender.com (2022).

1.2.2. Antibodies and paratope shaping

Each immunoglobulin consists of two light L-chains and two heavy H-chains. These in turn are divided into the constant and variable regions (C-, and V-regions), the latter of which contain the binding sites, the paratope. This paratope is formed in the first instance by V(D)J recombination. Here, V- (variable), D- (diversifying), and J-genes (joining) are recombined, i.e. rearranged (Figure 1.2). Random recombination of the V, D, and J genes allows a B cell to generate a virtually infinite repertoire of paratopes and thus of B cell receptors and

antibodies [28, 29].

The H-chains also carry a C-region, which determines the isotype class of the antibody. In general, five different isotypes are known, the immunoglobulins M, D, A, E, and G. Each immature B cell starts with an IgM BCR and can, after activation and in the appropriate environment, perform a class switch (isotype switching) to either IgA, IgE or IgG and their respective subclasses. Each Ig isotype has its own specific task field for which it has been optimized. For example, circulating, low-specificity IgM is the first line of humoral defense in the periphery. The secreted IgA dimer is mainly found in mucous membranes, while the highly specific and affine IgE and IgG molecules primarily serve to defend against parasites (IgE) or pathogens in general (IgG). However, the functions of antibodies are much more complex, especially concerning allergy, autoimmunity, tolerance, and tolerance induction. During isotype switching, so-called somatic hypermutations (SHM) take place, which alter the specificity and affinity of the Ig. These somatic mutations, mostly single-base substitutions, happen with an increased probability compared to normal and primarily occur in the complementarity determining regions (CDR) 1, 2, and 3. The mutations on the Ig paratopes can lead to an increase in the affinity of an antibody for the corresponding antigen. To ensure the clonal expansion of B cells with the highest affinity to a particular antigen, they are preferentially supplied with survival signals by T_h cells. These two steps, SHM and T cell-dependent clonal

expansion, are collectively referred to as affinity maturation [30–32].

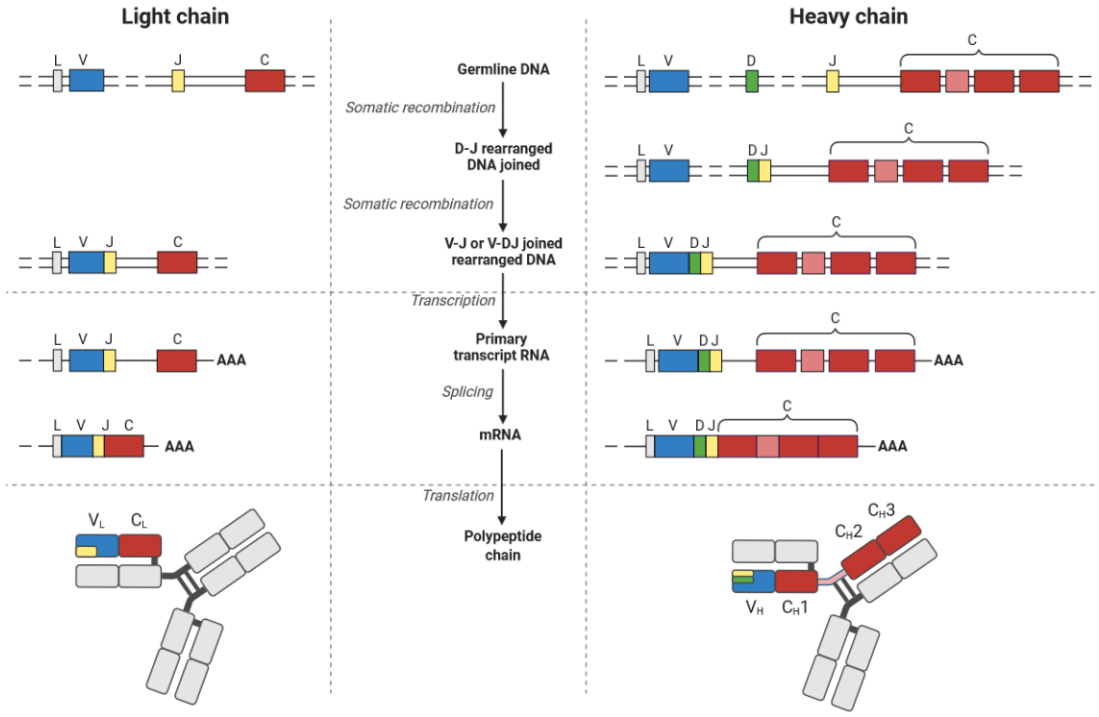

Figure 1.2.: Structure and generation of immunoglobulins from DNA to the protein level. Light chain comprising one variable and one constant region on the left. Heavy chain with one variable and three constant regions on the right. V, D, and J-genes are rearranged and the transcript spliced leading to the highly diverse variable regions allowing the immunoglobulin paratope to bind virtually all possible epitopes. Variable, blue; diversifying, green; joining, yellow; constant, red. Adapted from "B Cell Receptors (Light and Heavy Chains)", by BioRender.com (2022).

1.3. B cells in allergy

Allergies and their classical symptomatology depend on allergen-specific IgE. Generally, two different pathways lead to IgE-producing plasma cells. On the one hand, a direct isotype switch from IgM^+-B cells to IgE^+-B cells or plasma cells is possible [33]. On the other hand, there is an alternative pathway from IgM^+-

via $IgG1^+$- to IgE^+-B cells [34, 35]. The additional step of affinity maturation produces high-affinity IgE, which seems to be of greater importance in allergic patients [36–38].

Because of the short IgE half-life of two to three days in blood, a pool of long-lived IgE producers is assumed. Presumably, these long-lived IgE-secreting plasma cells are found in the bone marrow, from where a constant IgE titer can be maintained in the blood. These long-lived IgE^+ plasma cells have been described in mouse studies [39] on the one hand, and in the context of bone marrow transplantation also in humans [40–42].

1.4. Prevalence of Hymenoptera venom allergy

Most people (56.6-94.5%) are stung by a Hymenoptera at least once during their lifetime [43–45]. A fundamental distinction must be made between sensitization on the one hand and the symptomatic manifestation of an allergy on the other. While the prevalence of sensitization to Hymenoptera venoms is up to 31.7% [46], symptomatic reactions are much rarer. 2.4-26.4% of the population suffer from a large local reaction [44, 47–49] after a sting, which corresponds to a swelling diameter of more than 10 cm at the sting site. Systemic, anaphylactic reactions are reported by about 0.3 to 7.5% of people in the general population [44, 46, 48–51]. In general, it can be assumed that 20.2% of severe anaphylaxis

cases in children are due to insect stings, while in adults it is up to 48.2% [52]. Accordingly, insect venom allergies are not niche diseases, but relevant and life-threatening conditions.

1.5. Venom-specific immunotherapy

To protect patients from severe sting reactions, venom specific immunotherapy (VIT) is essential and the only curative approach. VIT is recommended for adults and children with measurable sensitization and systemic reactions beyond generalized skin symptoms, as well as for adults with generalized skin symptoms and impaired quality of life [53].

It is not conclusively understood how tolerance induction by VIT occurs. However, a variety of immunological mechanisms are thought to contribute in part. For example, proallergic T_h2 cells are suppressed by newly induced T_{reg} and T_h1 cells. This suppression results in reduced IL-4, IL-5, IL-9, and IL-13 levels, leading to desensitization of mast cells and basophils [54]. In addition, induction of regulatory B cells is considered a relevant component of successful VIT [55]. Regulatory B cells suppress proliferation of venom-specific T cells and support the induction of T_{reg} [56, 57]. Furthermore, class-switch in B cell populations leads to increased production of antigen-specific IgG4, which has anti-inflammatory properties as a competitive (blocking) antibody [58].

During VIT, venom extracts are applied subcutaneously. Generally, different protocols are discriminated with which the maintenance dose of 100 μg of venom can be reached. While conventional approaches provide for a slow increase in the amount of toxin over several weeks to months, the maintenance dose is reached within a few hours up to a few days with so-called rush or ultra-rush protocols. The last variant to be mentioned is the cluster protocols, in which patients receive several injections per day at an interval of 1-2 weeks. The maintenance dose is subsequently given at intervals of 4 weeks (first year), 6 weeks (second year) or 8 weeks (third to the fifth year) following the up-dosing phase [53, 59]. Clinical protection is achieved in most patients as soon as the maintenance dose can be applied [60, 61]. Overall, VIT lasts 3-5 years and should be continued beyond the third year if the success of therapy cannot be verified by sting provocation during therapy [62, 63]. Discontinuation of VIT should only occur after 3 years in patients with mild to moderate reactions. The minimum duration of 5 years successfully protects most of the patients in the long term [64, 65]. VIT with wasp venom is successful in 91-96% of patients [66, 67].

1.6. Hymenoptera venom proteomes

Figure 1.3 shows the phylogenetic tree of venom allergy-relevant Hymenoptera species. Allergies to Hymenoptera venoms are, as most allergies, triggered by

proteins. Accordingly, in the context of allergic disease, the proteome of the venoms is of utmost relevance. Published numbers on the protein components contained in the venoms vary considerably. For example, *Solenopsis invicta* venom contains 46 proteins, while honeybee venom contains 113, and *Polybia paulista* venom reportedly even contains over 1673 different proteins [68–70]. This striking discrepancy is partly due to differences in methodology, and partly due to the purity of the extracted venom. Many of the identified proteins have no direct effect or function in the venom and are referred to as 'venom trace molecules'. The contamination of the venom by venom trace molecules occurs during the extraction process of the venom by disrupting the cell membranes of the cells of the venom gland. Furthermore, in the case of *P. paulista*, it is likely that the use of databases comprising similar proteins from different species has resulted in peptides being aligned multiple times, resulting in a high false-positive rate. Therefore, depending on the degree of purity, Hymenoptera venoms likely contain between 40 and 150 different proteins.

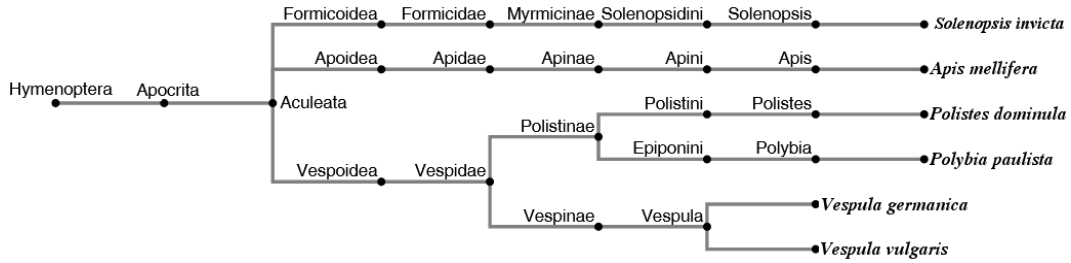

Figure 1.3.: Phylogenetic tree of closely related, allergy-relevant Hymenoptera. The splitting of the phylogenetic tree on the level of the family Vespidae leads to the species *P. dominula*, as well as *V. vulgaris* and *V. germanica*. Besides the Vespidae, the honey bees (*A. mellifera*) and the fire ants (*S. invicta*) are shown as exemplary representatives of their respective families.

1.7. Aim of the project

The superior goal of this work was to improve venom-specific immunotherapy to provide patients with the most successful therapy possible. Since it is of elementary importance to treat allergic patients with the right venom, the proteome of the venoms of the species *P. dominula* and *V. vulgaris/germanica* was elucidated by mass spectrometry and examined for differences and similarities. In a second part, the transcriptome of immune cells from patients undergoing *V. vulgaris* venom immunotherapy was examined in more detail in the hope of describing transcriptional differences as markers for therapeutic success. In the course of this, a method for the identification of antigen-specific B cells was developed and established.

Hypotheses:

1. *P. dominula* and *V. vulgaris* venoms contain proteins, which may be established as marker allergens for component resolved diagnostics to discriminate wasp venom allergies.

2. Transcriptomic changes in peripheral blood mononuclear cells of patients undergoing venom immunotherapy reveal unique genetic patterns that may be established as markers for predictive measurements.

3. Tag-based DNA barcoding of B cell receptors in scRNAseq allows the monitoring of transcriptional changes in Ves v 5-specific B cells.

2. Methods

2.1. General

2.1.1. Patient recruitment

Informed consent was obtained from all subjects involved in the study. The study was conducted according to the guidelines of the Declaration of Helsinki and approved by the Ethics Committee of the Faculty of Medicine of the Technical University of Munich (538/17).

Single cell transcriptomics

Inclusion criteria were full legal age, a credible history of allergic reaction after *V. vulgaris* sting incidents and the start of allergen-specific immunotherapy. Patients were diagnosed based on a thorough anamnesis, intradermal tests and molecular diagnostics (Table B.3). Patients included were sampled right before immunotherapy started, after four days, and after two weeks after completing the up-dosing phase or seven days after a maintenance shot of their VIT. Venous

blood was sampled, peripheral blood mononuclear cells (PBMC) isolated and stored until measured.

2.2. Molecular biology

2.2.1. Agarose gel electrophoresis

The separation of DNA following polymerase chain reaction (PCR) was performed by agarose gel electrophoresis. For this purpose, 1 g agarose in 100 ml 1 x TAE/ddH_2O was heated in a 250 ml glass flask until the agarose was completely dissolved, i.e. free of streaks. After brief cooling, 5 μl of SERVA DNA Stain Clear G was added, the mixture filled into the gel slide and the comb inserted. To each sample, 1/6 6 x DNA Loading Dye was added and pipetted into the gel pockets. DNA Ladder Mix was used as a marker, of which 7 μl was applied. Electrophoresis was performed at 120 V for 25 min and the gels were inspected under UV light.

2.2.2. Gel extraction using GeneJET Gel Extraction Kit

For the extraction of DNA from the gel, the corresponding band was cut out with a scalpel and transferred to a microreaction tube (1.5 ml). Using a precision balance and an empty reaction tube, the weight of the gel fragment was determined and binding buffer was added 1:1 (volume : weight). After incuba-

tion for 10 min at 50°C, the solution was pipetted onto a GeneJet purification column, centrifuged at 13000 relative centrifugal acceleration (rcf) for 1 min, and the flow-through discarded. 700 μl of wash buffer was added to the column, centrifuged again for 1 minute at 13000 rcf, the flow-through discarded, and the column transferred to a new microreaction tube. Elution was performed with 20 μl ddH_2O at the same centrifuge settings as in the previous steps.

2.2.3. Restriction enzyme digest

To generate sticky ends on the PCR products, these had to be digested with the restriction enzymes XbaI and NotI. For this purpose, 2 μl of 10 x FastDigest Buffer, 1 μl of restriction enzyme and 0.1 μg of DNA were pipetted together and filled up to 30 μl with ddH_2O. Incubation was carried out at 37°C for 10 minutes.

2.2.4. Ligation

For ligation of predigested pacGP67B vector and the inserts, 2 μl of 10 x T4 DNA ligase buffer, 1 μl of T4 DNA ligase and 50 ng of vector were pipetted together on ice. Insert was added at a molar ratio of 3:1 (insert : vector) and finally filled up to 20 μl with ddH_2O. Incubation was either at 22°C for 10 minutes or overnight at 4°C.

2.2.5. Transformation

The competent *E. coli* strains used were stored at -80°C and thawed on ice for 10 min before starting transformation. XL10-Gold Ultracompetent Cells and 2 μl of the ligation mixture or 25 ng of plasmid was transferred to 14 ml BD FalconTM Round-Bottom Tubes, 100 μl of bacteria was added and mixed briefly. 30 minutes on ice were followed by a heat shock for 35 seconds at 42°C before the batch was again placed on ice for 2 minutes. Next, 900 μl of LB medium was added and incubated at 37°C for 1 hour at 220 rpm. Centrifugation was performed at 800 rcf for 5 minutes, the supernatant was discarded, and the cell pellet was resuspended in 100 μl of fresh LB medium and spread on an agar plate. Incubation was performed at 37°C overnight.

2.2.6. Colony PCR

In order to screen the clones for the insert after transformation, colony PCRs were performed. For this purpose, depending on the strain used, one of the approaches in Tables 5 and 6 was pipetted together, parts of a clone were picked from the plate with the aid of a pipette tip and placed in the microreaction vessel.

Table 2.1.: Colony-PCR mix calculated for one clone and thermocycler settings.

PCR mix		**PCR protocol**	
EconoTaq	10 μl	Denaturation	98°C for 5 min
$Primer_{forward}$	0.5 μl	30 cycles	94°C for 30 sec
$Primer_{reverse}$	0.5 μl		55°C for 30 sec
ddH_2O	9 μl		72°C for 105 sec
Colony pick		Elongation	72°C for 5 min

2.2.7. Plasmid preparation using GeneJet Plasmid Miniprep Kit

After positive colony PCR and overnight culture, cells were centrifuged at 3200 rcf and completely dissolved in 250 μl of resuspension solution. 250 μl of the lysis solution, after inverting, lead to a viscous and clear solution to which 350 μl of neutralizing agent was added. Centrifugation at 13300 rcf for 5 minutes resulted in pelleting of the cell debris and chromosomal DNA. The supernatant was added to the GenJET spin column and centrifuged for 1 minute. After washing twice with 500 μl wash solution and centrifugations for 1 minute each, another centrifugation step (1 minute) followed to remove excess ethanol from the membrane. 31 μl of ddH_2O was added to the membrane and the column was incubated for 2 minutes at room temperature. DNA was eluted by centrifugation.

2.3. Sf-9 cell culture and recombinant protein expression

2.3.1. Adherent cells

In a 175 cm^2 cell culture flask, $4*10^6$ cells per cm^2 were seeded and insect cell medium added to a final volumen of 20 ml. The bottle was then placed in the incubator for seven days at 27°C.

2.3.2. Suspension cells

Suspension cells were maintained in Erlenmeyer flasks at a concentration of $1.5*10^6$ (4 to 5 days incubation) cells per ml medium. Incubation was performed at 27°C in a shaking incubator at 120 rpm.

2.3.3. Transfection

In a 25 cm^2 cell culture flask, $1*10^6$ cells were prepared with 5 ml medium and incubated for 30 minutes at 27°C. For the transfection mix, 100 μl of insect cell medium were mixed with 10 μl of cellfectin. Then, 2 μg of plasmid and 2.5 μl of ProGreen BaculoDNA or 2 μg of recombinant DH10Bac BacmidDNA were dissolved in another 100 μl of insect cell medium. These two preparations were combined, mixed well for 15 seconds, and then incubated at room temperature

for 30 minutes. At the end of the 30 minutes, the microreaction vessel was refilled with 800 μl of insect cell medium and the medium was aspirated from the cell culture flask. The transfection mix was added dropwise to the cells, which were then incubated for 4 h at 27°C. The bottle was then refilled with an additional 4 ml of medium and placed in the incubator for five days. Virus was harvested by centrifuging the supernatant at 3200 rcf for 5 min.

2.3.4. Virus amplification

In a 175 cm^2 cell culture flask, 5 ml of transfection supernatant (or 1 ml of amplification supernatant) was added to $24*10^6$ Sf-9 cells. After five days of incubation at 27°C, the virus-containing supernatant was centrifuged at 3200 rcf for 5 minutes and then stored at 4°C.

2.3.5. Recombinant expression

In a 1000 ml Erlenmeyer flask, 400 ml were prepared with $1.5*10^6$ Sf-9 cells per ml medium. These were then mixed with 1 ml of virus supernatant and incubated at 27°C for three days in a shaking incubator. The expression mixture was centrifuged at 3000 rcf for 20 minutes, the cell pellet discarded and the supernatant collected.

2.4. Protein biochemistry

2.4.1. Metal chelate affinity chromatography

Protein purification was performed by metal chelate affinity chromatography using a coexpressed polyhistidine tag. The nickel column matrix used was 1 ml HisTrapTM excel (GE Healthcare) and the chromatography system was an ÄKTApure. Elution was performed with 300 mM imidazole in PBS (pH 7.4) - subsequently referred to only as elution buffer (Ni-NTA). Initially, the column was equilibrated with 5 column volume (CV) ddH_2O as well as with 5 CV of sample buffer (PBS, pH 7.4) before loading at a constant rate of 1 ml of sample per minute. This was followed by a gradient wash step with a total of 10 CV, starting from 3% elution buffer (Ni-NTA) and working up to 15%. A constant 15% elution buffer (Ni-NTA) was used to wash 40 CV. The actual elution was performed in two steps: 7 CV with 70% elution buffer (Ni-NTA) followed by 100% elution buffer (Ni-NTA) with 4 CV. The eluate was collected in fractions of 2 ml.

2.4.2. Buffer exchange

Buffer exchange was performed using 4 ml Amicon®Ultra filter with a cut-off of 10 kDa. Samples were centrifuged at 3220 rcf to one remaining milliliter, flow-through discarded, and 3 ml of PBS replenished. This step was repeated

three times.

2.4.3. SDS polyacrylamide gel electrophoresis

For the analysis of protein expressions, the proteins were denatured and subsequently separated according to their size using freshly casted 10% Tris-Tricine SDS PAGE. The gels used were cast according to the scheme in Table 2.2, wrapped with moist cloths and stored at 4°C in the refrigerator. (Reducing) 5x PAGE running buffer was added to the samples at the beginning and samples boiled for 10 minutes at 90°C until denaturation and/or breaking of hydrogen bonds. If working under reducing conditions, the 5x PAGE running buffer contained DTT at a ratio of 16:1. For electrophoresis, the gels were placed in the electrophoresis chamber and the cathode was filled with Tris-tricine cathode buffer (5x) and the anode with Tris-tricine anode buffer (5x). The samples and 4 μl of Prestained Protein Ladder (Thermo Scientific, Schwerte, Germany) were slowly pipetted into the gel pockets before the samples were then separated at 120 V for 70 min. The gel was then briefly washed with ddH_2O and placed in Coomassie Brilliant Blue G-250 (AppliChem, Darmstadt, Germany) staining solution for 24 h. If the background staining was too intense, the gel was destained with Coomassie destainer until an ideal contrast was achieved.

Table 2.2.: Composition of 10% Tris-Tricine separating and stacking gels for five SDS gels.

	Separating gel	**Stacking gel**
Acrylamide (30%)	10 ml	2 ml
Tris-Tricine gel buffer (3x)	10 ml	5 ml
ddH_2O	6.2 ml	7.9 ml
Glycerol (85% v/v)	3.65 ml	- - -
TEMED	15 μl	10 μl
APS stock solution (10%)	150 μl	100 μl

2.4.4. Western blot

As blotting system, semi-dry blotters from SCIE-PLAS (Cambridge, UK) were used. At the beginning, six Whatman filter papers were placed in transfer buffer together with a cellulose nitrate membrane (nitrocellulose - NC) and the polyacrylamide gel to be blotted. Per gel, three filter papers, the NC membrane, the gel and again three filter papers were placed on the positive pole - in this order - and the chamber was sealed with the negative pole. Each of these packets required 100 mA of constant current and 90 minutes of blotting time. The membranes were then blocked for 60 minutes, followed by incubation with the first agent at 4°C overnight. After washing with PBS three times (5 minutes each), the 2nd agent was added for 60 minutes (room temperature (RT)). Washing was repeated three times for 5 minutes and in the meantime the detection solution was prepared. For this, 10 ml of AP detection buffer were mixed with premixed 100 μl BCIP (5-bromo-4-chloro-3-indolyl phosphate (AppliChem, Darmstadt, Germany)) and 100 μl NBT (nitrotetrazolium blue chloride). This solution was

added to the membrane and incubated until visible bands formed.

Four percent non-fat milk powder (AppliChem, Darmstadt, Germany) in PBS (M-PBS) was used as blocking agent. The antibodies were dissolved in 2% M-PBS (Table 2.3).

Table 2.3.: Workflow and corresponding reagents used for western blots.

	α-v5	**α-Rho1D4**
Blocking	4% M-PBS	4% M-PBS
1st agent	α-v5 Ab (0.2 μl/ml)	α-Rho1D4 Ab (0.2 μl/ml)
2nd agent	α-mouse IgG-AP (0.4 μg/mL)	α-mouse IgG-AP (0.4 μg/mL)
Detection	NBT/BCIP (1/1, 1:50)	NBT/BCIP (1/1, 1:50)
	α-FLAG	**Strep-tag**
Blocking	4% M-PBS	1% PVP-PBS
1st agent	α-FLAG Ab (0.2 μl/ml)	ExtrAvidin-AP (1:20000)
2nd agent	α-mouse IgG-AP (0.4 μg/mL)	
Detection	NBT/BCIP (1/1, 1:50)	NBT/BCIP (1/1, 1:50)

2.5. Immunology

2.5.1. ELISA

ELISA were performed on 96- or 384-well plates. Volumes in brackets are referring to 96-well plates. 20 (50) μl of protein was coated at a concentration of 40 μg/ml over night at 4°C. Wells were washed three times with 100 (300) μl D-PBS per washing step. Blocking was performed with 50 (300) μl 4% M-PBS for 60 min at RT. Cell culture supernatants were added and incubated over night at

4°C. Anti-FLAG antibody (1:5000) was applied and incubated at RT for 60 min. Following a washing step, secondary antibody (anti-mouse IgG AP, 1:20000) was added and after 60 min, the wells were washed. 5 mg/ml PNPP was dissolved in AP detection buffer (20 (50) μl per well) and absorbance was measured at 405 nm. As positive control, FLAG-tag carrying proteins were coated at a concentration of 40 μg/ml. No cell culture supernatant was applied. Other than that, the controls were handled analogously.

2.5.2. Flow cytometry

Cells were thawed, transferred to 50 ml RPMI complete medium and centrifuged at RT for 5 min and 500 rcf. The supernatant was discarded and the pellet resuspended in RPMI complete medium. The cells were transferred to a 25 cm^2 flask and incubated for 60 min at 37°C. After centrifugation at RT for 5 min and 500 rcf, the cells were transferred to FACS buffer (1% FCS in D-PBS) and sowed in a 96-well polystyrene conical bottom plate (Thermo Scientific). The plates were centrifuged for 5 min at 6°C and 500 rcf. Supernatant was discarded, Fc block (1:20) applied to each sample and incubated for 20 min at 4°C. After centrifugation (5 min, 6°C, 500 rcf) and discarding of the supernatant, 5000 ng Ves v 5 were applied to each well and incubated for 30 min at 4°C. Afterwards, cells were washed twice with FACS buffer, centrifuged and antibodies (Table 2.4) added (30 min, 4°C). Finally, all wells were washed twice and cells resuspended

in 50 μl of FACS buffer.

Table 2.4.: Reagents and their dilution in flow cytometry.

	Dilution	**Fluorochrome**
α-CD3	1:50	FITC
α-CD14	1:50	FITC
α-CD19	1:200	BV650
α-CD56	1:50	FITC
α-FLAG Ab	1:150	PE
α-Rho1D4 Ab	1:200	PE
α-v5 Ab	1:200	PE
Zombie NIR™	1:1000	Near infrared
Strep-Tactin®	1:200	PE

2.5.3. PBMC isolation

Heparinized blood was dissolved 1:1 with D-PBS without Ca/Mg. 25 ml of the mix was stacked on 10 ml of lymphoprep density gradient medium (STEMCELL Technologies, Vancouver, Canada) and centrifuged for 15 min at RT and 975 rcf without brake. PBMCs were harvested, D-PBS without Ca/Mg and 5 mM EDTA added and centrifuged for 10 min at RT and 515 rcf. The supernatant was discarded and the pellet resuspended in D-PBS without Ca/Mg and 5 mM EDTA, before being centrifuged for 10 min at RT and 300 rcf. Cells were resuspended, counted and transfered to freezing medium. Vials with $10*10^6$ cells were frozen away with a rate of -1°C/min and stored at -80°C.

2.6. Mass spectrometry

2.6.1. Sample preparation

Capillary-extracted venoms of *Polistes dominula* and *Vespula spp.* (*V. vulgaris* and *V. germanica*) (Entomon, Florence, Italy) were purified and trypsin-digested using both the SP3 on-bead and polyacrylamide in-gel methods. The SP3 method was performed according to Hughes et al. [71]. Briefly, the venom extracts were clarified by centrifugation and the cysteine disulfide bonds were reduced and alkylated with dithiothreitol or iodoacetamide. SP3 beads (Thermo Fisher Scientific, Waltham, Massachusetts, USA) were added to the samples to capture the proteins and washed three times with 70% ethanol solution. Proteolysis was performed by incubating the beads with a trypsin/LysC mixture (Promega, Madison, Wisconsin, USA) overnight at 37°C. After digestion, peptides were captured on the beads by adding pure acetonitrile. The beads were washed three times with acetonitrile and finally peptides were eluted from the beads with a solution of 2% DMSO in water. Samples were acidified to pH 4 with formic acid before liquid chromatography (LC) - mass spectrometry (MS) analysis. For the in-gel digestion protocol, samples were first migrated into an SDS-polyacrylamide gel. Migration traces were then cut into small pieces and washed 10 times in 100 mM ammonium bicarbonate buffer and acetonitrile baths. Samples were then reduced and alkylated with dithiothreitol (50 mM) and iodoacetamide

(150 mM), respectively. Proteolysis was performed by incubating the gel pieces in a trypsin/LysC mixture (Amount, Promega) overnight at 37°C. Digested peptides were finally extracted by successive incubations in 25 mM ammonium bicarbonate, 25 mM ammonium bicarbonate/acetonitrile (1/1, v/v), 5% formic acid, and 5% formic acid/acetonitrile (1/1, v/v). Buffer. Samples were finally vacuum dried and suspended in trifluoroacetic acid 0.05%, acetonitrile 1% (v/v) in water (volume).

2.6.2. Mass spectrometric analysis

The LC-MS setup consisted of a Dionex U3000 RSLC liquid chromatography system operated in column switching mode coupled to a Q-Exactive Plus or a Q-Exactive HF mass spectrometer (Thermo Scientific). The samples (200 ng peptide content) were loaded onto a trap column (75 μm × 20 mm, acclaim C18 pepmap 100, 3 μm, Thermo Scientific) through a loading phase (1% acetonitrile, 0.05% trifluoroacetic acid in water) at a flow rate of 5 μl/min. Samples were then eluted onto an analytical column (75 μm × 150 mm, C18 for Acclaim pepmap 100, 2 μm, Thermo Scientific) with a linear gradient starting from 2% A to 35% B in 66 min. Solvents A and B consisted of water with 0.1% formic acid and acetonitrile with 0.1% formic acid, respectively. MS acquisition was performed in data-dependent acquisition mode. The acquisition loop consisted of a survey scan acquired at a resolution of 70,000 at 200 m/z (60,000 at 200 m/z for Q-

Exactive HF), followed by selection and fragmentation of the 12 most intense precursor ions. The resolution of the MS/MS scans was set to 17,500 at 200 m/z (15,000 at 200 m/z for Q-Exactive HF) and the precursor ions that were already fragmented were excluded for 30s.

2.6.3. Data processing and analysis - LC-MS/MS

MS data were processed by Peaks Studio v.10.0 and v10.5 (Bioinformatics Solutions Inc., Waterloo, Canada) with an NCBI database containing protein sequences known for *P. dominula*, *V. germanica*, and *V. vulgaris* (21,442 entries). *Vespula spp.* samples were also processed using a protein sequence database containing all entries from the Hymenoptera order in Uniprot (601,844 entries). Protease specificity was set to trypsin, and error tolerance of precursor and fragment ion masses were set to 10 ppm and 0.015 Da, respectively. Carbamidomethylation of cysteine was specified as a fixed modification and oxidation of methionine and acetylation of the N-terminus of proteins as variable modifications. Identifications were filtered at a false discovery rate of 1% (peptides and proteins) using a reverse sequence database. The resulting proteomic datasets were screened for duplicate entries and reduced to one entry per protein. GenInfo identifiers (gi) were added where possible. Scanning included protein BLAST analysis to determine if duplicate entries were an artifact of using different databases for peptide identification in MS or if they were indeed different proteins. Inter-

ProScan version 5.39-77.026 was used to assign gene ontology (GO) terms to each protein for biological process, molecular function, and cellular component. Signal peptides were predicted using SignalP 5.0 with default parameters.

2.7. scRNAseq

2.7.1. Library preparation

All libraries for scRNAseq were prepared according to the manual (CG000330) of the Chromium Next GEM Single Cell 5′ Reagent Kits v2 (Dual Index) provided by 10x Genomics B.V. (Leiden, The Netherlands). A cell recovery of 8000 was targeted.

In short, the Chromium Next GEM Chip K is loaded with a master mix containing cell surface protein-labeled cells, barcoded single cell VDJ 5′ gel beads and partitioning oil. The gel bead is then dissolved and the cells within the GEMs are lysed. Each gel bead primer comprise an Illumina TruSeq Read 1 sequence, a 16 nt 10x barcode, a 10 nt unique molecular identifier (UMI), and a 13 nt template switch oligo, in addition to the master mix consisting of reverse transcription (RT) reagents and poly(dT) primers. Full-length cDNA with 10x barcode is generated starting from poly-adenylated mRNA. Cell surface protein feature barcodes with a Nextera-Read 2, a 15 nt feature barcode and the capture sequence are produced simultaneously in the same compartment. The GEM-RT

supernatant is separated and the GEMs are disssolved. Using silane magnetic beads, the 10x barcode first-strand cDNA and the DNA from the cell surface protein feature barcodes are purified. Both are then amplified. Based on their size, the amplified DNA is separated to generate 5' gene expression, V(D)J and cell surface protein libraries.

For the generation of the 5' gene expression library, the size of the amplicons is optimized using enzymatic fragmentation and size selection.

The V(D)J segments are enriched by amplification of the BCR constant region coding transcripts. Fragments of different lengths that together cover the complete V(D)J segments are generated by enzymatic fragmentation and size selection.

For the surface protein library, the procedure was analogous to the 5' gene expression library.

End repair, A-tailing, adapter ligation and sample index PCR are used to add P5, P7, i5 and i7 sample indexes and the Illumina R2 sequence to all libraries. Therefore, all final libraries contain the P5 and P7 priming sites used in Illumina sequencers.

2.7.2. Sequencing

Libraries were sequenced using a NovaSeq 6000 System with SP or S1 flow cells (Illumina Germany, Berlin Germany).

Sequencing was performed based on the manufacturer's recommendations.

Briefly summarized, each nanowell of the flow cell is coated with oligonucleotides that provide an anchor point for adapter binding. Using bridge amplification PCRs, clusters of DNA fragments are generated. Primers and modified nucleotides are then applied to the flow cell. After each round of synthesis, the attached base is determined based on fluorescence and the step is repeated until the complete fragment has been sequenced.

2.7.3. Data processing and analysis - scRNAseq

Raw sequencing data were demultiplexed and subsequently processed using RNA StarSolo for mapping and gene quantification [72]. The reference genome and splice junctions were based on GRCh38 (2020). For UMI deduplication, the CellRanger2-4 algorithm was used. Cell barcodes with N bases were matched to the whitelist (CellRanger3). Lower count UMIs that could be mapped to more than one gene were excluded (CellRanger3). Next, empty Droplets were filtered out using EmptyDrops approach via DropletUtils [73].
Data were analyzed using Seurat 4.0.5 [74]. The following inclusion/exclusion criteria were used:

- nFeature RNA > 50
- nFeature RNA < 2000
- Percentage of mitochondrial RNA < 8

- Percentage of mitochondrial RNA > 0.25
- Percentage of ribosomal protein > 0.25

The datasets were combined into a list, data normalized, and the 2000 genes with the highest variance were selected. Based on this, integration anchors were determined and the datasets were integrated into each other. Then the data was scaled and a principal component analysis was run. Relevant principal components were determined via JackStraw analysis to exclude redundant background noise during dimensional reduction. Finally, cells were clustered with a resolution of 0.5.

3. Material

3.1. Cell lines and plasmids

Cell lines	
Sf-9 (*Spodoptera frugiperda*)	Thermo Fisher Scientific
XL-10 Gold Ultracompetent Cells (*E. coli*)	Agilent Technologies
Plasmids	
pAcGP67B	BD Biosciences

3.2. Media and buffers

The media, buffers, and solutions used were all prepared with double distilled H_2O (ddH_2O) unless purchased or explicitly stated differently. The prepared media were autoclaved before use.

Agarose gel electrophoresis

1 x TAE	40 mM Tris
	1 mM EDTA
	pH 8,5 (Acetic acid)
6 x DNA Loading Dye	60% (v/v) Glycerol (85%)
	60 mM EDTA
	0,09% (w/v) Bromophenol blue
	0,09% (w/v) Xylene Cyanol FF
SERVA DNA Stain Clear G	SERVA

Buffers

Elution buffer (Ni-NTA)	300 mM Imidazole
	1x PBS, pH 7,4
FACS buffer	1% (w/v) FCS
	1x PBS, pH 7,4
D-PBS	Thermo Fisher Scientific

Media

2YT medium	CARL ROTH
Insect-XPRESS®	Lonza
LB medium	1,0% (w/v) Trypton

	0,5% (w/v) Yeast extract
	0,8% (w/v) NaCl
TYE medium	1,0% (w/v) Tryptone
	0,5% (w/v) Yeast extract
	0,8% (w/v) NaCl
	1,5% Agar

SDS-PAGE

APS stock solution	10% (w/v) Ammonium persulfate
Coomassie staining solution	0,1% (w/v) Coomassie-Brilliant-Blue R-250
	45% (v/v) Methanol
	10% (v/v) Acetic acid
Coomassie destaining solution	80% (v/v) ddH_2O
	20% (v/v) Acetic acid
SDS running buffer (5x)	0,125 M Tris
	0,96 M Glycin
	0,5% (w/v) SDS
Tris-Tricine anode buffer (5x)	0,2 M Tris
	pH 8,9
Tris-Tricine gel buffer (3x)	3 M Tris
	0,3% (w/v) SDS

	pH 8,45
Tris-Tricine kathode buffer (5x)	0,5 M Tris
	0,5 M Tricine
	0,5% (w/v) SDS
	pH 8,6

Western blot

AP substrate	0,01% (v/v) NBT (10x) stock solution
	0,01% (v/v) BCIP stock solution
	ad detection buffer AP
BCIP stock solution	0,5% (w/v) BCIP
	ad DMF
Detection buffer AP	100 mM Tris
	10 mM $MgCl_2$*H_2O
	100 mM NaCl
	pH 9,5
NBT stock solution (10x)	1% (w/v) NBT
	0,1 M Tris-HCl, pH 9,5
Transfer buffer	25 mM Tris
	19,2 mM Glycine
	20% (v/v) 2-Propanol

pH 8,3

3.3. Molecular-weight size markers and kits

5′ Feature Barcode Kit	10x Genomics
Chromium Next GEM Chip K Single Cell Kit	10x Genomics
Chromium Next GEM Single Cell 5′ Kit v2	10x Genomics
Chromium Single Cell Human BCR Amplification Kit	10x Genomics
Dual Index Kit TN Set A	10x Genomics
Dual Index Kit TT Set A	10x Genomics
GeneJET Gel Extraction Kit	Thermo Fisher Scientific
GeneJET Plasmid Miniprep Kit	Thermo Fisher Scientific
GeneRuler DNA Ladder Mix	Thermo Fisher Scientific
Library Construction Kit	10x Genomics
PageRuler™Prestained Protein Ladder	Thermo Fisher Scientific
MACS Kits (live/dead & bcells)	keine Ahnung
BioAnalyzer	keine Ahnung

3.4. Antibodies and flow cytometry reagents

Anti-human CD3 FITC	OKT3	BioLegend
Anti-human CD14 FITC	63D3	BioLegend
Anti-human CD19 BV650	SJ25C1	BioLegend
Anti-human CD56 FITC	HCD56	BioLegend
Anti-FLAG	FG4R	invitrogen
Anti-FLAG PE	L5	BioLegend
Anti-mouse IgG AP	polyclonal	Sigma-Aldrich
Anti-Rho1D4	1D4	Cube Biotech
Anti-Rho1D4 PE	1D4	Cube Biotech
Anti-v5		Invitrogen
Anti-v5 PE	TCM5	eBioscience
Human TruStain FcX™		BioLegend
Strep-Tactin® AP		IBA-Lifesciences
Strep-Tactin® PE		IBA-Lifesciences
Zombie NIR™		BIOZOL

3.5. Chemicals

Acetic acid (CH_3COOH)	Merck Millipore
Agar	PanReac AppliChem
Ammonium persulfate ($(NH_4)_2S_2O_8$)	PanReac AppliChem
5-Bromo-4-chloro-3-indolyl phosphate (BCIP)	PanReac AppliChem
Bromophenol blue	Sigma-Aldrich
Coomassie-Brilliant-Blue R250	Bio-Rad
Dimethylformamide (DMF - C_3H_7NO)	Fluka
EDTA	PanReac AppliChem
Gentamicin sulfate 50 mg/ml	CARL ROTH
Glucose	CARL ROTH
Glycerol	Merck Millipore
Imidazole	PanReac AppliChem
Magnesium chloride hexahydrate ($MgCl_2$*6 H_2O)	PanReac AppliChem
Methanol (CH_3OH)	Merck Millipore
Nitro blue tetrazolium chloride (NBT)	VWR Chemicals
4-Nitrophenyl phosphate disodium salt hexahydrate ($C_6H_6NO_6P$*H_2O)	PanReac AppliChem
Nonfat dried milk powder	PanReac AppliChem
2-Propanol (C_3H_8O)	VWR Chemicals

Sodium chloride (NaCl)	Sigma-Aldrich
Sodium dodecyl sulfate (SDS)	Sigma-Aldrich
Sodium hydroxide (NaOH)	Sigma-Aldrich
Tricine ($C_6H_{13}NO_5$)	PanReac Millipore
Tris - Base ($NH_2C(CH_2OH)_3$)	PanReac AppliChem
Tris - HCl ($NH_2C(CH_2OH)_3$ HCl)	PanReac AppliChem
Tryptone	PanReac AppliChem
Xylene Cyanol FF	Merck Millipore
Yeast extract	PanReac AppliChem

3.6. Enzymes and enzyme buffer

BcuI (SpeI) restriction enzyme	Thermo Fisher Scientific
10 x FastDigest Buffer	Thermo Fisher Scientific
NotI restriction enzyme	Thermo Fisher Scientific
T4 DNA Ligase	Thermo Fisher Scientific
10 x T4 DNA Ligase Buffer	Thermo Fisher Scientific
Q5™ High-Fidelity DNA-Polymerase	New England Biolabs
5 x Q5™ Polymerase Reaction Buffer	New England Biolabs
XbaI restriction enzyme	Thermo Fisher Scientific

3.7. Equipment and columns

2100 Bioanalyzer Instrument	Agilent
Amicon®Ultra Filter	Merck
AKTApure	GE Healthcare
BD Falcon™Round-Bottom Tubes	BD Biosciences
BioVanguard Green Line	Telstar Life Science
Centrifuge 5810 R	eppendorf
Centrifuge 5424 R	eppendorf
Chromium Controller	10x Genomics
Eclipse TS100	Nikon
Gel iX Imager	Intas Science Imaging
HisTrap^{TM}excel (1 ml)	GE Healthcare
Infinite®200 PRO	Tecan
Innova®42 Incubator Shaker	New Brunswick Scientific
Innova®43 Incubator Shaker	New Brunswick Scientific
Peltier-cooled incubator IPP260	memmert
PB303 DeltaRange	Mettler Toledo
peqPOWER 300 Power Supply	VWR International
peqSTAR 96X Thermocycler	VWR International
PerfectBlue gel system™Mini S	VWR International

ROCKER 2D basic	IKA
ROLLER 6 basic	IKA
SE250 Vertical Protein Elektrophoresis Unit	Hoefer
Sigma®25 cm cell culture flask	Merck
Sigma®75 cm cell culture flask	Merck
Sigma®175 cm cell culture flask	Merck
ThermoMixer®C	eppendorf
V20-SDB semi-dry blotter	SCIE-PLAS

3.8. Webserver and software

BioRender.com	Figure design	
BLAST	Sequence alignment	[75]
Clustal W	Sequence alignment	[76]
DropletUtils	Filter empty droplets	[73]
InterProScan v5	Functional analysis	[77]
ProtParam	Protein characteristics	[78]
R 4.1.1	Data analysis	
RNAStarSolo	Mapping and gene quantification	[72]
SignalP 5.0	Signal sequence predicition	[79]
GraphPad Prism 7	Data analysis	

R packages

cowplot_1.1.1	Nebulosa_1.2.0	scCATCH_3.0
dplyr_1.0.7	patchwork_1.1.1	SCORPIUS_1.0.8
ggplot2_3.3.5	pheatmap_1.0.12	Seurat_4.1.0
ggplotify_0.1.0	RColorBrewer_1.1-2	SeuratObject_4.0.4
gridExtra_2.3	Rcpp_1.0.8	SeuratWrappers_0.3.0
harmony_0.1.0	reshape2_1.4.4	writexl_1.4.0
Matrix_1.3-4	rliger_1.0.0	

4. Results

4.1. Venom proteomes - *P. dominula & V. vulgaris*

This part of the thesis aimed to describe the protein components of the venoms of three allergy-relevant, closely related wasp species. The capillary-extracted venoms of the species *P. dominula* (PDV), *V. germanica* and *V. vulgaris* (YJV) were analyzed and compared by mass spectrometry [80]. Based on these venom proteomes, potential new allergens were identified in further research, which may be added to the palette of allergens used in component-resolved diagnostics (CRD) [81].

4.1.1. Protein diversity

P. dominula and *Vespula* spp. venom (mixture of the venoms of the closely related species *V. vulgaris* and *V. germanica*) were analyzed by mass spectrometry. The analysis yielded 1140 proteins for *Vespula* spp. venom. However, after removing

duplicate entries caused by similar proteins from different Hymenoptera species, 157 proteins remained. *P. dominula* venom was found to be less rich in protein diversity, as 100 unique proteins were identified (Figure 4.1a). An overlap of 48 results in 109 and 52 unique venom proteins, respectively (Figure 4.1b). Further-

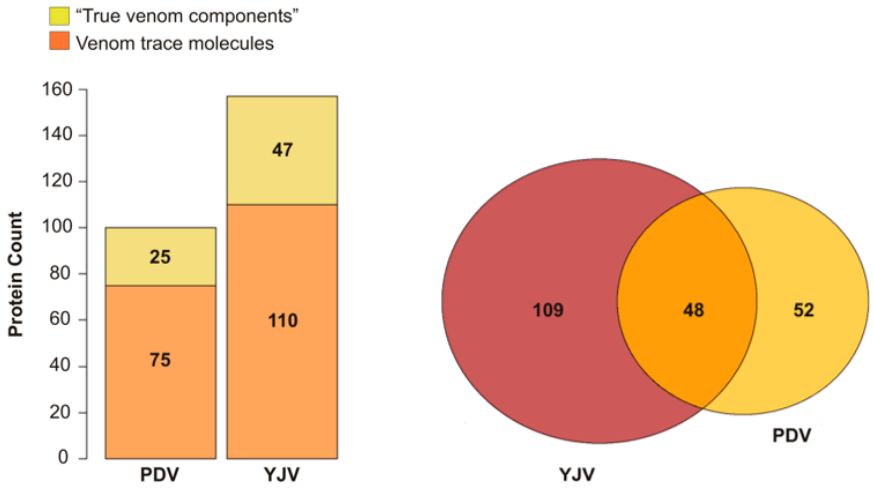

(a) (b)

Figure 4.1.: Identified proteins in *P. dominula* and *Vespula* spp. venom. (a) Total number of proteins identified in the venoms. The proteins are divided into venom components with leading sequence for the extracellular space, annotated allergens or a known function in the venom ('true venom components') and into venom trace molecules lacking signal peptides. (b) Venn diagramm of all proteins found in YJV and PDV and the overlap containing proteins identified in both venoms. PDV, *Polistes dominula* venom; YJV, yellow jacket venom.

more, the two data sets were subdivided into three different groups: allergens already annotated, secreted proteins / proteins with a known venom function (these two groups were classified as 'true venom components'), and venom trace molecules not exhibiting a signal sequence for secretion to the extracellular space.

A brief comparison of the protein function at the molecular level and an eval-

uation of the biological processes involved was achieved by assigning *Gene Ontology* (GO) terms to the identified proteins. Figures 4.2a and b show the frequency of GO terms. As the variety of proteins present in the two venoms differs, the relative abundance is of greater importance in this context. While the venoms generally show similar composition, YJV comprises 20% of proteins with catalytic activity, PDV on the other hand 7% (Figure 4.2a). This discrepancy, as noticeable as it may be, is presumably caused by greater contamination of housekeeping proteins in the YJV analyzed, as mostly metabolic active enzymes are assigned to this GO term. One exception are the venom hyaluronidases, which, are present in both venoms. Briefly summarized, the proteins found in the two venoms only show minor differences concerning molecular functions or biological processes (Figure 4.2a and b).

4.1.2. Annotated allergens

Apart from the high molecular weight protein vitellogenin (Ves v 6), the analysis yielded all allergens of the here investigated venoms that had already been annotated (Table B.1). These allergens were, except Pol d 4 - the PDV serine protease - also part of the aforementioned overlap [82].

The phospholipase A1 (PLA1) is a known allergen from venoms of various Vespoidea species [83–85] and also present in PDV and YJV (Pol d 1 and Ves v 1) [86]. It hydrolyzes the sn-1 position of phospholipids and, therefore, disrupts

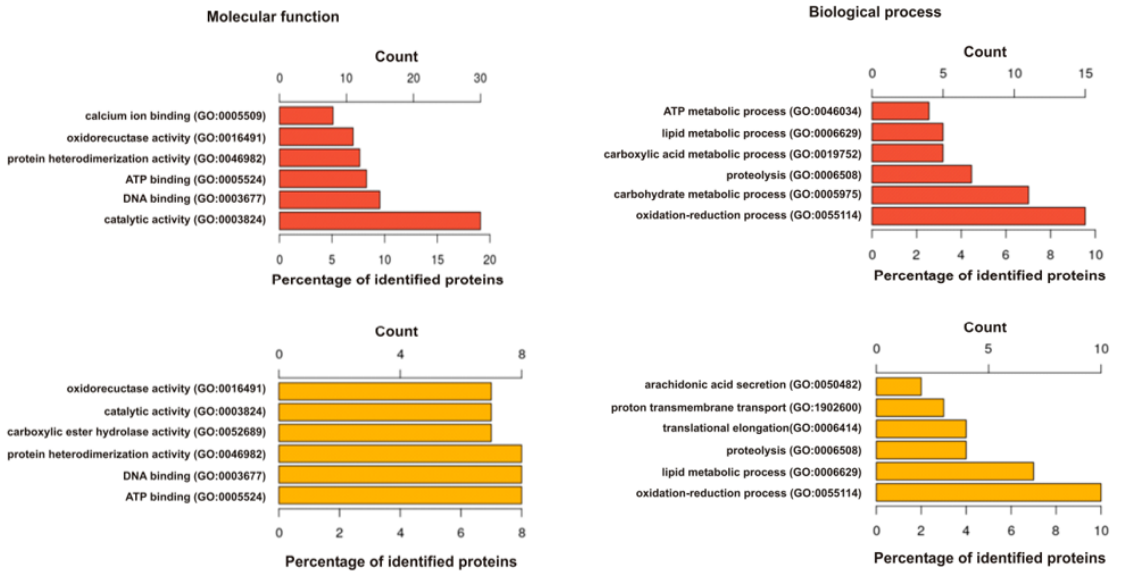

(a) (b)

Figure 4.2.: Top six GO terms for (a) molecular function and (b) biological process of proteins from YJV (red) or PDV (yellow). On the x-axis above the plots the absolute counts are given, on the lower axis the relative abundance in [%].

cells due to the high amount of phospholipids in pro- and eukaryotic cell membranes.

Hyaluronidases are promoting the spread of venom at the puncture site by cleaving hyaluronan [87], the most abundant glycosaminoglycan in the vertebrate extracellular matrix. They have been annotated as allergens for at least eight Hymenoptera species, including *A. mellifera*, *P. paulista*, and *V. vulgaris* [82]. The sequence identity of the newly identified *P. dominula* hyaluronidase Pol d 2 and the venom hyaluronidases of the abovementioned species is approximately 53% (Api m 2, query coverage 90%), 91% (Poly p 2, query coverage 79%), 74% (Ves v 2.0101, query coverage: 90%), and 57% (Ves v 2.0201, query coverage:

92%).

Dipeptidyl peptidases IV (DPP IV) are aminopeptidases present in the venom, separating dipeptides from the main chain at the N-terminus of a protein. This allows the activation or inactivation of the substrate, protecting the host insect from undirected and unintended toxic effects [88]. DPP IV is, for instance, part of honey bee venom (HBV - Api m 5) [89], where it catalyzes the reaction of promelittin to melittin (Api m 4), a cytotoxic polypeptide [90]. Similarly, Ves v 3 activates the venom polypeptide mastoparan [91]. However, in PDV, there is no known and susceptible propeptide present, that has the requirements to act as a substrate. While it was characterized as a relevant allergen in PDV (Pol d 3) [92], its venom function remains elusive.

Pol d 4, the trypsin-like serine protease from PDV, was described as a putative allergen in 2003 [93, 94]. So far, there is no homologous protein described in YJV. Its function in the venom is likely connected to coagulation and tissue damage, as serine proteases present in snake venoms fulfill similar roles [95].

Antigens 5 are part of the CAP superfamily (cysteine-rich secretory proteins, antigen 5, and pathogenetic 1 proteins). Most CAP superfamily proteins are secreted and act as endocrine or paracrine modulators [96], the function of venom antigen 5s is unclear. Various functions in venoms and / or saliva are part of current scientific discussion, such as blocking ion channels, including ryanodine receptors, Ca^{2+} and K^{+} channels [97–99] or influencing platelet aggregation

and thus modulating the immune system [100]. Nevertheless, their role in Hymenoptera venoms remains unclear.

4.1.3. Secreted proteins and proteins with known venom function

Assuming that all proteins with venom function must be actively shuttled out of the cell, the primary structures of all identified PDV / YJV proteins were analyzed for the presence of signal sequences [79]. Table B.2 gives an overview of the analyzed venom components with a signal sequence for extracellular transport.

Among the proteins identified exclusively in PDV, surprisingly, is an icarapin-like protein. The eponym is Api m 10 (icarapin), a major HBV allergen with unknown molecular function and structure [101, 102]. Despite its originally reported instability, it is used in CRD as a marker allergen for the diagnosis of HBV allergy [103, 104]. Recent work has raised doubts about the instability of Api m 10 [105]. PDV icarapin-like protein has a sequence identity of 43% to the canonical Api m 10 primary structure. To date, no studies have been published that address the allergenicity of icarapin-like protein.

The venoms of different Hymenoptera, such as *Apis* spp. or *B. terrestris*, but also snake and spider venoms contain phospholipases A2 (PLA2) [106, 107], which act as neuro- and myotoxins. The lytic effect on cells is achieved by hydrolyzing

phospholipids of the cell membrane in motor nerves [106]. Two different isoforms with 99% sequence identity have been identified in PDV. Moreover, one of the isoforms is also present in YJV. The two PDV PLA2 differ only at one residue and have around 45% sequence identity to Api m 1 (HBV PLA2) [108].

PDV also contains three variants of the protein lethal (2) essential for life-like (PLELL) which differ in length (246, 201, 196 amino acids) and the presence of leading sequences. The sequence identity of the 246 amino acid variant to the other two is relatively low at 41% and 39%, respectively. PLELLs can be assigned to the HSP20 family, which are small heat-shock proteins that function as chaperones. Exactly what role is assumed by PLELL in Hymenoptera venom is not clear.

The vascular endothelial growth factor C (VEGF C) protein is part of the PDGF family (PF00341). Members of this family are present in HBV, PVF-1 [109], and also in snake venom [110]. PVF-1 is part of current allergological research, as about 40% of HBV-allergic patients show sensitization to PVF-1. However, no basophil activation has been achieved with PVF-1, so its relevance as an allergen remains unclear [111]. The function of VEGF C in PDV is not entirely clear. The PDGF family includes several members with three corresponding receptors: VEGFR-1, -2, and -3. Depending on receptor binding, proteins in this family are either hemangiogenic, lymphangiogenic, or both. VEGF Cs bind to VEGFR-2 and -3 and are therefore predominantly lymphangiogenic, but also play a role

in blood epithelial cell mitogenesis [112–114]. This hemangiogenic function also induces an increase in blood vessel permeability and may contribute to the envenoming process [115]. VEGF Cs occur naturally as prepropeptides and depending on the cleavage progress, the binding affinity for VEGFRs is altered, i.e. increased [115].

The bulk of the proteins identified exclusively in YJV (Table B.2) are predicted for *P. dominula* and, accordingly, are probably not specific to *Vespula* spp.. In addition, the descriptions of most proteins listed here imply that they do not serve a venom-specific function but are venom trace molecules [69].

Several small peptides were identified; namely dominulin A and B in PDV as well as mastoparan, vespakinin, and vespulakinin in YJV. Although no signal sequences were predicted, these peptides are treated as 'true venom components' and are therefore listed in Table B.2. The line between actively transported venom components and housekeeping contaminants is not always clear, because not all underlying shuttling mechanisms are fully elucidated and precursor proteins are sometimes unknown.

For example, the mastoparans discussed earlier are closely associated with DPP IV (Ves v 3). Their precursors contain N-terminal sequences that are released after cleavage of the signal peptide and are DPP IV substrates. Therefore, the shuttling mechanisms are based on transit peptides present in precursor proteins. This also explains how mastoparans can end up in the venom despite the absence

of a signal peptide [91]. However, no mastoparan precursors were found in the proteomic analysis performed here, probably due to the lack of genomic data on *Vespula* spp.

Dominulins A and B from PDV are small peptides of 17 amino acids with twelve identical residues. These peptides show antibacterial properties and are probably closely related to mastoparans [116]. Drawing a link between dominulins and *P. dominula* DPP IV (Pol d 3) seems obvious, but no link has been reported in the literature to date. Moreover, no precursor of dominulin A or B is known or predicted. In previous studies, the two variants were found both on the cuticle and in the venom, with the latter occurring more irregularly [116]. While the presence of mastoparan in the venom and its role as a true venom component seems clear [117], dominulins remain elusive.

Vespulakinins/vespakinins are vasoactive glycopeptides containing the nine amino acid long bradykinin [118]. This peptide has mainly three different pharmacological effects after injection in the victim: release of histamine from mast cells, lowering of blood pressure [118], and induction of pain [119]. The analyses presented here revealed vespulakinin/vespakinin in YJV, whereas polisteskinin, a rather similar peptide previously described in *Polistes* spp. venoms, was not detected in PDV. However, the detection of such short peptides is unlikely in a shotgun run.

A total of 47 (YJV) and 25 (PDV) proteins that are secreted or have a known

function in venom were identified, with a cut set of 14 proteins. These include the proteins listed in Table B.2 and the annotated allergens from Table B.1.

4.1.4. Venom trace molecules

All proteins not exhibiting properties needed for the classification as a true venom component were labeled as 'venom trace molecules'. These proteins are derived from adjacent tissue to the venom in the venom gland and are either naturally occurring contaminants or due to the venom extraction process. A more detailed characterization and the complete list of proteins can be found in Grosch et al. [80].

4.2. Monitoring transcriptional changes in patients undergoing VIT

This project aimed to describe the transcriptional changes in patient PBMCs during the first two weeks of VIT. Most Hymenoptera venom-allergic patients achieve good protection against systemic reactions after the up-dosing phase [60, 61]. Therefore, there might be changes in the immune cells involved, which, if identified, allow a prospective statement about the course of immunotherapy. Markers of successful immunotherapy can be identified either at the protein or transcriptome level, the latter providing broader insight into the cells to get a

first overview of promising candidates [120–123].

4.2.1. Patient recruitment and sample preparation

All subjects included were *V. vulgaris* venom-allergic patients undergoing venom-specific immunotherapy. Venom immunotherapy can generally be divided into two different phases: the up-dosing phase and the maintenance phase. The therapy protocol used for the treatment of the here included patients provides for a stationary up-dosing over a period of three days. Two weeks after the end of therapy, the first maintenance dose is given, which is then administered at intervals of four to six weeks for the first three years. Patients gave blood before and after up-dosing as well as 2 weeks after leaving the hospital (Figure 4.3). PBMCs were isolated from the blood of the patients and stored frozen. After thawing, cells from eight patients (Table B.3) were pooled per time point and dead cells were removed before being submitted to the scRNAseq workflow.
The samples of individual patients were pooled, as influencing factors like age, sex, underlying medical conditions, lifestyle, and epigenetic changes in general, can be reduced. The heterogeneity of the patients, also with regard to peculiarities of the respective allergy phenotype, would, in case of an analysis of individual patient transcriptomes, lead to too many, not relevant, differences. By pooling the samples, all changes can be attributed to the therapy, as this is the only element all patients have in common. Included were three biological

women and five men. The average age was 42 years (28-62 years).

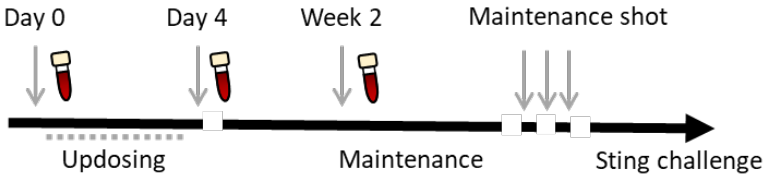

Figure 4.3.: Treatment scheme for VIT and timeline for patient sampling. Blood was drawn before the up-dosing phase began, on days 4 and 18, as indicated by a blood vial.

4.2.2. Data processing and cell counts

Table 4.1 gives the number of cells remaining after mapping, gene quantification, and empty droplets filtering including the abbreviations used from here on. The abbreviations include the day of sample collection and a letter to identify unstimulated (c) samples (e.g. 'd14c' = unstimulated sample 14 days after the end of the up-dosing phase). Dead cells were excluded based on the content of nFeature RNA, mitochondrial RNA, and ribosomal proteins.

Table 4.1.: Abbreviations used in the following and cell counts of RNAseq samples before (top) and after (bottom) excluding cells with too high or too low nFeature RNA, mitochondrial RNA and ribosomal proteins.

Abbreviation	**d0c**	**d4c**	**d14c**
Cell count	4816	8998	726
Living cells	4476	8307	673

4.2.3. Clusters and cluster assignment

Figure 4.4a and b show the dimensionally reduced and clustered cells of comparison d0c-d4c-d14c as well as extracted and re-clustered T cells. To roughly assign clusters, the expression of unique cell markers was considered. Figure 4.4c shows the expression of PTPRC (CD45) on the left to confirm that all clusters comprise leukocytes and that no significant contamination was present. On the right, MS4A1 (CD20), as a marker for B cells, ITGAX (CD11C), as a marker for monocytes and macrophages, and CD3E, CD3G, CD3D, and CD247, to identify T cells, are shown. Based on these genes, cluster 7 is B cells (including plasmablasts and circulating plasma cells), cluster 5 is monocytes and macrophages, and clusters 0, 1, 2, 3, 4, and 6 are presumably various T cells. Cluster 8 is not readily assignable. Therefore, two further markers, CD68 and LYZ, were used. Figure 4.4d shows violin plots with the expression levels of CD68 and LYZ. As can be seen, LYZ is only expressed in clusters 5 and 8, with a higher level of expression in cluster 8. According to Zhu et al. [124], this combination of CD68 and LYZ allows differentiation between monocytes and dendritic cells (DC) and defines cluster 8 as DCs.

The partially low numbers of cells expressing the aforementioned genes, especially CD3E, CD3G, and CD3D positive clusters, are due to the fact that not every cell constantly transcribes all surface proteins [125]. To provide a more in-depth analysis of peripheral T cells, clusters 5, 7, and 8 were excluded and

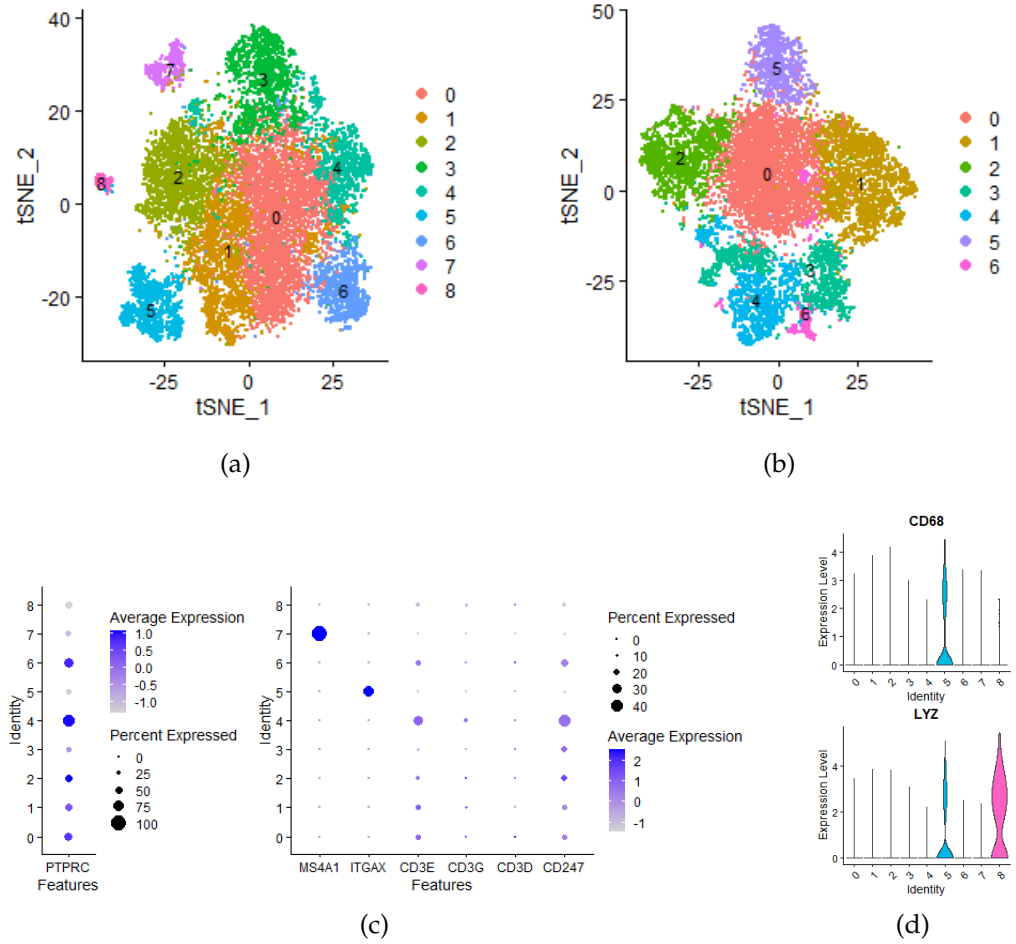

Figure 4.4.: (a) Clusters in tSNE embedding (whole PBMCs). (b) T cells extracted from original dataset and newly clustered in tSNE embedding. (c) Dot plots of cell markers unique for leukocytes in general (PTPRC - CD45), B cells (MS4A1 - CD20), monocytes / macrophages (ITGAX - CD11C) and T cells (CD3E, CD3G, CD3D and CD247). Cluster numbering refers to the original clustering in 4.4a. (d) Violin plots of expression level of CD68 and LYZ to discriminate monocytes / macrophages and dendritic cells. Cluster numbering refers to the original clustering in 4.4a.

the remaining cells clustered again (Figure 4.4b). In the following, cluster IDs derived from the T cell-only analysis are referred to as t0 to t6 to avoid confusion. Some changes in the relative cluster sizes can be described (Table 4.2): Clusters 5, 7, and 8 remain stable during up-dosing, but are increased after 14 days. Partic-

ularly striking is the percentage growth of cluster 5 (monocytes/macrophages) from ~7% (d0c & d4c) to ~39% (d14c). Since the total cell counts for d14c are comparatively low, the overall percentage values should be treated with caution. Furthermore, it is not clear if there is an increase of monocytes/macrophages in PBMCs after 18 days of VIT or whether other cell types decrease and thus the relations are shifted. Nevertheless, this is a noteworthy observation.

Similar behavior is shown by the B cell cluster (cluster 7), which increases from 2.4% (d0c) to 3% (d4c) to 9.5% (d14c). Again, the limitations already mentioned apply. However, an increase of peripheral B cells, plasmablasts, and plasma cells can be expected after antigen exposure and is in line with published literature [126].

To make statements about changes in the T cell clusters, it is necessary to characterize the different clusters in more detail. This was done based on published marker genes for T cell subpopulations [127, 128]. The populations expected in peripheral blood are naïve (T_N), central memory (T_{CM}), effector memory (T_{EM}), effector memory re-expressing CD45RA (T_{EMRA}) and regulatory (T_{reg}) T cells. T_{CM} and T_{EM} cells differ mainly in the expression of homing factors such as CCR7, which guides cells from circulation to lymphatic organs [129]. T_{EMRA} cells re-express CD45RA, which is thought to be a marker for T_N cells. However, certain memory cells (especially - but not limited to - $CD8^+$ T cells) are $CD45RA^+$ [130]. Due to the bulky extracellular domain of CD45RA in comparison to

CD45RO, the homodimerization of CD45 is less efficient and, therefore, cells are less efficiently activated. This is thought to be an immune checkpoint to regulate autoimmunity [131]. Figure 4.5 shows a heatmap of clusters t0 to t6 with the pre-

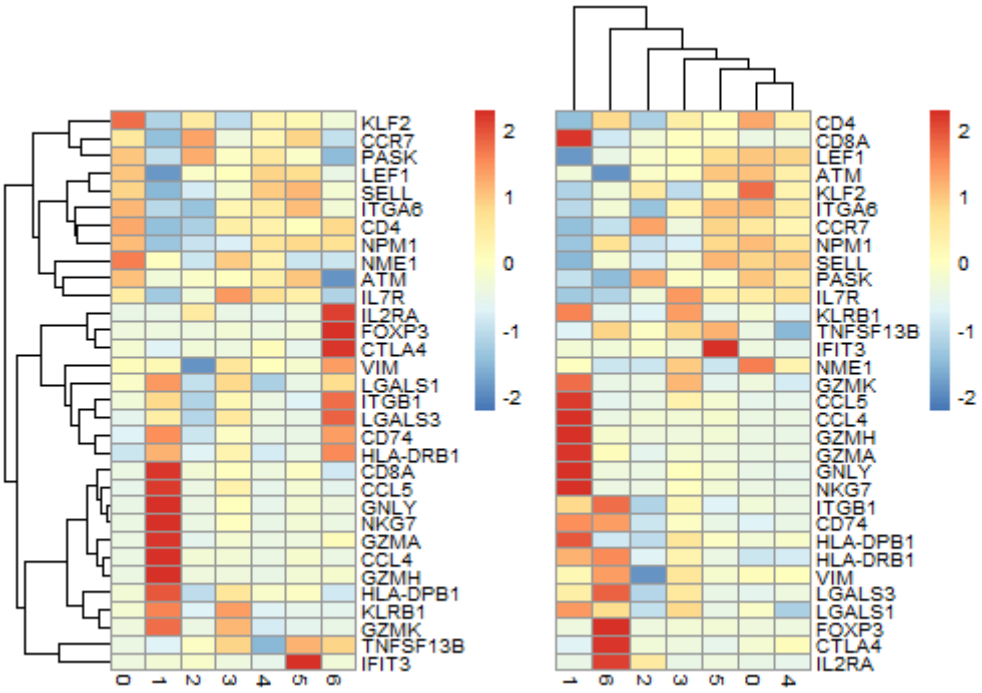

Figure 4.5.: Heatmap of clusters t0, t1, t2, t3, t4, t5, and t6 including differentially expressed marker genes for different T cell subpopulations clustered based on rows (left) or columns (right).

viously mentioned marker genes sorted by rows (left) or columns (right). Cluster t1 can be defined with high probability as T_{EMRA} based on the expression of KLRB1, GZMK, CCL4, CCL5, GZMH, GZMA, GNLY, NKG7, ITGB1, and CD74. Consistent with this is the increased CD8A expression. Figure 4.6 shows density plots of the expression of two natural killer cell (NK cell) markers, NCAM1 (CD56) and the transcription factor EOMES. Cluster t1 thus contains NK T and NK cells in addition to $CD8^+$ memory T cells. For the sake of simplicity, this

cluster will nevertheless be referred to as T_{EMRA} cells in the following. The

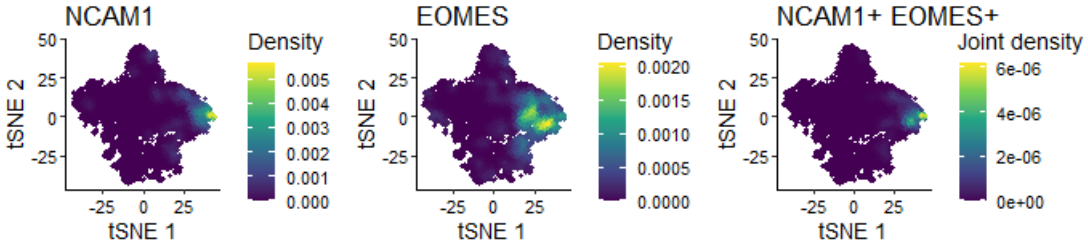

Figure 4.6.: Density plots of NCAM1 and EOMES expression in tSNE embedding.

T_{EMRA} cells are elevated after the up-dosing phase and remain elevated over the two-week period.

Cluster t6 shows the typical transcriptional profile of regulatory T cells with expression of FOXP3, CTLA4, and IL2RA. T_{reg} cells decline over the course of the first two weeks of VIT. The PASK and CCR7 genes, which are particularly highlighted in cluster t2, are considered markers for T_{CM} cells. This cluster initially grows moderately (from 11 to 15%) before the relative size with respect to total T cell numbers subsequently doubles to ~30%. IL7R, KLRB1, TNFSF13B as well as GZMK, and CCL5 are indicative for T_{EM} cells and in combination are upregulated especially in cluster t3. Before the start of therapy, this cluster is at around 34% but shrinks to virtually 0% within the first four days. Two weeks after the end of the up-dosing phase, cell counts seem to slowly recover. Clusters t0, t4, and t5 are the most similar among the T cell clusters, and all show transcriptional profiles indicative of naïve T cells. Differentially regulated are mainly TNFSF13B / IFIT3 (t5) and NME1 / KLF2 (t0) (Figure 4.5). Similar

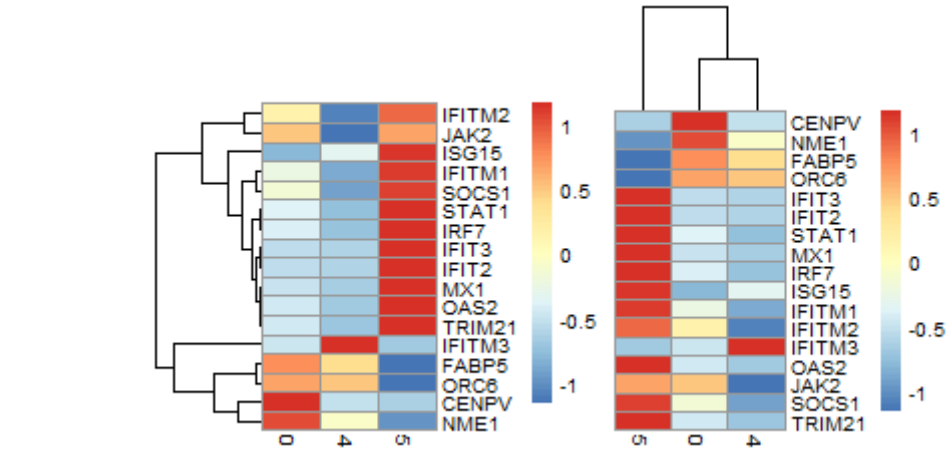

(a)

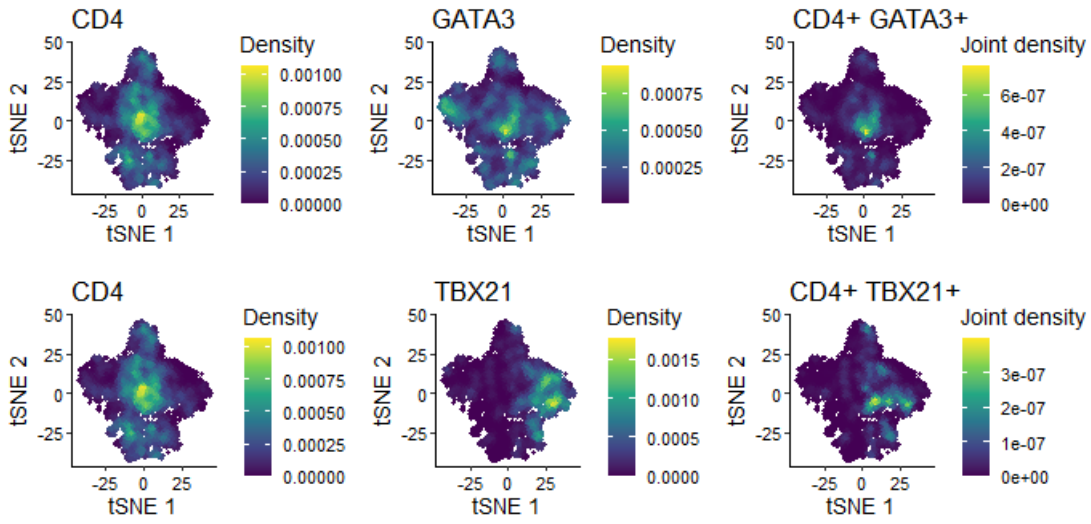

(b)

Figure 4.7.: (a) Heatmap of clusters t0, t4, and t5 including differentially expressed marker genes for the identified T_N cell subpopulations clustered based on rows (left) or columns (right). (b) Density plots of CD4, GATA3 and TBX21 to locate T_h2 and T_h1 cells.

to cluster t3, the relative size of cluster t4 decreases to zero (d4c) and seems to slowly recover after two weeks. This cluster is presumably non-activated (i.e. resting), naïve T cells. The situation is different with cluster t0, which also shows the typical transcriptional profile of naïve T cells (CCR7, NPM1, SELL), but

additionally has the genes NME1 and KLF2 upregulated. NME1 is a long-lasting activation marker [127], while KLF2-positive T cells represent a transitional state between the naïve and memory compartments [132]. The third cluster of naïve T cells, t5, is notable for the upregulation of TNFSF13B and IFIT3, both of which are activation markers. In contrast to NME1, which can be up-regulated for several days after activation, IFIT3 transcripts are depleted after approximately two days [127]. Thus, cluster t5 are more acute activated naïve T cells. Cluster t5 is increased in size on day four compared to day zero and is, two weeks after the up-dosing phase, slowly progressing back to the initial level.

To further describe the function of each naïve T cell cluster, the expression of interferon-response (IFN-response) and proliferation-associated genes in clusters t0, t4, and t5 was examined in more detail (Figure 4.7a). IFN-response genes (IFIT3, IFIT2, STAT1, MX1, IRF7, ISG15, IFITM1, IFITM2, IFITM3, OAS2, JAK2, SOCS1, TRIM21) are upregulated in naïve T cells that were activated in a TCR-dependent manner [127]. These cells form a transitional state between resting T_N cells and proliferating T cells. The CENPV, NME1, FABP6, and ORC6 genes can be used as marker genes for proliferating T cells. The IFN-response cassette seems to be active mainly in cluster t5. Genes associated with proliferation are upregulated mainly in cluster t0.

To localize T_h1 as well as T_h2 cells, density plots were generated using CD4, GATA3, and TBX21. As shown in Figure 4.7b, both populations are primarily

located in cluster t0. To further define cluster t0, cytokine expression of $CD4^+$

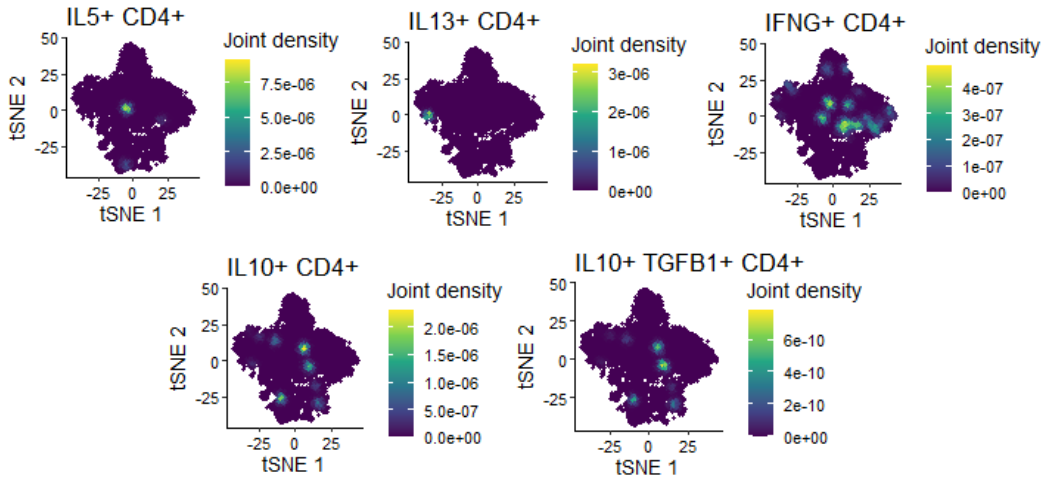

Figure 4.8.: Marker cytokine expression for T_h1 (IFNγ), T_h2 (IL5, IL13) and T_{reg} (IL10, TGFβ) cells in density plots.

T cells was examined in more detail. As can be seen in Figure 4.8, the cytokines of T_h1 (IFNγ) and T_h2 response (IL5) are increased in the region of cluster t0. IL13 is primarily produced by T_{CM} cells, whereas the regulatory cytokines IL10 and TGFβ are produced at multiple sites. This is related to the diffuse representation of the T_{reg} cluster in tSNE-embedding and is an artifact of the two-dimensional representation of the high-dimensional data set. Thus, the density plots locate $CD4^+$ T_h1 and T_h2 effector T cells primarily in cluster t0. Summarized, this puts the T cell clusters t0, t4, and t5 in the following relationship: t4 are resting T_N cells. Interferon-response T_N cells are clustered in t5. Cluster t0, where KLF2 regulates cytokine expression, markers for proliferation can be found and T_h1 as well as T_h2 cells are present, is presumably a cluster of activated T cells (T_{Akt}) [132, 133]. However, the assignment here is to be understood generously. In

this context, 'activated' includes different cell states between resting T_N and T effector cells on the verge of becoming memory T cells.

Table 4.2.: Cluster IDs with assigned celltypes and the cluster sizes of day 0, day 4, and week 2. Top: Cluster IDs refer to the initial clustering in Figure 4.4a. Cluster size is in relation to all cells analysed. Bottom: Cluster IDs refer to the in depth analysis of T cells in Figure 4.4b. Cluster size is in relation to T cells analysed. M/M, monocytes/macrophages; DC, dendritic cells; $T_{N\text{-}Mem}$, naïve - memory T cells; $T_{N\text{-}IFN}$, naïve - interferon response T cells.

		Percentage [%]			**Trend**	
ID	**Population**	**Day 0**	**Day 4**	**Week 2**	**Day 4**	**Week 2**
5	M/M	7	6	39	→	↗
7	B cells	2	3	10	→	↗
8	DC	1	1	5	→	↗
t0	T_{Akt} cells	2	46	29	↗	↘
t1	T_{EMRA} cells	13	24	26	↗	→
t2	T_{CM} cells	11	15	30	↗	↗
t3	T_{EM} cells	34	0	4	↘	↗
t4	T_N cells	34	0	3	↘	↗
t5	$T_{N\text{-}IFN}$ cells	1	13	6	↗	↘
t6	T_{reg} cells	6	2	3	↘	→

4.2.4. Memory T cells - trajectories and DEGs

The clusters of CD45RA re-expressing T cells (t1) and of central memory T cells (t2) were looked at in more detail over the time course of the initial phase of VIT. As already established in Figure 4.6, the T_{EMRA} cluster also includes, but to a lesser extent, NK and NKT cells. Nevertheless, transcriptional differences from time point zero to time point one can be observed in the trajectory analysis. Two weeks after the end of the up-dosing phase, the cells of cluster t1 seem to approach their initial state again (Figure 4.9a). An analogous picture is provided by Figure 4.9b, where the trajectory of the T_{CM} cells is shown. Again, transcriptional differences are most pronounced immediately after the up-dosing phase, whereas pre- and post-up-dosing appear to be similar. To further characterize

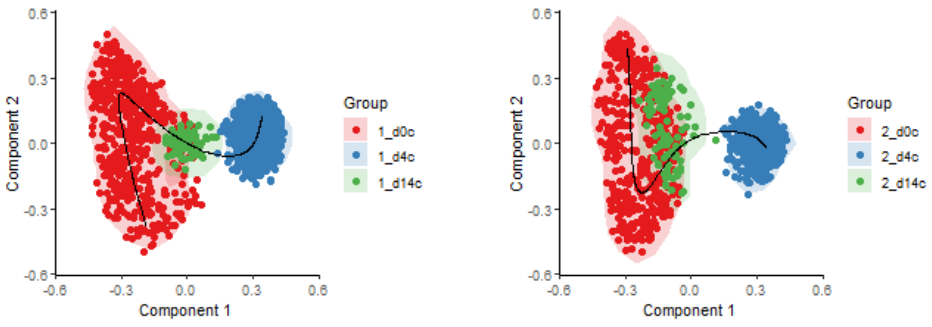

(a) (b)

Figure 4.9.: PCA of progression of development of T_{EMRA} (a) and T_{CM} (b) cell clusters. The trajectory is indicated as solid black line. d0c, red; d4c, blue; d14c, green.

the evolution of the transcriptome shown in 4.9 and identify genes relevant in

the context of therapy, the differentially expressed genes (DEG) of each time point were calculated. Figure 4.10a shows a heatmap with the DEGs of the T_{EMRA} cells. Among others, genes such as MX2 and STAT2 are differentially expressed, even after two weeks of antigen abstinence. A similar pattern can be observed for the T_{CM} cells. Again, interesting transcriptional differences are found, for example, MX1, IL6ST, or RELA (Figure 4.10). Intriguingly, there is also parallelism between the clusters, for example in the form of CD6 expression. However, whereas T_{EMRA} cells upregulate CD6 expression over time, expression in T_{CM} cells rises to a maximum after the up-dosing phase and subsequently decreases again.

4.2.5. Interferon-response T cells - trajectories and DEGs

$T_{N\text{-}IFN}$ cells, i.e. naïve T cells either primed by interferons or early-activated T cells, presumably assume a kind of high-alert status and are thought to be a developmental intermediate step between resting naïve and effector T cells [127]. The trajectory in Figure 4.11a indicates the evolution of the transcriptome of this intermediate state at the three time points. The already known pattern can be confirmed here: the differences are largest after the four days of antigen exposure before they seem to stabilize again. Figure 4.11b shows the corresponding DEGs. Certainly of interest are candidates such as SIGMAR1 or RNASET2, which are similarly regulated in the non-acute antigen exposure stages day zero and day

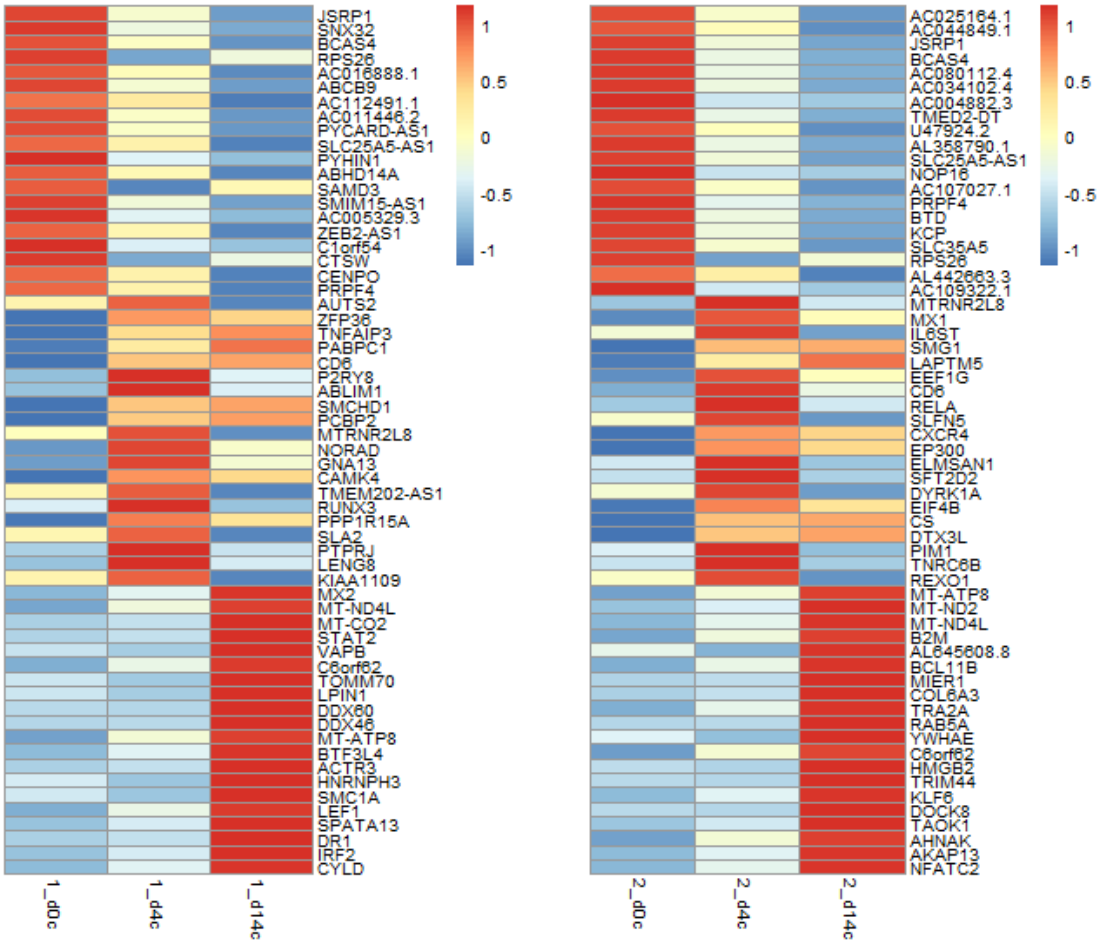

(a) (b)

Figure 4.10.: Heatmap of top DEGs of T_{EMRA} (a) and T_{CM} (b) cell clusters.

14 after the up-dosing phase. However, the highly expressed genes of day four, for example IFIT2 or OASL, could also provide information about the course of therapy.

In addition, to further characterize the interferon-response cluster, the DEGs of the $T_{N\text{-}IFN}$ cells at day four were assessed in comparison with all other T cells (Figure A.1 shows a selection of the top DEGs). Based on all DEGs thus identified,

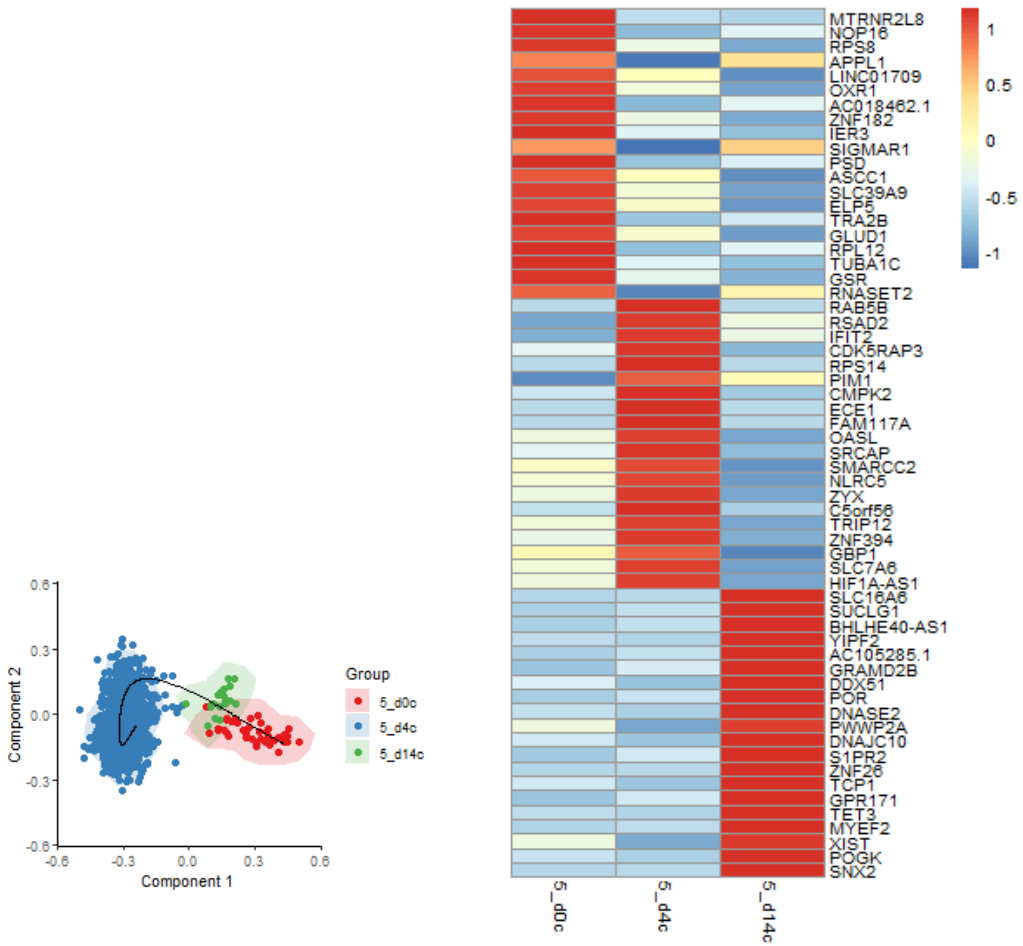

(a) (b)

Figure 4.11.: (a) PCA of progression of development of $T_{N\text{-}IFN}$ cell cluster. The trajectory is indicated as solid black line. d0c, red; d4c, blue; d14c, green. (b) Heatmap of the top 20 DEGs of $T_{N\text{-}IFN}$ cells for the time points pre and post up-dosing.

GSEA and network analyses were performed (Figure 4.12) to highlight relevant differences in pathways. The most affected pathways are shown as nodes in the upper right of Figure 4.12. Of particular interest in this context are those genes, such as MX1 or OAS3, that are involved in all identified relevant pathways. These genes, so-called hub genes, which represent highly interconnected genes,

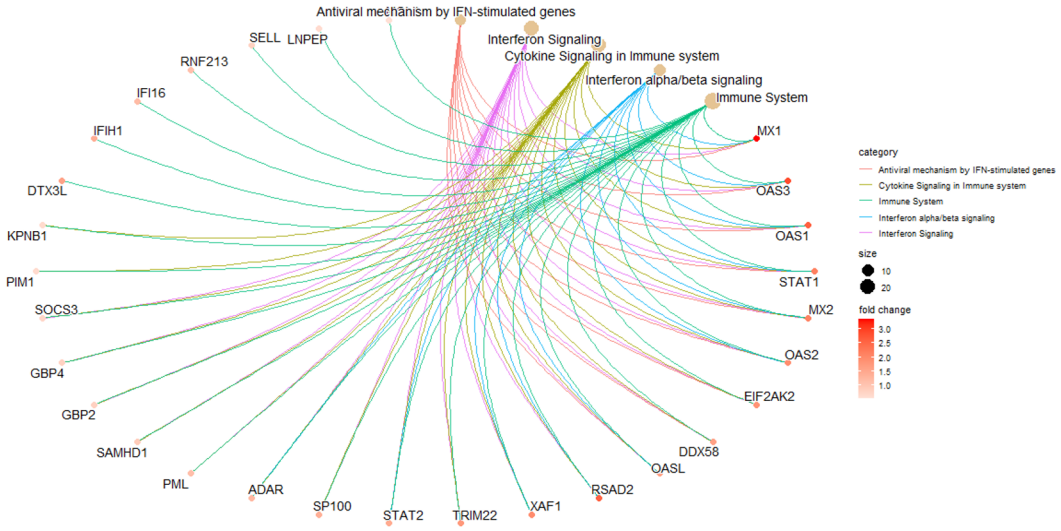

Figure 4.12.: Network analysis of gene set enriched pathways of day four of $T_{N\text{-}IFN}$ cells.

are particularly suitable candidates for further research due to their privileged key role. The genes are ordered clockwise in Figure 4.12 according to their connectivity and thus their relevance in the context of hub gene identification.

4.2.6. Activated T cells - trajectories and DEGs

Clusters t0 (T_{Akt}), t3 (T_{EM}), and t4 (T_N) were analyzed together as these clusters are developmentally connected. T_{Akt} are virtually absent at day zero but develop during the up-dosing phase. On the one hand, it can be assumed that there is *de novo* activation of T_N cells, which are present at day zero but gone at day four, on the other hand, re-activation of T_{EM} cells by re-exposure to antigen and a resulting shift towards T_{Akt} cells can be expected. Accordingly, the cells of the T_{Akt} cluster at the time points after the up-dosing phase are recruited

from clusters t3 and t4. Thus, the time points d0c of T_{Akt}, T_{EM} and T_N cells were chosen as a baseline and compared with the time points d4c and d14c of the T_{Akt} cells. Figure 4.13a shows the evolution of the clusters just mentioned.

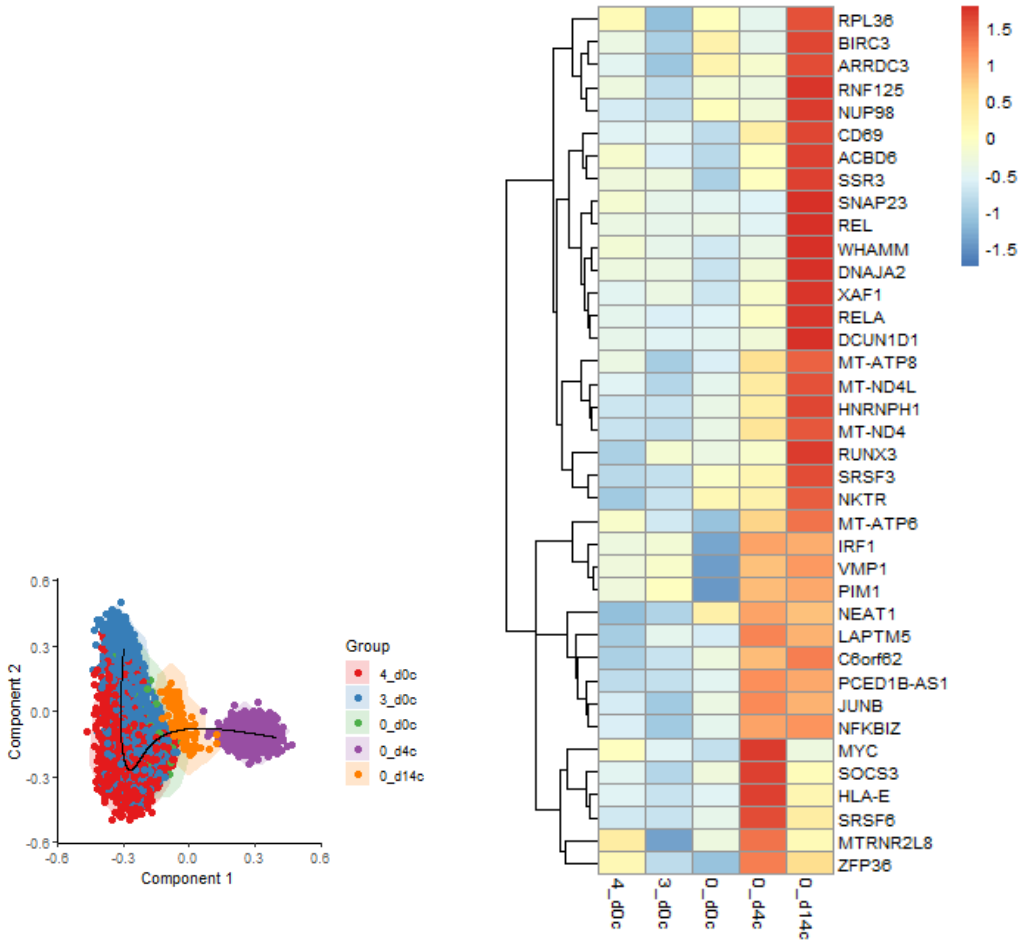

(a) (b)

Figure 4.13.: (a) PCA of progression of development of T_N, T_{EM}, and T_{Akt} cell clusters. The trajectory is indicated as solid black line. d0c, red, blue and green; d4c, purple; d14c, yellow. (b) Heatmap of the top 20 DEGs of T_{Akt} as based on T_N and T_{EM} cells.

The three clusters of the baseline show fewer differences among each other than the two post up-dosing clusters of the T_{Akt} to the reference before the

up-dosing phase. Two weeks without antigen exposure leads to a realignment of the transcriptional profiles to the baseline. The DEG of the post up-dosing time points of T_{Akt} cells were also related to the artificial baseline (Figure 4.13b). A variety of DEG, including IRF1, CD69, REL, RELA, SOCS3, and NFKBIZ, were identified as time-dependent markers.

4.2.7. Regulatory T cells - trajectories, pathway analyses and DEGs

As the last T cell cluster, T_{reg} cells were examined in more detail. Figure 4.14a shows the effect of therapy on T_{reg} cells. Again, the main transcriptomic shift happens between baseline and day four. After two weeks post up-dosing, most of the effects on the transcriptional level of T_{reg}s have disappeared. However, due to the low T_{reg} cell numbers for d14c, these results should be handled with caution. For the same reason, no top DEGs were determined for the time point two weeks post up-dosing. Nevertheless, the time point was included for completeness in Figure 4.14b. Again, interesting time-dependent changes in the transcriptome can be described. For example, the increased expression of CD25 (IL2RA), MX1, or IRF1 at day four. Figure 4.15 gives barplot diagrams of the gene set enrichment analysis (GSEA) for the more relevant cytokine candidates in the context of venom allergy immunotherapy. It is striking that the bulk of cytokine signaling pathways were less expressed in T_{reg} cells two weeks after the end of

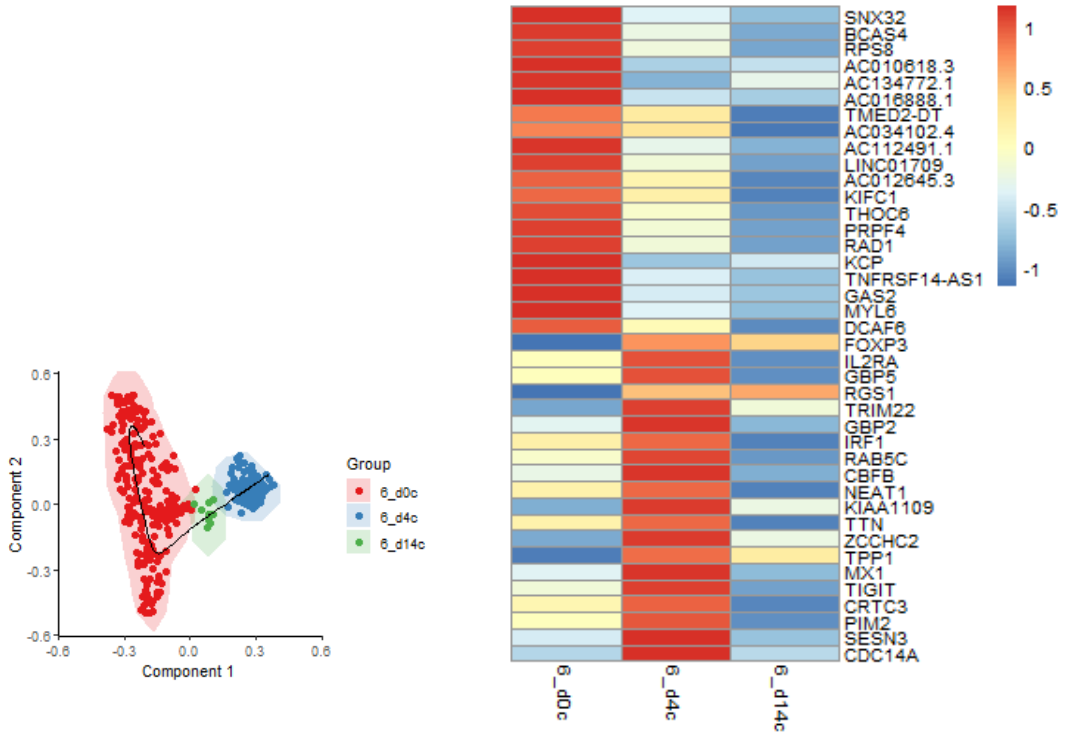

(a) (b)

Figure 4.14.: (a) PCA of progression of development of T_{reg} cell cluster. The trajectory is indicated as solid black line. d0c, red; d4c, blue; d14c, green. (b) Heatmap of the top 20 DEGs of T_{reg} cells for the time points pre and post up-dosing.

the up-dosing phase, while there seems to be none or close to no difference from baseline to day four. The IL33 signaling pathway has to be addressed separately, as the expression is on its low on day zero, remarkably increased on day four, and on its way back to baseline at time point d14c. In general, it can be noted that the pathway analyses indicate that T_{reg} cells exhibit less cytokine signaling pathway expression two weeks after the end of the up-dosing phase than before the start of VIT. However, the low cell numbers might influence the analysis.

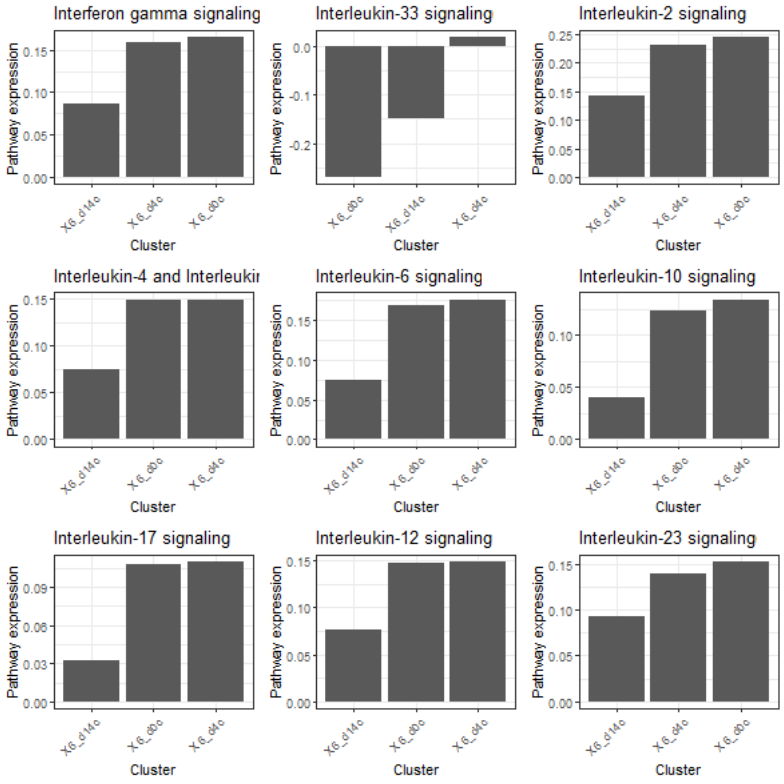

Figure 4.15.: Expression of selected signaling pathways for T_{reg} cells on days 0, 4 and 14. Order of time points is based on the level of expression.

4.2.8. Monocytes and macrophages - trajectories and DEGs

The initial cluster 5, monocytes and macrophages, shows distinct transcriptional changes during the up-dosing phase of VIT. Figure 4.16 indicates this development. There is a visible shift from day zero to day four. Day zero and day 14 after up-dosing, however, show an overlapping area. Thus, this area contains cells that exhibit a comparable transcriptome before and after the up-dosing phase. Nevertheless, not all cells return to the initial level but form a distinct, new population that differs from day four and day zero. To better understand

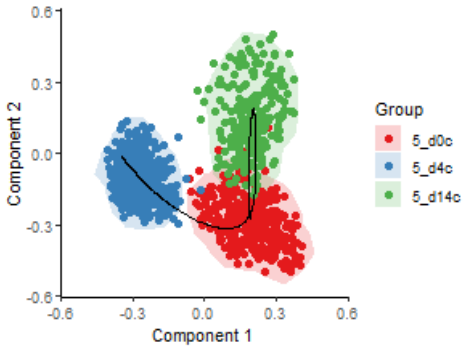

(a)

Figure 4.16.: PCA of progression of development of monocytes and macrophages on day 0, day 4 and week 2. Temporal course of VIT was used as pseudotime. The trajectory is indicated as solid black line. d0c, red; d4c, blue; d14c, green.

the transcriptional changes of M/M cells during the first two weeks of therapy, the 20 most differentially regulated genes were analyzed for each time point and summarized as a heatmap in Figure 4.17. In addition to a large number of lncRNAs, inflammation-associated genes such as - but not limited to - IKBKG, IL1B, CD300E, IFIT1, or IFI6 are also differentially expressed in a time-dependent manner.

4.2.9. Dendritic cells - trajectories and pathway analyses

Dendritic cells were examined in more detail. Figure 4.18a shows the effect of the first weeks of venom immunotherapy on DCs. There is a shift from day zero to day four, but also from day zero and day four to day 14 post up-dosing. The DCs did not return to the initial level over the 14 days without

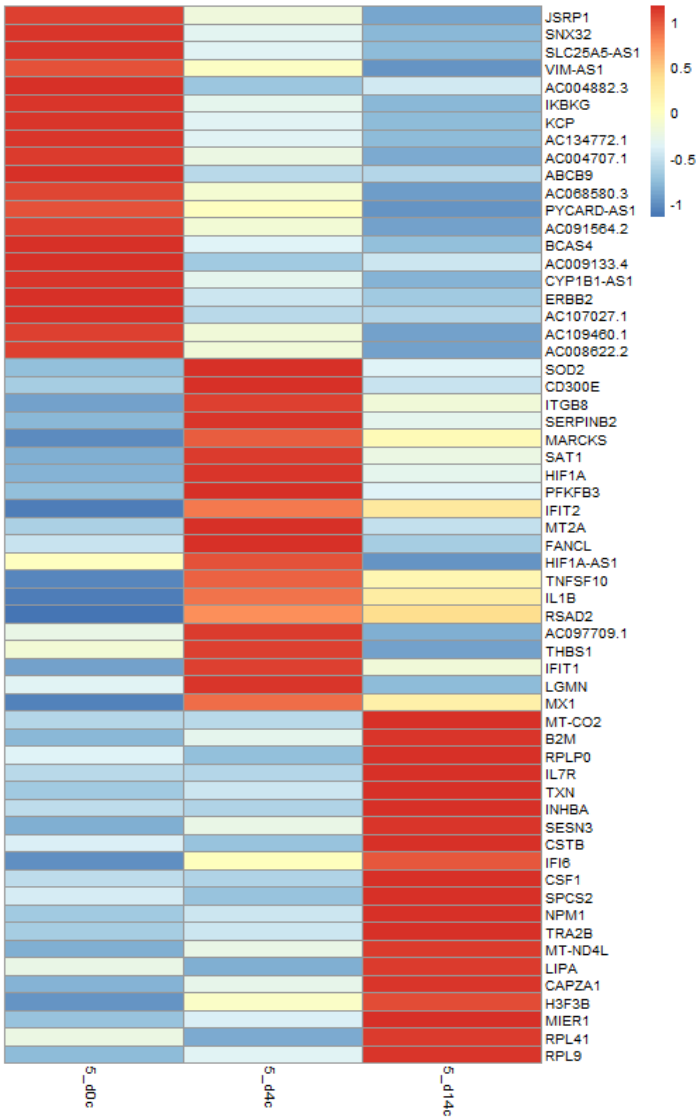

(a)

Figure 4.17.: Heatmap of the top 20 differentially expressed genes of monocytes and macrophages for each time point.

antigen exposure but further developed transcriptionally during this period. Figure 4.18b shows a selection of cytokine signaling pathways. Looking at these pathways, it can be observed that day four has a consistently increased expression. However, the scaling of the data should also be considered here

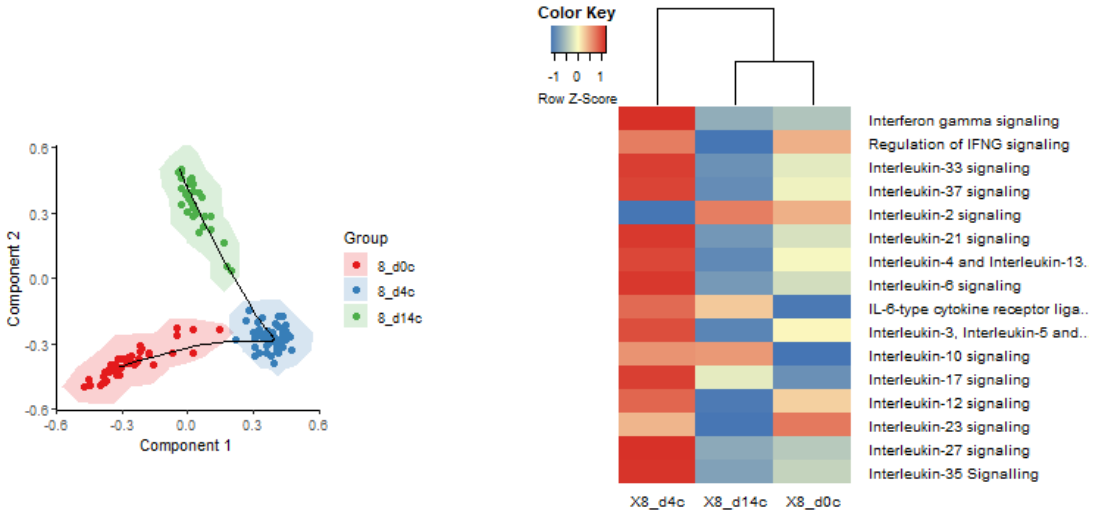

(a) (b)

Figure 4.18.: (a) PCA of progression of development of dendritic cell cluster. The trajectory is indicated as solid black line. d0c, red; d4c, blue; d14c, green. (b) Column-clustered heatmaps of pathway analysis of selected cytokines for DCs on days 0, 4 and 14.

and Figure 4.19 shows the absolute values of the GSEA for the more relevant candidates in the context of venom allergy immunotherapy. On the one hand, it is striking that the bulk of cytokine signaling pathways were more highly expressed in DCs at day four (Figure 4.18b). On the other hand, most of these differences are marginal variations from day zero and day 14. Only the IL-33 signaling pathway is remarkably upregulated at day four compared with day zero and downregulated at day 14 compared with day four (Figure 4.19). Since DCs show great differences in their transcriptional profile, which were still visible two weeks after the start of therapy, trajectory analyses were used to identify marker genes. These marker genes indicate the evolution of DCs from day zero to day four to day 14 post up-dosing and can be considered as potential

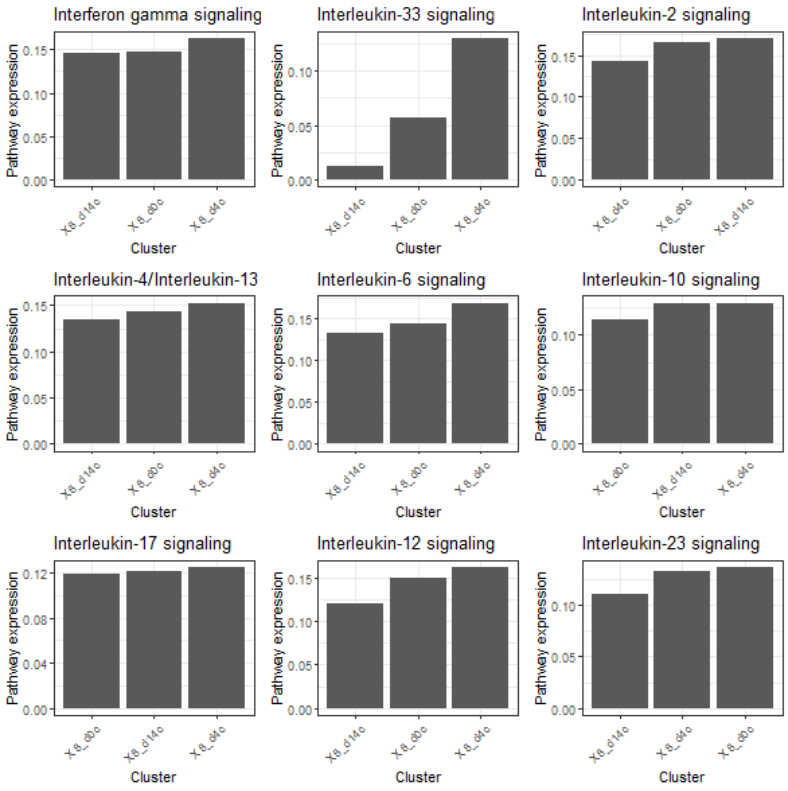

Figure 4.19.: Expression of selected signaling pathways for DCs on days 0, 4 and 14. Order of time points is based on the level of expression.

therapy markers. Thus, these are genes that are up- or down-regulated in DCs depending on the time point. Figure 4.20 shows a heatmap of differentially expressed genes during DC progression. All genes listed are possible marker genes for the course of therapy. There are generally four different scenarios:

1. A gene is up-regulated at steady-state (day zero), becomes down-regulated with the start of therapy (day four), and remains at a low level (day 14).

2. A gene is up-regulated at steady-state (day zero), is regulated to intermediate expression with the start of therapy (day four), and subsequently

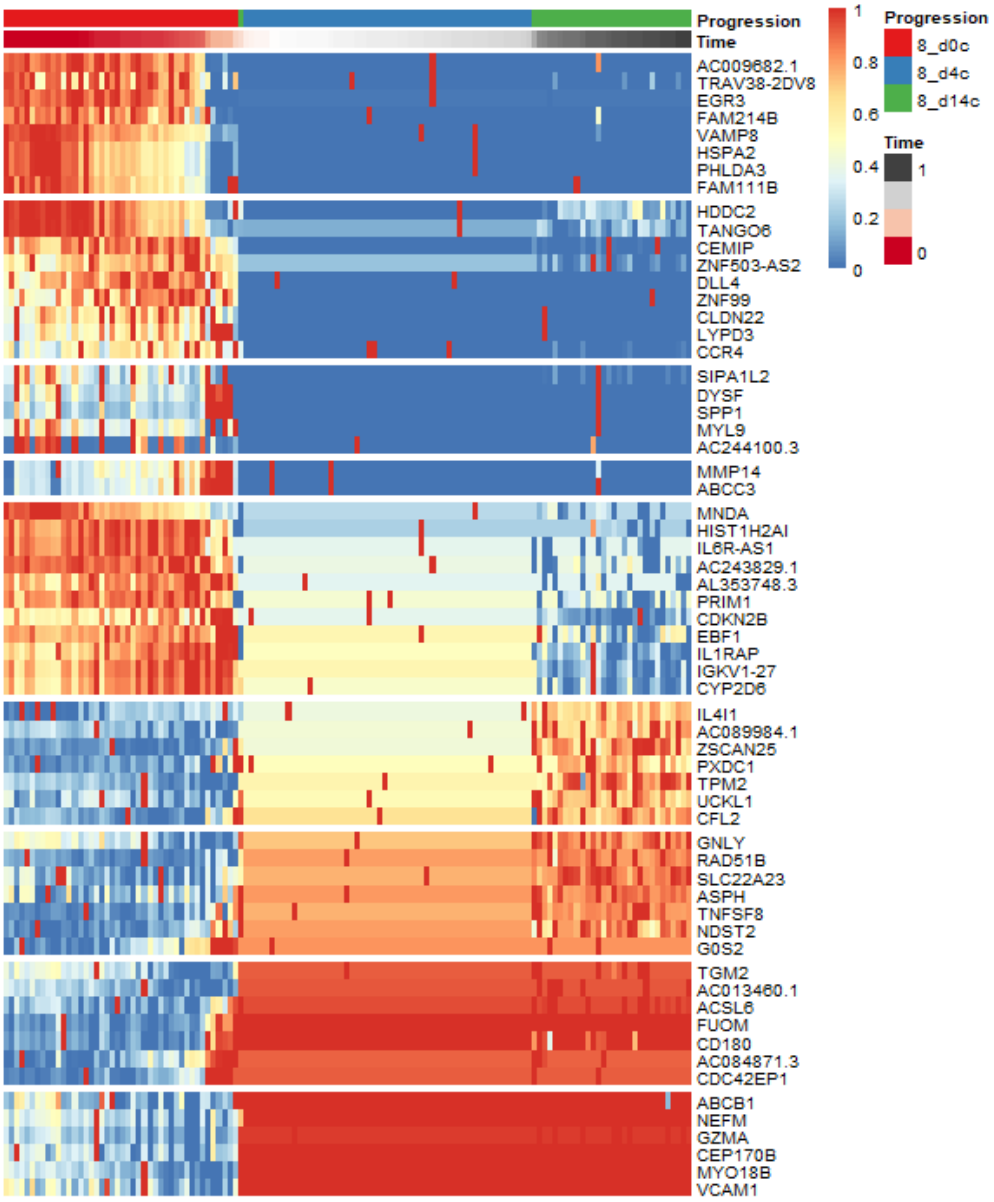

Figure 4.20.: Heatmap of the transcriptional progression of dendritic cells under immunotherapy. Only the most differentially expressed genes are shown. Temporal course of VIT was used as pseudotime. d0c, red; d4c, blue; d14c, green.

decreases further (day 14).

3. A gene is down-regulated at steady-state (day zero), is regulated to intermediate expression at the start of therapy (day four), and continues to

increase thereafter (day 14).

4. A gene is down-regulated in steady-state (day zero), becomes up-regulated with the start of therapy (day four), and remains at a higher level (day 14).

All four different possibilities can be found in Figure 4.20. Some intriguing candidates have been identified, such as IL4I1, CD180, or IL1RAP.

4.2.10. B cells - trajectories and pathway analyses

Care should be taken when analyzing the B cell data, as different populations, such as B_{reg}, naïve B cells, plasmablasts, and plasma cells, are analyzed together due to the low cell numbers. Thus, a very heterogeneous cluster is present. Figure 4.21a shows the trajectory of the B cell cluster over the already known time points. Delineated is day four, which comes up with a special transcriptional profile. Day zero and day 14 seem to be very closely intertwined. The trajectory (solid black line) is striking. The B cells appear to develop from a population in the upper left (d0c) into the demarcated day four population and then differentiate into a second population of day zero (lower left) at day 14. Presumably, activation of B cells is observed here. Since naïve and memory B cells (also to a lower degree plasmablasts and plasma cells) are already present in the cluster at day zero (whether specific or not does not matter), the day zero and day 14 clusters overlap at the bottom of day zero (likely memory B cells) (Figure 4.21a).

Figure 4.21b shows the expression of selected cytokine signaling pathways. As

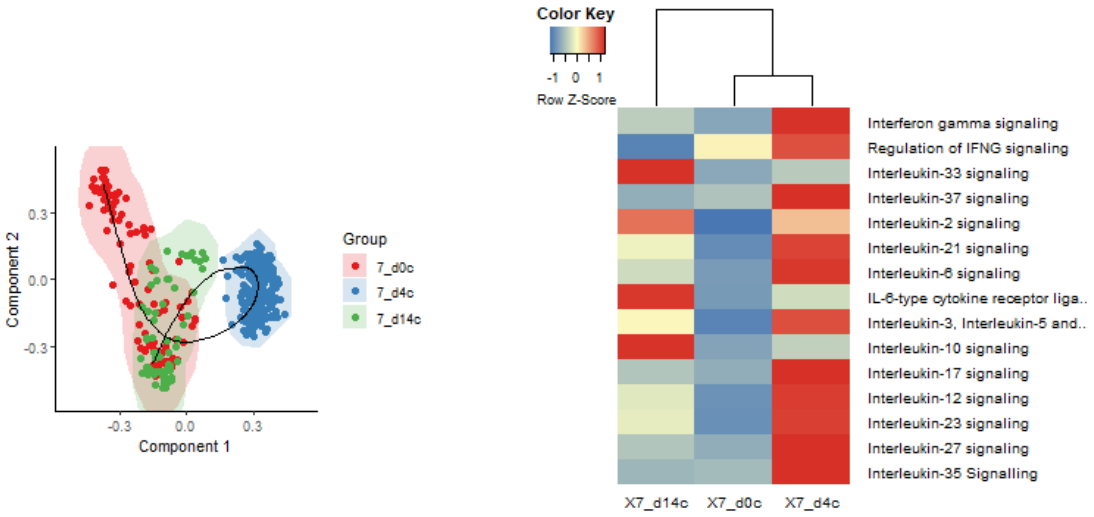

(a) (b)

Figure 4.21.: (a) PCA of progression of development of B cell cluster. The trajectory is indicated as solid black line. d0c, red; d4c, blue; d14c, green. (b) Column-clustered heatmaps of pathway analysis of selected cytokines for B cell cell cluster on days 0, 4 and 14.

indicated in Figure 4.21a, day four has a different profile than day zero and day 14. The expression of most pathways seems to be increased immediately after the up-dosing phase compared to day zero and day 14 . To make a more reliable statement beyond scaled data, individual signaling pathways were examined for calculated pathway expression (Figure 4.22). The pathways selected here generally show the picture already drawn: there is slightly increased cytokine signaling pathway expression at day four. However, the IL33 signaling pathway stands out again. There are remarkable differences in IL33 signaling, i.e. induction, in B cells two weeks after initiation of VIT. IL10 signaling is also increased after 14 days compared to baseline and immediately after the up-dosing phase.

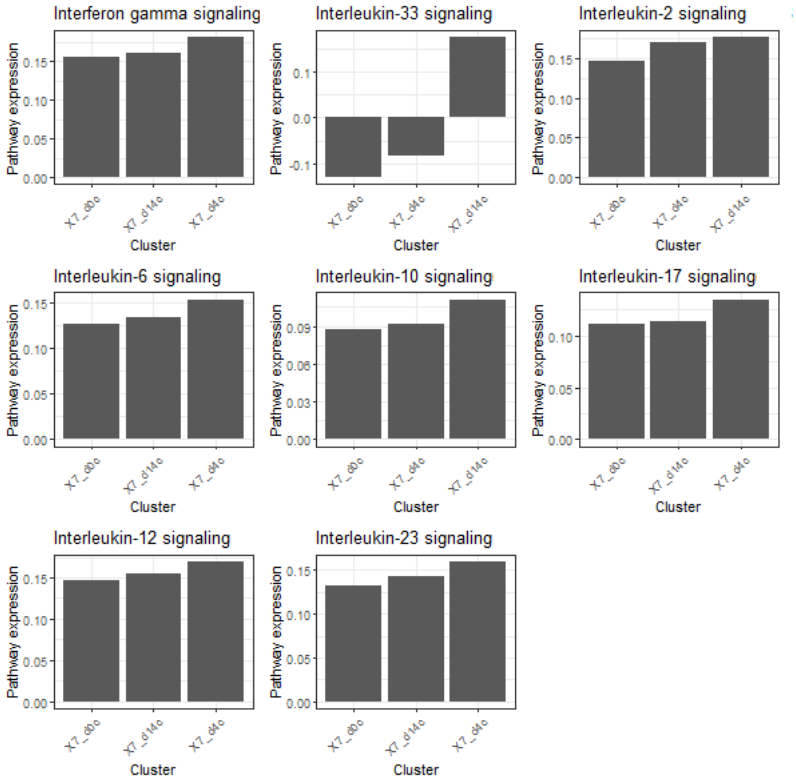

Figure 4.22.: Expression of selected signaling pathways for B cells on days 0, 4 and 14. Order of time points is based on the level of expression.

To identify possible biomarkers for the progression of VIT, the most differentially expressed genes in the B cell cluster over the course of therapy are shown in the heatmap in Figure 4.23. Due to the heterogeneity of the cluster, the expression of individual genes also varies within time points. The same four possibilities as described in chapter 4.2.9 are again applicable here. However, the classification of individual marker genes into one of the categories is somewhat complicated by said heterogeneity. Nevertheless, interesting markers, such as IDO1, were identified.

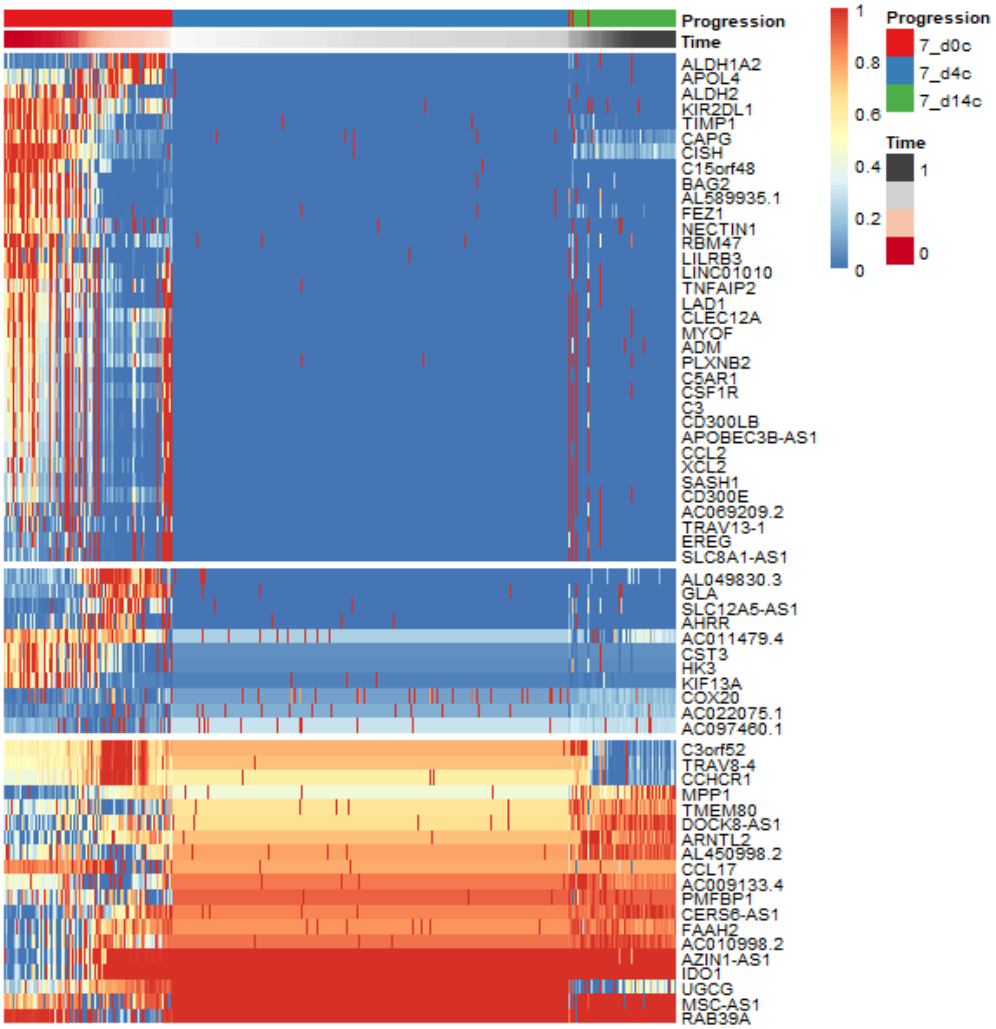

Figure 4.23.: Heatmap of the transcriptional progression of B cells under immunotherapy. Only the most differentially expressed genes are shown. Temporal course of VIT was used as pseudotime. d0c, red; d4c, blue; d14c, green.

4.3. Allergen-specific B cells

To be able to make more than just general statements about whole cell populations in the future, a further step was to label Ves v 5-specific B cells and read out the transcriptome. This would allow to monitor transcriptional changes of allergen-specific B cells. By V(D)J-enrichment, it would also be possible to

simultaneously produce allergen-specific antibodies. The generation of specific antibodies would have a wide range of therapeutic and diagnostic applications, which are not limited to the field of allergy research. This project is based on the idea of peptide tagging antigens and thus detecting the binding of the B cell receptor to the antigen [126]. Instead of directly labeling the antigen with fluorochromes [134–137], a monoclonal antibody directed against a peptide tag is DNA barcoded and the binding of the antigen to a B cell receptor is detected in a high throughput scRNAseq setup. As a model allergen Ves v 5 was chosen because it can be easily produced recombinantly in sufficient quantities and the bulk of wasp venom-allergic patients (~85%) react to it [138].

4.3.1. Experimental design

Figure 4.24 gives a first overview of the experimental course of the project. In a first step, blood was drawn from patients, and PBMCs were isolated. Subsequently, B cells were enriched and DNA barcoded. This was accomplished by incubating Ves v 5, which was recombinantly produced and carried a peptide tag, with the cells. Afterward, a monoclonal antibody (mAb) specific for the peptide tag was coupled with a DNA barcode and mAb+barcode were incubated with the Ves v 5-labeled B cells (Figure 4.25). Next, the cells were placed in an scRNAseq pipeline, which was used to read the 5' transcriptome, V(D)J gene sequences, and the additional introduced cell surface-bound DNA barcodes.

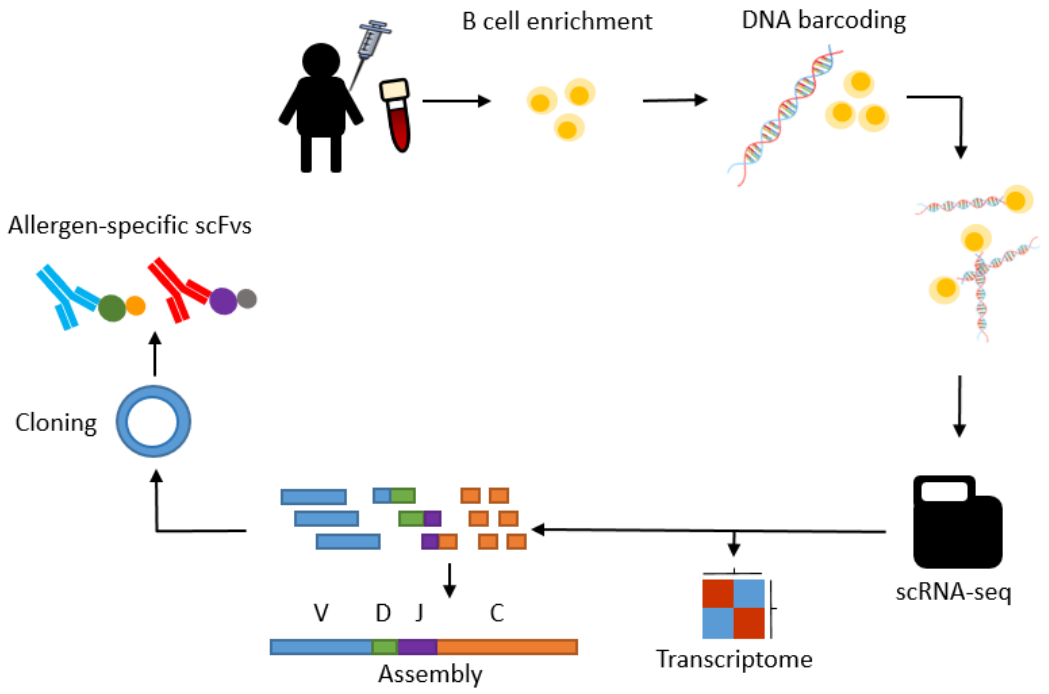

Figure 4.24.: Experimental design and workflow of tag-based transcriptomic profiling and generation of allergen-specific scFvs.

After bioinformatic assembly of the V(D)J-C sequences, scFv constructs were designed and cloned. As a final check whether the identified cells were indeed Ves v 5-specific B cells, the recombinant scFvs were tested for their binding to Ves v 5.

4.3.2. Patient recruitment

In this project, blood was drawn from a male patient with confirmed *V. vulgaris* venom allergy and sensitization to Ves v 5 six days after receiving maintenance shot. PBMCs were isolated from the blood sample. This time point was chosen to boost peripheral, Ves v 5-specific B cells [126]. This is necessary because mature

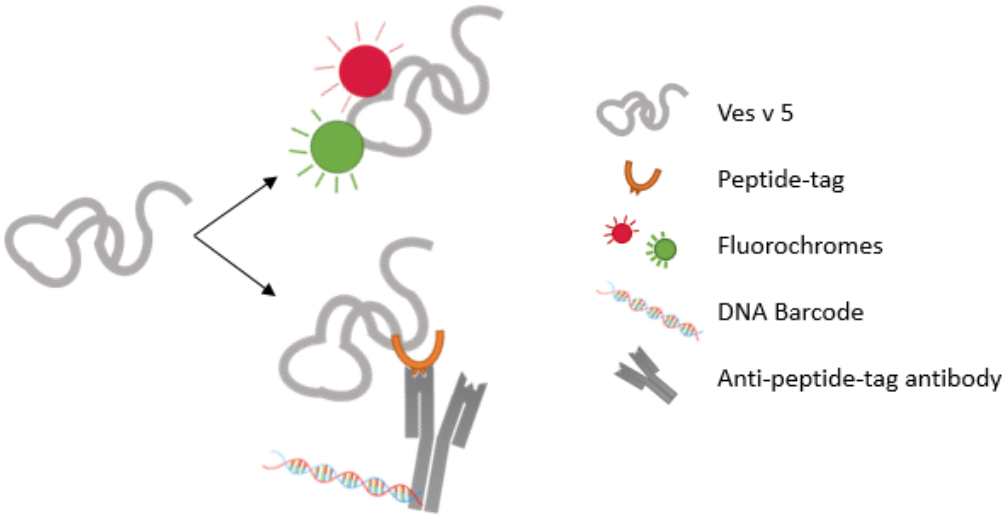

Figure 4.25.: 'Classical' (top) and tag-based (bottom) approach to label B cells in an effort to identify antigen-specific B cells. The protein is either labelled with two fluorochromes and B cells single cell sorted ('classical') or recombinantly produced carrying a peptide tag and detected via barcoded mAbs in scRNAseq.

B cells are relatively rare in peripheral blood (5-10%) and reside there primarily during migration from lymphatic centers to the site of action. The timing of six days after maintenance dose ensures that the patient has been exposed to the allergen and thus increased differentiation, proliferation, and migration behavior in B cells can be exploited.

4.3.3. Recombinant production of peptide tagged Ves v 5

Figure A.3 shows an alignment of the primary structures of the included Ves v 5 constructs. A total of four constructs were tested with different tags: Rho1D4, v5, FLAG, and Strep-tagII. All constructs also carried a His-tag for purification. The tags were separated from the actual protein by linker amino acids to create

a flexible tag region and thus prevent steric influences of the tag on the folding of the protein as well as on the binding of B cell receptors. The v5 tag is derived from the P and V protein of simian virus 5 and is 14 amino acids long [139]. It is used in some common methods, such as ELISA, Western blot, immunofluorescence, and flow cytometry. The Rho1D4 tag - nine amino acids long - originates from bovine rhodopsin and is used in e.g. Western blot, ELISA, and immunofluorescence [140]. The DYKDDDK tag - or FLAG tag - shows a dissociation constant of ~100 nM to the M1 mAb [141]. At eight amino acids, the FLAG-tag is the shortest peptide tag cloned here [142]. The Strep-tag II is based on the binding of streptavidin to biotin and is traditionally used for the physiological purification of proteins. However, other fields of application, such as ELISA, are also possible [143].

Since the v5-tagged Ves v 5 construct was already available, only the three remaining ones were cloned. The gene strands were digested and ligated with pAcGP67B vector before XL10Gold bacteria were transformed with the vector. After the expansion of the transformed bacteria under antibiotic selection, the plasmid was extracted and PCR was performed to confirm the presence of the insert. As can be seen in Figure 4.26a, the generated vectors all carry the respective insert, which leads to the prominent bands right below 1kbp. For each construct, two clones were tested. Subsequently, the inserts in the vectors were sequenced to exclude random mutations. Finally, adherent Sf9 cells

were co-transfected with vector and viral DNA to generate high-titer transgenic baculovirus for inoculation of expression cultures.

Proteins were recombinantly expressed in Sf9 cells and purified by IMAC and His-tag. Western blots were performed to test the binding of the antibody clones and to confirm the presence of peptide-tag carrying Ves v 5 (Figure 4.26b). The anti-FLAG Western blot results in a single clear band at approximately 35

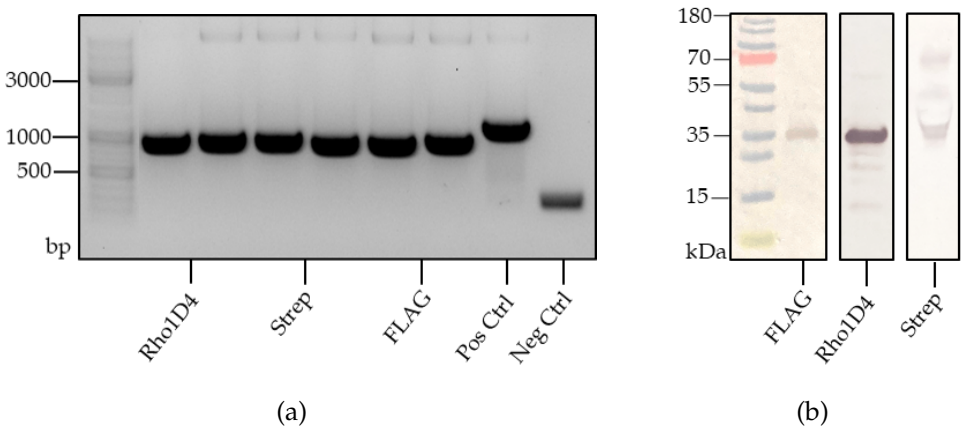

(a) (b)

Figure 4.26.: Agarose gel and Western blot of the Ves v 5 constructs. (a) Agarose gel of PCR-amplified Ves v 5 inserts in pAcGP67B vector. The marker indicates the size of the fragments in basepairs. (b) Western blots of the recombinant Ves v 5 constructs carrying FLAG, Rho1D4 or Strep-tag purified by IMAC and His-Tag.

kDa. The blots with anti-Rho1D4 antibody as well as with Extravidin-AP each show a prominent band at 35 kDa, but additional bands are discernible here. The ~35 kDa protein is Ves v 5. The additional, much weaker bands in the Rho1D4 and Strep blots are either due to multimerization (however unlikely, since the separation was performed under reducing conditions), signs of protein degradation, or indicate a partially altered running behavior due to the changed

primary structure. The possibility that the primary antibody used - as well as the Extravidin-AP - binds non-specifically, cannot be fully excluded.

4.3.4. Identification of Ves v 5-specific B cells via flow cytometry

To establish the stimulation and staining protocol for the scRNAseq experiments and to identify the most appropriate peptide tags, the setup and antibodies used were tested using flow cytometry. B cells enriched from PBMCs were incubated with the different constructs described in Figure A.3 and stained as explained in chapter 2.5.2. Figure 4.27a-d shows the percentage of tag-positive B cells in relation to live, pregated $CD3^-$, $CD19^+$ cells. The largest population

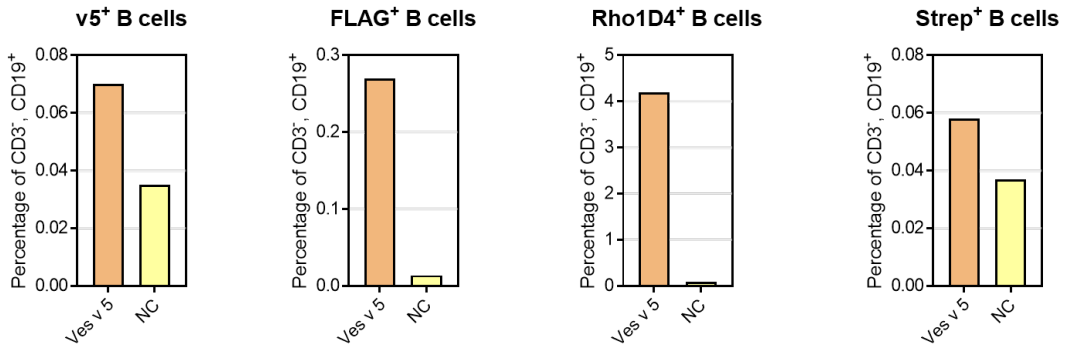

Figure 4.27.: Identification of Ves v 5-specific B cells via flow cytometry. Percentage of CD3 negative and CD19 positive cells incubated with Ves v 5 (including negative control without Ves v 5) and stained with (a) anti-v5, (b) anti-FLAG, (c) anti-Rho1D4 antibody and (d) Strep-Tactin®. NC, negative control.

(~4%) of possibly Ves v 5-specific B cells is achieved using the Rho1D4 tag. The signal-to-noise ratio (SNR, ratio of population size of Ves v 5 incubated cells

to negative control) is found to be remarkable (Figure 4.27c). A similarly good SNR is achieved with the FLAG tag, but here the total stained population is much smaller (~0.3%, Figure 4.27b). Strikingly, the stainings based on v5 or Strep-tagII have comparatively poor SNR and the populations are again lower by a magnitude (Figure 4.27a and d). Based on these results, the tags with low SNR in flow cytometry, i.e. FLAG as well as Rho1D4 tag, were selected for the following scRNAseq experiments.

4.3.5. Analysis of V(D)J- and C-genes of barcoded B cells

Once the most promising Ves v 5 constructs were selected and the protocol for using the tag-specific antibodies was established, the actual scRNAseq experiment was performed. B cells were enriched from PBMCs, incubated with FLAG- or Rho1D4-tagged Ves v 5, and then the tag-specific antibodies were added. A 5' gene expression library, a V(D)J enriched library, and a cell surface library were produced, sequenced and the data processed (Chapter 2.7).

In total, analyzable data was generated for 3555 B cells in the FLAG and 4665 B cells in the Rho1D4 approach. In the FLAG approach, 1.8% of the total cells were barcoded, corresponding to an absolute number of 64 B cells. The majority of these cells carry a BCR of the IgM isotype (89%). IgD (3.1%), IgA (1.6%), and IgG (6.3%) BCRs were detected but were present in smaller amounts. The general isotype distribution was well confirmed in the Rho1D4 approach (IgM

90%, IgD 3.1%, IgA 1.9%, and IgG 4.8%), but there are relevant deviations in the absolute amount of barcoded B cells. In total, 872 B cells carried a DNA barcode, which corresponds to about 18% of all cells. Thus, in the Rho1D4 approach, about ten times as many B cells were bound to DNA barcodes as in the FLAG approach. It is not directly obvious how this discrepancy occurs. Possibilities include underrepresentative binding of the anti-FLAG antibody to the FLAG-Ves v 5 tagged B cells or nonspecific binding of the anti-Rho1D4 antibody. In the next step, the BCRs were analyzed for clonal relatedness. This

Table 4.3.: Amount of BCR isotypes in absolute numbers and percentage of barcoded and total cells as detected by scRNAseq. DNA Barcodes were coupled to anti-FLAG- and Rho1D4 antibodies.

	FLAG$^+$			**Rho1D4$^+$**		
	Count	**[%]**	**[%] total cells**	**Count**	**[%]**	**[%] total cells**
IgM	57	89	1.6	786	90.1	16.8
IgD	2	3.1	0.06	27	3.1	0.58
IgA	1	1.6	0.03	17	1.9	0.36
IgG	4	6.3	0.11	42	4.8	0.9
Total	64		1.8	872		18.64

was made possible by comparing the amino acid sequences of the CDR3 of each BCR, with the CDR3 of all other BCRs. The randomly generated and highly variable CDR3 are most affected by SHM during affinity maturation of B cells. Thus, if two B cells have very similar CDR3 (sequence similarity >70%), a clonal relatedness is probable. Clonal relatedness would allow preselection of BCRs to be tested for their binding to Ves v 5. Since the patient was exposed to the

maintenance dose of wasp venom one week before sampling, extensive clonal relatedness of B cells in the periphery should be related to VIT. Figure 4.28a

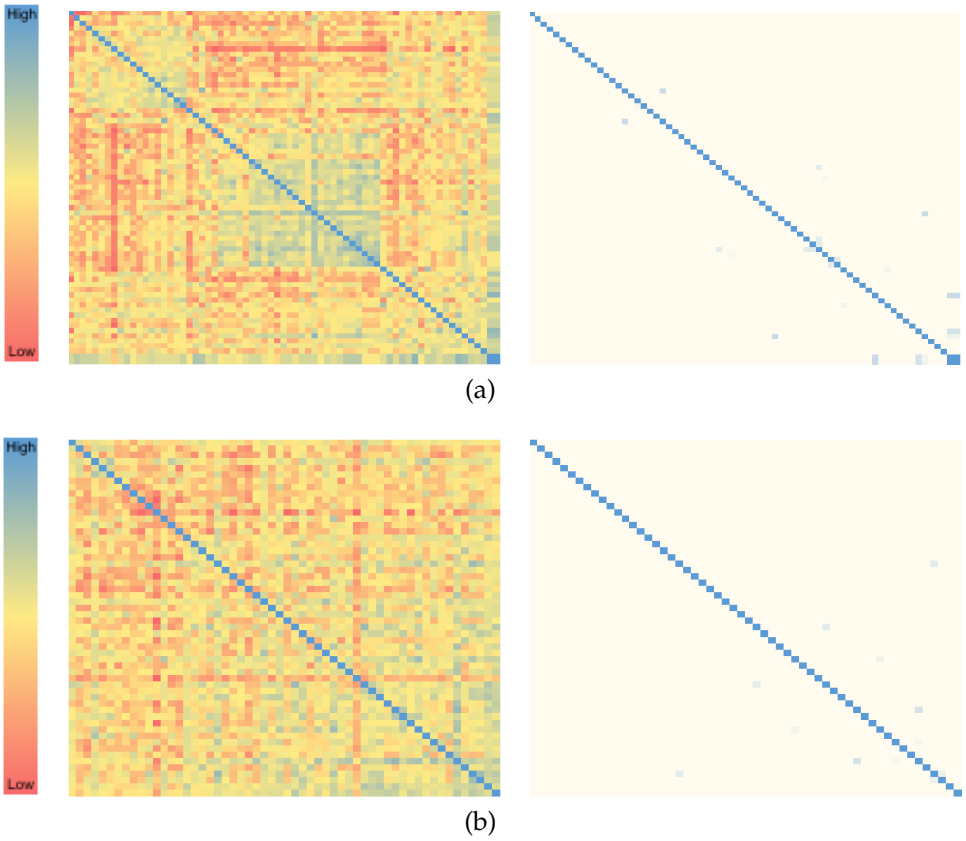

Figure 4.28.: Color coded similarity matrix of CDR3 amino acid sequences of (a) FLAG-based heavy chains of all BCR isotypes and (b) Rho1D4-based heavy chains of IgG BCRs. Each square represents the similarity of a CDR3 to the CDR3 of a different BCR (or itself: blue diagonal). Three colors scale on the left (red - yellow - blue); 2 colors scale with a cut-off of 70% (yellow - blue) at the right.

and b give color-coded similarity matrices of CDR3 amino acid sequences of FLAG-based heavy chains of all BCR isotypes (Figure 4.28a) and Rho1D4-based heavy chains of IgG BCRs (Figure 4.28b). Clonal relatedness of single or multiple B cells would show up in the matrices as blue areas around the diagonal. While in the FLAG-based approach single areas suggest clonal relatedness of isolated

cells, such areas are not present in the Rho1D4 approach. Overall, it can be said about both approaches that, if a clonal relationship is present at all, it can only be confirmed in isolated cases and to a small extent.

4.3.6. Design and recombinant production of scFvs

The sequenced V(D)J regions of the barcoded B cells were used to design and recombinantly produce scFvs. For this purpose, the 5′ UTR and the constant region were first removed. Subsequently, the gene segments were translated *in silico*, the signal sequence was truncated, and the sequence was reverse translated to nucleotides. The sequences thus obtained were combined into an scFv (Figure A.4). The constructs contain a GP64 signal sequence followed by the H-chain. The L-chain is connected to the H-chain via a flexible $(GGGGS)_3$-linker. C-terminally, two peptide tags, a FLAG-tag for identification, and a His-tag for purification, were fused. To prevent readthrough, two stop codons were cloned in series. BcuI (SpeI) and NotI restriction sites were inserted for digestion and ligation with the target vector. Transgenic baculovirus was generated and amplified. Cell culture supernatant of the virus amplifications was used to test for expression of scFvs. For this purpose, Western blots were performed with anti-FLAG antibody (Figure 4.29). In total, ten scFvs were successfully cloned and expressed. All scFv constructs lead to a band at around 35 kDa. The Rho 322 construct shows another band between 55 and 70 kDa.

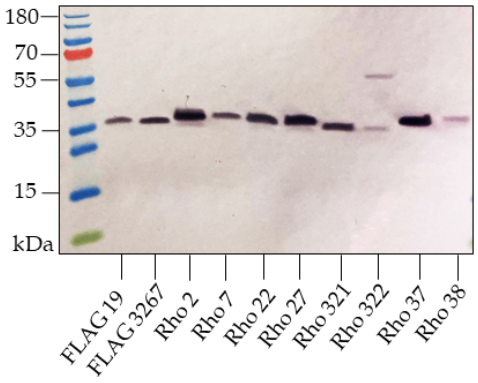

Figure 4.29.: Western blot with anti-FLAG antibody of baculovirus infected, adherent Sf9 cells expressing FLAG-carrying scFv-constructs.

4.3.7. Binding of scFvs in ELISA

After successful production of ten scFvs in Sf9 cells was confirmed by Western blot (Figure 4.29), binding of scFvs to Ves v 5 was tested. This was done by

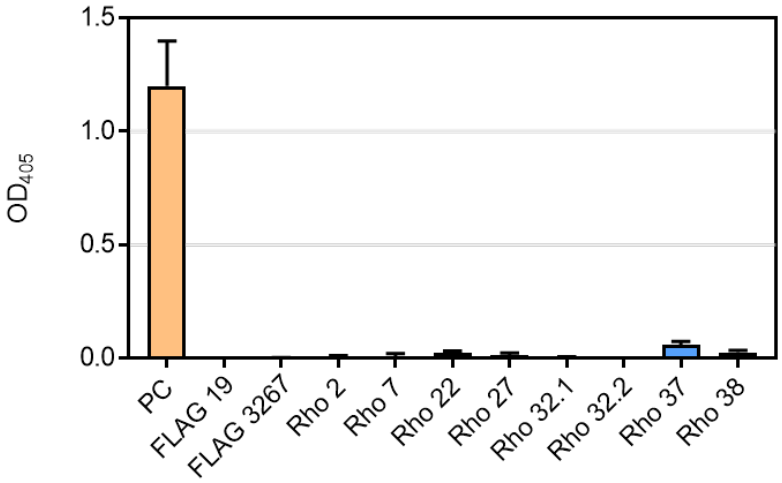

Figure 4.30.: Binding of scFvs as tested in ELISA. OD measured at 405nm. PC, positive control.

ELISA. Recombinant Ves v 5 with v5-tag was coated onto a plate and incubated with cell culture supernatant. Figure 4.30 shows the OD measured in an ELISA

at 405 nm. The data shown are exemplary for several ELISA. As a positive control, FLAG-tag carrying Ves v 5 was applied and incubated with the same primary and secondary antibodies as the scFv samples. As can be seen, no relevant signal was measured for any of the scFvs. In summary, although B cells were DNA barcoded in scRNAseq, evidence that they expressed Ves v 5-specific BCRs on the surface was not obtained.

5. Discussion

In the course of this work, the hypotheses introduced at the beginning were addressed by using biochemical, molecular biological, and bioinformatic methods. Venoms of the species *P. dominula* and *Vespula* spp. were analyzed for their protein composition. The transcriptome of peripheral immune cells from patients under YJV immunotherapy was described and an approach to identify B cells of a certain specificity was developed and tested.

The CRD success story begins with the identification of particularly relevant allergens. The growing knowledge of the composition of allergen sources through proteomic analyses has greatly facilitated the identification of interesting allergen candidates. Classical CRD requires the use of marker allergens to distinguish allergies to venoms from closely related Hymenoptera species. CRD has already been shown to provide a more reliable diagnosis of Hymenoptera venom-allergic patients [103, 144]. However, detailed proteomic data of PDV and YJV have not been available. Through mass spectrometric analysis, the proteomic composition

of the crude venoms of said three species were analyzed.

Of a total of 157 proteins identified in YJV venom, 109 were specific for *Vespula* spp. and 33 of these carried a signal peptide. Another 14 secreted proteins, including most allergens described, have homologous counterparts in PDV. PDV showed 52 unique proteins, for a total of 100 identified. Of these, eleven carried signal sequences for the extracellular space. Since most of the additional proteins identified in YJV are household contaminants, it can be assumed that the higher protein diversity is due to a lower degree of purity of the venom - e.g. due to slight differences in the extraction process. The high cross-reactivity of the already identified allergens from PDV and YJV significantly complicates the correct diagnosis of PDV and YJV. For example, antigens 5 show marked cross-reactivity and therefore cannot be used as reliable markers in CRD [145]. The same is true for PLA1 and DPP IV [86, 89, 92]. The identified hyaluronidases also show high cross-reactivity (data not shown). Species-specific marker allergens that allow a clear differentiation between PDV and YJV allergy have not been described yet. Some of the identified secreted proteins, such as PLA2 or icarapin-like protein, are promising new allergen candidates, since their homologs are known to be major allergens in other Hymenoptera venoms such as HBV [108]. PLA2, meanwhile, has already been described as an allergen by us [81]. Since the allergens from PDV and YJV show pronounced cross-reactivity, their use in classical CRD is limited. However, cross-reactive allergen pairs can be used to

measure relative sIgE levels. By using Ves v 1 and Pol d 1, as well as Ves v 5 and Pol d 5, 69% of PDV/YJV double-sensitized allergic patients could be successfully diagnosed [86]. Nevertheless, this method determines the correct venom for VIT in a majority but not all patients [146]. Additional cross-reactive allergens from PDV and YJV would add value to routine diagnostics for discrimination between true mono- and true double-sensitization. In summary, proteins could be identified in PDV and YJV that could function as marker allergens in the diagnosis of venom allergy. However, the three species studied seem to be so closely related that such a clear distinction as between HBV and YJV allergy using unique allergens is unlikely.

VIT, the only curative therapy for venom allergies, can confidently be described as a 'black box'. While many therapy mechanisms have been elucidated and described in fragments, a prospective statement about the course and the chances of success is not yet possible. This would require reliable biomarkers in the form of proteins or genes that change during the course of VIT and whose changes are primarily associated with the outcome of the therapy. Therefore, in a first step to address this issue, blood was drawn from YJV allergic patients during the up-dosing phase of their VIT to describe the change in the transcriptional profile of PBMCs. These transcriptional differences allow the rough identification of gene candidates that may be used as biomarkers. For this purpose, data were acquired using scRNAseq and, subsequently, network, trajectory, and pathway

analyses were performed and differentially expressed genes described.

The size changes of the individual clusters during the course of therapy are not easily evaluated. Especially since noticeably less cells were available for analysis of the d14c sample than at time points d0c and d4c. This difference may lead to a larger error and thus to significant variations in the relative number of cells in each cluster. However, there are three changes in the original clustering worth mentioning, which concern clusters 5 (monocytes / macrophages), cluster 7 (B cells), and cluster 8 (DCs). All three clusters remain in a similar range from day zero to day four, whereas they have grown in percentage 14 days after the end of the up-dosing phase. It is not clear whether this increase is due to a decrease in the relative proportions of naïve and / or memory T cells or is caused by expansion. Of course, it must also be taken into account that clusters 5 and 7 are particularly heterogeneous. Thus, an expansion of individual cell types within these clusters may well occur, which will transfer the effect to the whole clusters. There is e.g. no literature available that could explain the significant increase in monocytes / macrophages during the initial phase of VIT. However, the percentage increase of B cells in PBMCs after antigen exposure has been described and explained previously [126]. This is due to the activation of mature (naïve) B cells as well as long-lived memory B cells and the subsequent differentiation into short-lived antibody-producing plasmablasts, long-lived antibody-producing plasma cells, and new long-lived memory B cells

migrating in peripheral blood [24–26]. DCs, which act as antigen-presenting cells at the interface between antigen and T helper cells, are known to change their phenotype as well as abundance in PBMCs under immunotherapy [147, 148]. It has previously been shown that $CD123^+$ DCs increased one year after therapy begin, while other subtypes, such as $CD1c^+$, $CD141^+$, or $CD16^+$ DCs remain the same in frequency. The increase in $CD123^+$ DCs is accompanied by increased FcϵRI expression. FCϵRI may be involved in tolerance induction by triggering the production of IL10 in DCs, which impairs the abilities of DCs to activate T helper cells [149].

In addition to the frequency changes of the individual cell types during the first phase of VIT, some time-dependent transcriptional changes could be observed within the clusters. For example, the increased expression of CD300E in monocytes/macrophages. Myeloid cells express CD300E at their cell surface, which is known to be involved in releasing proinflammatory cytokines, sending survival signals, and initiating activation marker expression [150, 151]. However, there is also evidence that CD300E-activated monocytes express fewer HLA class II molecules at the surface, thus impairing the activation of the T helper cell response [152]. In the context of VIT, this would mean that DCs could be less efficient in eliciting the T_h2 response required for allergy. Another identified gene, IL1B, is up-regulated in monocytes after the up-dosing phase and is still above the initial expression level after two weeks. IL1B is expressed at higher

levels only after TLR stimulation of monocytes [153]. The corresponding protein, interleukin-1β (IL-1b) has a variety of functions and is involved in diverse mechanisms. For example, IL-1b leads to the differentiation of monocytes into conventional DCs or, in combination with IL23, to the enhancement of the T_h17 response [154, 155]. However, IL-1b produced by APCs also has another function: it leads to induction of T_h1 cells [156, 157]. This induction may possibly contribute to the shift of T_h2 to T_h1 cells and thus be involved in therapeutic success.

The memory T cell clusters T_{EMRA} and T_{CM} behave comparably during the first two weeks of VIT. Generally, two weeks after the end of the up-dosing phase, there are more memory T cells than at baseline. However, while T_{EMRA} increases abruptly from day zero to day four and remains relatively stable thereafter, the cluster of central memory T cells increases slowly during the first four days but then increases again. It can only be speculated why memory T cells are formed at different rates. $CD45RA^+$ re-expressing T cells show unresponsiveness to reactivation and are considered pre-senescence cells, i.e., cells that possess characteristics of an effector cell (cytokine secretion and cytotoxicity) but hardly proliferate due to senescence [131, 158]. However, this state is reversible, given the right stimulus, and proliferation is possible [159]. Since extended proliferation is unlikely due to the pre-senescence status, the cluster probably feeds from another compartment. Differentiation from the T_{EM} cluster can be treated

as likely since the period of four days is not sufficient for complete *de novo* differentiation starting from T_N cells [160]. Since this shortcut is not possible for T_{CM} cells, which recruit from early effector T cells [161], it takes the full time for T_N cells to differentiate to effector T cells and, subsequently, to T_{CM} cells. This difference in recruiting might explain the dissimilar development.

One gene that is differentially expressed in a time-dependent manner in both memory clusters is CD6. The CD6 protein is part of the early regulation of T cell activation via the binding of CD166 and CD318 and the subsequent signaling pathway [162, 163]. It has not been conclusively determined whether CD6 is involved only in negative or positive regulation or whether it can act in both directions [164–168]. However, CD6 is involved in TCR-dependent activation, thus, regardless of positive or negative regulation, it is upregulated on *V. vulgaris* venom-specific T cells and, therefore, a valuable clue to develop therapy-supporting intervention methods.

The identification of an interferon-response T cell cluster was surprising, as these tend to be associated with an anti-viral response rather than immunological changes during immunotherapy [169, 170]. However, in addition to its role as an anti-viral population, there is also debate as to whether $T_{N\text{-}IFN}$ cells are an intermediate activation state, located between resting T_N and effector T cells [127]. Both possibilities would be in line with the observation that in the steady state before the onset of VIT, hardly any cells can be assigned to this cluster, but

after four days of antigen exposure, a significant proportion can be detected. Antigen abstinence for two weeks leads to a reduction in cell numbers, again confirming its function as an intermediate activation state with or without anti-viral activity. Antigen exposure leads first to activation of T cells and second to release of interferons from cells of the innate as well as the adaptive immune system, which are then present in the (lymph node) microenvironment and may lead to transcriptional changes in T_N cells through interferon receptors. Again, interesting differences in the time-dependent transcriptional profile could be elaborated. For instance, PIM1, which is upregulated at day four compared to the other two time points, is considered a downstream effector of γc cytokine family signaling, which is elementally important as a co-stimulatory signal for T cell activation by inducing anti-apoptotic and pro-metabolic signals [171–173]. This leads to the conclusion that the interferon-response status of the cluster should indeed be considered an intermediate-activation step, as these cells appear to be more susceptible to γc family cytokines. However, due to the diversity of the associated cytokines (e.g. IL2, IL4, IL9, and IL21), no conclusion can be drawn about the direction of subsequent activation / differentiation.

Because this interferon-response status of T cells is poorly understood even independent of allergy and immunotherapy, GSEA of DEGs of $T_{N\text{-}IFN}$ cells were performed in comparison with all other T cells. This allows identification of enhanced activated pathways and thus closer characterization of this cell popu-

lation. $T_{N\text{-}IFN}$ cells have DEGs particularly in the interferon α and β signaling pathway. The MX1, OAS3, OAS1, STAT1, MX2, and OASL genes stand out for their particularly high connectivity and are identified as hub genes in this context. The MX genes encoding the MX dynamin like GTPases are involved in the defense against RNA and DNA viruses, such as influenza A viruses [174]. Similarly, the OAS genes form oligoadenylate synthetase proteins that are also involved in the antiviral response. For example, the OAS1 protein can bind cytosolic double-stranded RNA, activate RNAse L and thus degrade viral RNA [175, 176]. It is surprising that during VIT T cells take this antiviral status. Provided that the therapy products used are not contaminated with viral components, this effect has to be attributed to the venom. Certain conserved structures in venoms, the so-called venom-associated molecular patterns (VAMP), can be recognized by the (innate) immune system [177, 178]. Possibly, these VAMPs are recognized by pathogen recognition receptors and an antiviral, T_h1 program is initiated in the T cells, contributing to the shift from T_h2 to T_h1 during therapy. This would explain, in part, the unusually high success rates of VIT in contrast to other immunotherapies [66, 67].

The size changes of the T_N, T_{EM} and T_{Akt} clusters are not easy to explain. In principle, it is reasonable to think that cells from the T_N and T_{EM} clusters are (re)activated and transition to the T_{Akt} cluster. However, it is surprising that virtually all T_N and T_{EM} cells disappear during the four days of the up-dosing

phase. Generally, T cell activation is TCR dependent but only a small proportion of T_N and T_{EM} cells are specific for *V. vulgaris* venom [179, 180]. Thus, one would expect a reduction in cell numbers in T_N and T_{EM} clusters, but the magnitude at which this is observed is unusual. However, the following things should be noted: first, a shift of T_N cells is not only to be expected in the direction of T_{Akt}, but also in the direction of $T_{N\text{-}IFN}$ cells. Second, due to the long period of antigen exposure, a large proportion of naïve T cells leave the periphery by expression of homing factors and migrate to secondary lymphoid organs to be presented with antigens [179, 180]. Third, effector memory T cells migrate to the inflamed tissue or terminally differentiate to T_{EMRA} cells [159]. Fourth, there is the phenomenon of 'bystander activation', which occurs independently of the TCR. Bystander activation in naïve and memory cells was observed for $CD8^+$ as well as $CD4^+$ T cells. Generally, there are two different pathways to activate a T cell independent of its TCR. One is based on pathogen recoginition receptors, such as toll-like receptors (TLR) [181], the other is cytokine-mediated [182]. The already mentioned VAMPs, can be recognized by the immune system via, for example, TLR2 or TLR4 [177, 178]. $CD4^+$, $TLR2^+$ T cells can adopt a T_h1-like phenotype after TLR2 stimulation and produce IFNγ [183, 184]. Other studies focused on the enhanced proliferation and cytokine expression of $CD4^+$ T_h17 cells after TLR2 stimulation [185]. Cytokine-mediated TCR-independent activation of T cells occurs primarily through the cytokines IL1, IL2, IL12, IL18, IL23,

IL27, and IL33 [182]. Depending on the status of the cytokine-binding T cell, different effects can be expected. For example, naïve T cells can be bystander activated by the cytokines IL2, IL18, or IL27 [186, 187]. To carry out just one example, stimulation of naïve T cells with IL27 prevents differentiation into T_h17 cells through activation of STAT1 [188–190]. Thus, the cellular shifts are not due to a monocausal effect, but the interplay of different immunological mechanisms that together form the phenotype observed here. However, no literature can be found that would confirm these extensive changes during therapy. Furthermore, these shifts of course do not mean that all originally naïve or effector memory T cells adopt an effector state, but only that they do not retain the transcriptome of a resting T_N or T_{EM} cell.

Since T_{Akt} cells are the cluster that grows the most within the first phase of VIT, some interesting DEGs are expected here. For example, REL, the gene encoding c-Rel involved in the NF-κB-signaling pathway, is upregulated two weeks after the end of the up-dosing phase compared to days zero and four. c-Rel is an important driver of the development and maintenance of nascent T_{reg} cells [191, 192]. Similarly, the closely related RELA is instrumental in shaping the effector function of T_{reg} cells [193]. However, the NF-κB-signaling pathway is also involved in the differentiation and function of T_h1, T_h2, T_h9, and T_h17 cells, and the conclusion that increased REL and RELA expression is only linked to T_{reg} induction would be presumptuous [194–196]. Another interesting observation is

the upregulation of SOCS3, the suppressor of cytokine signaling-3, at day four after the onset of VIT. As its name implies, SOCS3 is involved in the regulation of cytokine signaling, particularly the γc cytokine family. Increased expression of SOCS3 in T cells is associated with an enhanced T_h2 and an attenuated T_h1 response [197–199]. This is an indication that VIT does not abolish the T_h2 response within the four days of the up-dosing phase or that there is no *de novo* differentiation toward the T_h2 compartment. Thus, the early-onset tolerance to allergens after the up-dosing phase is probably not yet related to a suppressed T_h2 response, but is due to other, still unknown, factors [60, 61].

It is, however, known that the number of T_{reg} cells increases during the course of immunotherapy and many of the therapeutic effects can be attributed to this increase and the associated amplified regulation of the T_h2 immune response [200–202]. However, the bulk of the studies refer to long-term effects of immunotherapy. The decrease in T_{reg} cells after four days of antigen exposure and two weeks after the end of the up-dosing phase is in line with the results of Zissler et al. [200]. The authors of the study see an initial decrease of T_{reg} numbers with grass-pollen immunotherapy during the up-dosing phase and an increase only after several weeks of continuous therapy (no exact time in relation to the beginning of therapy is given). However, the comparatively low cell counts in the d14c sample must also be taken into account, which could easily falsify the result. An interesting finding on transcriptomic level is certainly the increased

IL33-pathway expression from d0c to d4c. IL33 is produced by a variety of cells and is commonly considered to be a T_h2-inducing alarmin [7, 203]. After binding to its receptor (ST2/IL1RAP), it leads to increased production of type 2 cytokines, which in turn fuel the inflammatory reaction and shape the allergic immune response [204–206]. IL33 is an elementary building block during the sensitization process. In mouse models, allergic sensitization can be prevented if soluble ST2 is applied simultaneously [207]. Interestingly, in a phase 2a study, a single dose of anti-IL33 antibody led to an increased tolerance to peanut food challenge in peanut-allergic patients, indicating the crucial role IL33 plays not only during sensitization but also after inducing an allergic reaction [208]. In the context of T regulatory cells, IL33 and increased expression of ST2 are associated with activation and increased migrating T_{reg} cells. IL33 not only inhibited IL17 production in T_{reg} cells but also negatively influenced differentiation in T_h17 direction [209]. In addition, IL33 also affects the stability and suppressive efficacy of T_{reg} cells [210]. Also of interest is the up-regulation of IL2RA after the up-dosing phase. T_{reg} cells can already take up and process small amounts of IL2 from the environment due to the high expression of CD25 (IL2RA) at the surface, which positively influences proliferation, differentiation, and function of T_{reg} cells [211, 212]. Since IL2 in larger amounts also has pro-proliferative effects on effector T cells, for the regulation of an immune response, the expression of IL2 is not increased, but that of its receptor CD25. This increases the sensitivity

of the T_{reg} population to IL2, thus ensuring the specific effect of IL2 on T_{reg} cells without affecting effector T cells. The upregulation of IL2RA after the up-dosing phase is indicative of increased IL2 sensitivity in T_{reg} cells, therefore, allowing a more efficient regulatory response to antigen exposure.

However, the statements made in this project should be treated with some caution for methodological reasons. First, the low cell count in the sample two weeks after the end of the up-dosing phase may influence the results. Second, scRNAseq datasets can be analyzed in different ways, which may affect the general conclusions. In the course of this work, the focus was on integrated data sets. Here, multiple scRNAseq datasets are combined based on anchor points of common cell states. This allows the identification of similarities between samples even if they were obtained from different individuals, experimental conditions, species, etc. However, this forced, joint analysis of data can result in some loss of information. The alternative, separate processing of the data sets and clustering specific for each time point, was performed for verification (data not shown), but no relevant differences were identified. Third, the resolution for identifying the clusters was intentionally set relatively low in order to be able to answer the broad question clearly and within an appropriate framework. However, the reality is much more complex and must be mapped more precisely, depending on the question. Although a low cluster resolution leads to a better clarity, it inevitably introduces a certain heterogeneity into the individual clusters. Thus,

for future studies, it may be necessary to consider these clusters at a higher resolution. Fourth, mRNA is subject to diverse mechanisms, such as stabilization of mRNA or prevention of translation at the ribosome by binding of antisense RNA, which affects the quantity and quality of proteins build. To confirm the identified genes as relevant, experiments at the protein level are essential. As a final remark, the hypothesis that there are transcriptional changes in the course of therapy, which have the potential to be markers, can be affirmed. In the course of this work, a multitude of different genes were identified, which could have effects on the immune system and together lead to a tolerance to allergens.

Activation of allergen-specific B cells *in vivo* by antigen exposure during VIT leads to transcriptional changes, which may turn out to be a promising target for targeted interventions during immunotherapy due to the elementary key role of antibody-producing B cells. In the course of this work, a staining procedure was developed and tested using recombinant allergen-tag fusion proteins to bind DNA barcodes to BCRs of certain specificity. Starting from isolated PBMCs, B cells were enriched, incubated with Ves v 5-tag fusion protein, and DNA barcode-carrying α-tag Ab were added. Four different tags were tested for their suitability: v5-, FLAG- and Rho1D4-tag as well as Strep-tagII. All constructs were succesfully produced and purified as recombinant proteins. In the first step, the tags were tested by Western blot. While v5- and FLAG-tag show single and distinct bands, Rho1D4-tag and Strep-tagII lead to multiple, hard to define

bands. This may be due to protein degradation or multimerization, for example. The possibility that the α-Rho1D4-tag Ab, as well as the Strep-tactin™ bind nonspecifically is also present. Next, all constructs and DNA barcode carriers were tested in flow cytometry. Strep-tagII and v5-tag each identified about 0.06-0.07% of $CD3^-$, $CD19^+$ cells as Ves v 5-specific. In the case of the FLAG tag, it was up to 0.3%, while the α-Rho1D4 Ab stained about 4% of the cells. Due to the poor SNR in $v5^+$ or $Strep^+$ B cells, these constructs and their corresponding DNA barcode carriers were deemed less suitable for use in scRNAseq. The large discrepancy in the frequency of $FLAG^+$ and $Rho1D4^+$ B cells cannot be easily explained, as there are no robust data on the frequency of Ves v 5-specific B cells in the periphery of allergic patients under immunotherapy. Accordingly, both results may be correct and following the thought, both Ves v 5 constructs were selected for final testing in scRNAseq.

The BCR isotype distribution gives the first indication of the comparability of the tags in scRNAseq. If both constructs are well suited, the frequency of the individual isotypes should be of a similar order of magnitude. However, compared to FLAG-tag, all isotypes were identified at approximately ten times the frequency by Rho1D4-tag. The difference in the frequency of $FLAG^+$ and $Rho1D4^+$ B cells was already observed in flow cytometry and was, thus, confirmed here. Color-coded matrices of CDR3 similarity of the identified, potentially Ves v 5-specific B cells were generated. This allows visual identification of clonally related B cells.

However, no extended clonal relatedness was described in either sample. Yet, this would be expected for class-switched B cells of a single specificity [135]. To confirm the specificity of the BCRs, ten scFv constructs were designed, cloned, and recombinantly expressed. All scFvs show a band at around 35 kDa in the western blot. One construct (Rho 322) shows another band of unknown origin between 55 and 70 kDa. Samples were separated under reducing conditions in SDS-PAGE, which theoretically precludes dimerization of the scFvs. There is a possibility that posttranslational modifications, such as methylation, phosphorylation, glycosylation, myristoylation, acetylation, or ubiquitination, altered the molecular weight of the recombinant protein. Moreover, since the recombinant proteins are produced in larger amounts in the baculovirus-mediated expression system and baculovirus negatively affects the metabolism of Sf9 cells, the post-translational modifications may not be incorporated into the entirety of the recombinant proteins leading to two different Rho 322 bands. The scFv constructs were tested for their binding to Ves v 5 by ELISA. For this purpose, cell culture supernatant of the scFv expressions was added to plates coated with Ves v 5 and the potential binding was tested with antibodies directed against the fused tag. For none of the scFvs, binding to Ves v 5 could be confirmed by ELISA. Since the experiment was repeated several times and both positive and negative controls worked in the expected manner, specific binding of the generated scFvs to Ves v 5 can be virtually ruled out. In principle, the production

of scFvs in insect cells using baculovirus-mediated expression system is possible and has been applied several times [213–215]. The most common problem, lack of secretion of scFvs into the cell culture supernatant [214, 216], did not occur with the scFvs produced during this work. The lack of binding to Ves v 5 may be due to different reasons. The expression system is one possible source of error. For example, Sakamoto et al. [217] report that the specificity of their scFv is dependent on expression in insect cells or *E. coli*. The design of the scFvs is another possible cause. The length of the linkers that link heavy- and light-chain is significantly involved in the binding capacity of the scFvs [218]. This is because proper assembly of the paratop regions occurs only if the linker used is long and flexible enough. The linker used has been tested for other scFvs, but may not be suitable for the correct folding of the scFvs designed in the course of this work. In addition, it is of course questionable whether the identified B cells were specific for Ves v 5 at all. The lack of clonal relationship casts doubt on this. The α-Rho1D4-tag Ab had already turned out to be possibly unspecific in the preliminary experiments, since, on the one hand, there were multiple bands in the Western blot and, on the other hand, the frequency of $CD3^-$, $CD19^+$ and $Rho1D4^+$ cells in flow cytometry was higher than in the other three samples. Yet, this is not true for the FLAG-tag, which not only produced a single, distinct band in Western blot but also had shown good SNR in flow cytometry. However, only a few $FLAG^+$ B cells from which scFvs could be designed were identified

and, therefore, only two of the total ten scFvs were based on $FLAG^+$ cells. To further address the question, different approaches should be pursued in the work to follow: first, scFvs with different linker lengths could be tested. To describe expression system-dependent changes in specificity, a second system, ideally the already established expression in *E. coli* can be added. In addition, the focus should be placed on identification by FLAG-tag, as the Rho1D4-tag is unlikely to bind specifically enough with the corresponding antibody. In short, the hypothesis posed at the beginning could neither be completely rejected nor confirmed. On the one hand, the established system of tag-based identification in flow cytometry works with low SNR for two of the four tested constructs. On the other hand, the results regarding the frequency of Ves v 5 specific-B cells differ widely depending on the tag and it was not possible to confirm the specificity of the BCRs for Ves v 5.

In conclusion, during the course of this work, the venom proteomes of relevant wasp species were elucidated and potential new allergens were identified. Transcriptional changes within peripheral immune cells, with main focus on T cell populations, of patients during the first two weeks of wasp venom immunotherapy were described and starting points for further work on therapy interventions were discovered. For example, time- and therapy-dependent regulated genes were REL, CD6, and PIM1 in T cell subpopulations or CD300E in monocytes and macrophages. Furthermore, a tag-based carrier system for staining of Ves v 5-

specific B cells was developed. However, the confirmation that the method can also be used in combination with a high-throughput scRNAseq platform was not successful. Finally, a T cell state was identified independent of the original hypotheses, whose role in venom immunotherapy has not yet been described. It is characterized by an interferon-response gene cassette, comprising antiviral genes such as MX1, MX2, OAS1, and OAS3.

A. Supplementary figures

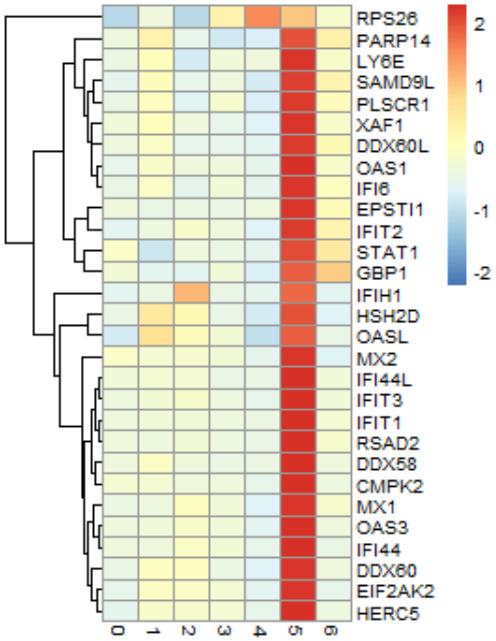

Figure A.1.: Row-clustered DEGs of $T_{N\text{-}IFN}$ cells in comparison to all other T cell clusters.

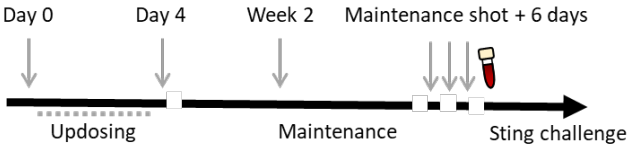

Figure A.2.: Treatment scheme for VIT and timeline for patient sampling. Blood was drawn 6 days after a maintenance shot as indicated by a blood vial.

Figure A.3.: Alignment of primary structures of peptide tagged Ves v 5 constructs. All constructs carry an N-terminal His-Tag for purification (blue). Linker amino acids are coloured green. The different peptide tags are highlighted (yellow).

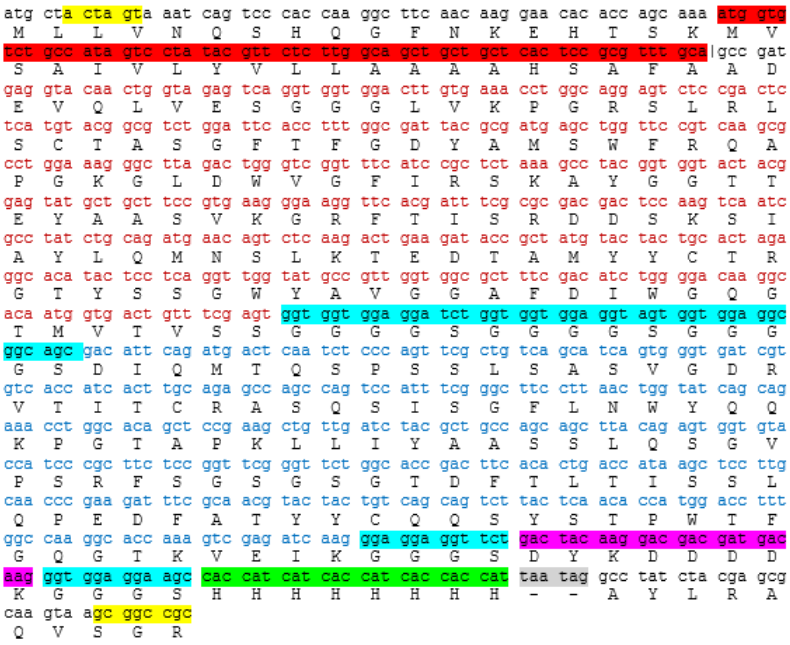

Figure A.4.: Exemplary scFv construct. Nucleotide sequence is given at the top, corresponding amino acids at the bottom of each line. Heavy chain (red text) and light chain (blue text) are joined by a $(GGGGS)_3$-linker (highlighted blue). The restriction sites are highlighted yellow, the FLAG-tag pink and the His-tag green. The double stop codon is highlighted grey.

B. Supplementary tables

Table B.1.: Identified proteins in *P. dominula* and *Vespula* spp. venom that are known allergens. From Grosch et al. [80].

Identifier	Description	Allergen
AAS67042.1	Phospholipase A1 2 precursor, partial	Pol d 1
AAS67043.1	Phospholipase A1 3 precursor, partial	Pol d 1
Q6Q249.1	Phospholipase A1 4	Pol d 1
AAS67044.1	Phospholipase A1 4 precursor, partial	Pol d 1
Q3ZU95	Phospholipase A1	Ves g 1
P49369	Phospholipase A1	Ves v 1
XP_015179722.1	Hyaluronidase	Pol d 2
P49370	Hyaluronidase A	Ves v 2.0101
Q5D7H4.1	Hyaluronidase B	Ves v 2.0201
XP_015174448.1	Dipeptidyl peptidase IV	Pol d 3/Ves v 3
ACA00159.1	Dipeptidylpeptidase IV preproprotein	Pol d 3/Ves v 3
NP_001310266.1	Venom serine protease precursor	Pol d 4
AAT95010.1	Allergen Pol d 5 precursor	Pol d 5
NP_001310265.1	Antigen 5 precursor	Pol d 5
P35784	Venom allergen 5	Ves g 5
Q05110	Venom allergen 5	Ves v 5

Table B.2.: Identified proteins in *P. dominula* and *Vespula* spp. venom that exhibit a signal peptide for transport into the extracellular matrix or have a known function in the venom. An X indicates in which species the protein was identified. The species for which the protein was originally annotated in the Hymenoptera database is given in square brackets. All *P. dominula* proteins were identified by annotated *P. dominula* proteins (identified or predicted). From Grosch et al. [80].

Identifier	Description	PDV	YJV
XP_015182550.1	60S acidic ribosomal protein P2	X	
XP_015183814.1	Acidic phospholipase A2 PA4-like isoform X1	X	
XP_015183815.1	Acidic phospholipase A2 PA4-like isoform X2 [*P. dominula*]	X	X
XP_015181576.1	Alpha-N-acetylgalactosaminidase isoform X1 [*P. dominula*]		X
XP_015181584.1	Alpha-N-acetylgalactosaminidase isoform X2 [*P. dominula*]		X
XP_015184655.1	Apolipophorins [*P. dominula*]	X	X
XP_015183810.	Apolipoprotein D-like [*P. dominula*]		X
XP_015179728.1	Cyclin-dependent kinase 8-like [*P. dominula*]		X
XP_015182852.1	Digestive cysteine proteinase 1 [*P. dominula*]		X
P0C1M6.1	Dominulin-A	X	
P0C1M7.1	Dominulin-B	X	
XP_015185362.1	FK506-binding protein 2 isoform X1 [*P. dominula*]		X
XP_015185363.1	FK506-binding protein 2 isoform X2 [*P. dominula*]		X
XP_015183963.1	Furin-like protease 1 isoform 1-CRR isoform X1 [*P. dominula*]		X
XP_015183982.1	Furin-like protease 1 isoform 1-CRR isoform X3 [*P. dominula*]		X
XP_015179268.1	Heat shock 70 kDa protein cognate 3 isoform X1 [*P. dominula*]	X	X
XP_015185877.1	Icarapin-like	X	
XP_015186100.1	Interferon-related developmental regulator 1-like [*P. dominula*]	X	
XP_015187740.1	Juvenile hormone epoxide hydrolase 1-like	X	
XP_015183311.1	Maltase 1-like [*P. dominula*]		X
P01514	Mastoparan-L [*Vespula lewisii*]		X

Continued on next page

Table B.2 – *Continued from previous page*

Identifier	Description	PDV	YJV
P0C1Q8	Mastoparan-V1 [*V. vulgaris*]		X
A0A310SDE3	Neuroblastoma suppressor of tumorigenicity 1 [*Eufriesea mexicana*]		X
XP_015173581.1	Nucleobindin-2-like isoform X1 [*P. dominula*]		X
XP_015173583.1	Nucleobindin-2-like isoform X2 [*P. dominula*]		X
XP_015173585.1	Nucleobindin-2-like isoform X3 [*P. dominula*]		X
XP_015173600.1	Peptidylglycine alpha-hydroxylating monooxygenase [*P. dominula*]		X
XP_015187119.1	Phospholipase A1-like [*P. dominula*]	X	X
XP_015190124.1	Phospholipid hydroperoxide glutathione peroxidase isoform X2 [*P. dominula*]		X
XP_015186079.1	Prosaposin isoform X1 [*P. dominula*]		X
XP_015186089.1	Prosaposin isoform X2 [*P. dominula*]		X
XP_015191732.1	Protein 5NUC-like [*P. dominula*]		X
XP_015181251.1	Protein D2-like [*P. dominula*]		X
XP_015189991.1	Protein disulfide-isomerase A3 [*P. dominula*]		X
XP_015190044.1	Protein lethal(2)essential for life-like	X	
XP_015171801.1	Renin receptor isoform X1 [*P. dominula*]		X
XP_015171802.1	Renin receptor isoform X2 [*P. dominula*]		X
XP_015171803.1	Renin receptor isoform X3 [*P. dominula*]		X
XP_015171804.1	Renin receptor isoform X4 [*P. dominula*]		X
AAP37412.1	Serine protease precursor	X	
A0A1B1JID1	Superoxide dismutase [Cu-Zn] [*A. mellifera*]		X
A0A0M9A935	Transferrin [*Melipona quadrifasciata*]		X
XP_015185020.1	Tyramine beta-hydroxylase [*P. dominula*]		X
XP_015179456.1	Uncharacterized protein LOC107067990	X	
XP_015181315.1	Uncharacterized protein LOC107068952	X	

Continued on next page

Table B.2 – *Continued from previous page*

Identifier	Description	PDV	YJV
XP_015183315.1	Uncharacterized protein LOC107070028 [*P. dominula*]		X
XP_015185303.1	Vascular endothelial growth factor C	X	
D0EY66	Venom CUB-protease [*V. vulgaris*]		X
A0A3S6I504	Vespakinin [*Parapolybia varia*]		X
P57672	Vespulakinin-1 [*Vespula maculifrons*]		X

Table B.3.: Clinical data of patients. The 8 patients included in monitoring transcriptional changes during VIT are listed at the top. Results of the *in vitro* diagnostics (ImmunoCAP) are given in CAP classes. All patients were diagnosed with *Vespula* spp. venom allergy. i.c., intradermic test; YJV, yellow jacket venom.

Age	Sex	Vespula spp. i.c. [μg/mL]	YJV (i3)	rVesv1 (i211)	rVesv5 (i209)	MUXF3 (O214)	Tryptase [μg/ml]
30	f	0.01	3	2	3	0	7.98
42	f	0.01	2	1	0	1	4.17
46	m	0.0001	2	1	0	0	6.78
32	m	0.01	3	2	0	1	9.69
61	m	0.0001	4	0	6	0	4.27
37	m	0.01	2	0	2	1	4.15
62	f	0.01	2	0	2	0	nA
28	m	nA	3	2	3	2	3.09
34	m	nA	2	0	2	0	nA

List of Figures

List of Tables

Bibliography

[1]A. Lanzavecchia, "Mechanisms of antigen uptake for presentation," Current Opinion in Immunology **8**, 348–354 (1996).

[2]R. M. Chicz, R. G. Urban, W. S. Lane, J. C. Gorga, L. J. Stern, D. A. Vignali, and J. L. Strominger, "Predominant naturally processed peptides bound to HLA-DR1 are derived from MHC-related molecules and are heterogeneous in size," Nature **358**, 764–768 (1992).

[3]E. E. Sercarz and E. Maverakis, "MHC-guided processing: Binding of large antigen fragments," Nature Reviews Immunology **3**, 621–629 (2003).

[4]M. I. Yuseff, P. Pierobon, A. Reversat, and A. M. Lennon-Duménil, "How B cells capture, process and present antigens: A crucial role for cell polarity," Nature Reviews Immunology **13**, 475–486 (2013).

[5]Z. Jinfang, "T helper 2 (Th2) cell differentiation, type 2 innate lymphoid cell (ILC2) development and regulation of interleukin-4 (IL-4) and IL-13 production," Cytokine **75**, 14–29 (2015).

[6]M. M. Fort, J. Cheung, D. Yen, J. Li, S. M. Zurawski, S. Lo, S. Menon, T. Clifford, B. Hunte, R. Lesley, T. Muchamuel, S. D. Hurst, G. Zurawski, M. W. Leach, D. M. Gorman, and D. M. Rennick, "IL-25 Induces IL-4, IL-5, and IL-13 and Th2-Associated Pathologies In Vivo," Immunity **15**, 985–995 (2001).

[7]A. S. Mirchandani, R. J. Salmond, and F. Y. Liew, "Interleukin-33 and the function of innate lymphoid cells," Trends in Immunology **33**, 389–396 (2012).

[8]M. Kopf, G. Le Grost, M. Bachmann, M. C. Lamers, H. Bluethmann, and G. Köhler, "Disruption of the murine IL-4 gene blocks Th2 cytokine responses," Nature **362**, 245–248 (1993).

[9]H. Shimoda, J. Van Deursen, M. Y. Sangster, S. R. Sarawar, R. T. Carson, R. A. Tripp, C. Chuo, F. W. Quelle, T. Nosaka, D. A. Vignali, P. C. Doherty, G. Grosveld, W. E. Paul, and J. N. Ihle, "Lack of IL-4-induced Th2 response and IgE class switching in mice with disrupted Stat6 gene," Nature **380**, 630–633 (1996).

[10]S. Romagnani, "The Thl/Th2 paradigm and allergic disorders," Allergy: European Journal of Allergy and Clinical Immunology **53**, 12–15 (1998).

[11]J. Kinet, "The high-affinity IgE receptor (FceRI): From Physiology to Pathology," Annual review of immunology **17**, 931–972 (1999).

[12]T. C. Moon, A. Dean Befus, and M. Kulka, "Mast cell mediators: Their differential release and the secretory pathways involved," Frontiers in Immunology **5**, 1–18 (2014).

[13]L. L. Reber, J. D. Hernandez, and S. J. Galli, "The pathophysiology of anaphylaxis," Journal of Allergy and Clinical Immunology **140**, 335–348 (2017).

[14]P. Mauriello, S. Barde, J. Georgitis, and R. Reisman, "Natural history of large local reactions from stinging insects," Journal of Allergy and Clinical Immunology **74**, 494–498 (1984).

[15]S. Blank, J. Grosch, M. Ollert, and M. B. Bilò, "Precision Medicine in Hymenoptera Venom Allergy: Diagnostics, Biomarkers, and Therapy of Different Endotypes and Phenotypes," Frontiers in Immunology **11**, 1–17 (2020).

[16]R. R. Hardy, C. E. Carmack, S. A. Shinton, J. D. Kemp, and K. Hayakawa, "Resolution and characterization of pro-B and pre-pro-B cell stages in normal mouse bone marrow.," Journal of Experimental Medicine **173**, 1213–1225 (1991).

[17]M. D. Cooper, "The early history of B cells," Nature Reviews Immunology **15**, 191–197 (2015).

[18]U. Fischer, J. J. Yang, T. Ikawa, D. Hein, C. Vicente-Dueñas, A. Borkhardt, and I. Sánchez-García, "Cell Fate Decisions: The Role of Transcription Factors in Early B-cell Development and Leukemia," Blood Cancer Discovery **1**, 224–233 (2020).

[19]T. H. Winkler and I. L. Martensson, "The role of the pre-b cell receptor in b cell development, repertoire selection, and tolerance," Frontiers in Immunology **9**, 1–10 (2018).

[20]F. Loder, B. Mutschler, R. J. Ray, C. J. Paige, P. Sideras, R. Torres, M. C. Lamers, and R. Carsetti, "B cell development in the spleen takes place in discrete steps and is determined by the quality of B cell receptor-derived signals," Journal of Experimental Medicine **190**, 75–89 (1999).

[21]J. B. Chung, M. Silverman, and J. G. Monroe, "Transitional B cells: Step by step towards immune competence," Trends in Immunology **24**, 342–348 (2003).

[22]T. Lopes-Carvalho and J. F. Kearney, "Development and selection of marginal zone B cells," Immunological Reviews **197**, 192–205 (2004).

[23]A. Cerutti, M. Cols, and I. Puga, "Marginal zone B cells: Virtues of innate-like antibody-producing lymphocytes," Nature Reviews Immunology **13**, 118–132 (2013).

[24]Antonio Lanzavecchia, "Antigen-specfic interaction between T and B cells," Nature **314**, 537–539 (1985).

[25]M. J. Shlomchik and F. Weisel, "Germinal center selection and the development of memory B and plasma cells," Immunological Reviews **247**, 52–63 (2012).

[26]J. S. Blum, P. A. Wearsch, and P. Cresswell, "Pathways of Antigen Processing," Annual Review of Immunology **31**, 443–473 (2013).

[27]S. Crotty, "A brief history of T cell help to B cells," Nature Reviews Immunology **15**, 185–189 (2015).

[28]D. Jung and F. W. Alt, "Unraveling V(D)J Recombination: Insights into Gene Regulation," Cell **116**, 299–311 (2004).

[29]D. B. Roth, "V(D)J Recombination: Mechanism, Errors, and Fidelity," Microbiology Spectrum **2**, edited by M. Gellert and N. Craig, 306 (2014).

[30]Z. Li, C. J. Woo, M. D. Iglesias-Ussel, D. Ronai, and M. D. Scharff, "The generation of antibody diversity through somatic hypermutation and class switch recombination," Genes and Development **18**, 1–11 (2004).

[31]V. H. Odegard and D. G. Schatz, "Targeting of somatic hypermutation," Nature Reviews Immunology **6**, 573–583 (2006).

[32]G. Teng and F. N. Papavasiliou, "Immunoglobulin somatic hypermutation," Annual Review of Genetics **41**, 107–120 (2007).

[33]O. Talay, D. Yan, H. D. Brightbill, E. E. M. Straney, M. Zhou, E. Ladi, W. P. Lee, J. G. Egen, C. D. Austin, M. Xu, and L. C. Wu, "IgE+ memory B cells and plasma cells generated through a germinal-center pathway," Nature Immunology **13**, 396–404 (2012).

[34]A. Erazo, N. Kutchukhidze, M. Leung, A. P. Christ, J. F. Urban, M. A. Curotto de Lafaille, and J. J. Lafaille, "Unique Maturation Program of the IgE Response In Vivo," Immunity **26**, 191–203 (2007).

[35]H. Xiong, J. Dolpady, M. Wabl, M. A. Curotto de Lafaille, and J. J. Lafaille, "Sequential class switching is required for the generation of high affinity IgE antibodies," Journal of Experimental Medicine **209**, 353–364 (2012).

[36]H. H. Jabara, R. Loh, N. Ramesh, D. Vercelli, and R. S. Geha, "Sequential switching from mu to epsilon via gamma 4 in human B cells stimulated with IL-4 and hydrocortisone.," Journal of immunology (Baltimore, Md. : 1950) **151**, 4528–33 (1993).

[37]L. Cameron, A. S. Gounni, S. Frenkiel, F. Lavigne, D. Vercelli, and Q. Hamid, "SϵSμ and SϵSγ Switch Circles in Human Nasal Mucosa Following Ex Vivo Allergen Challenge: Evidence for Direct as Well as Sequential Class Switch Recombination," The Journal of Immunology **171**, 3816–3822 (2003).

[38]T. J. Looney, J.-Y. Lee, K. M. Roskin, R. A. Hoh, J. King, J. Glanville, Y. Liu, T. D. Pham, C. L. Dekker, M. M. Davis, and S. D. Boyd, "Human B-cell isotype switching origins of IgE," Journal of Allergy and Clinical Immunology **137**, 579–586.e7 (2016).

[39]S. Asrat, N. Kaur, X. Liu, L. H. Ben, D. Kajimura, A. J. Murphy, M. A. Sleeman, A. Limnander, and J. M. Orengo, "Chronic allergen exposure drives accumulation of long-lived IgE plasma cells in the bone marrow, giving rise to serological memory," Science immunology **5**, 1–17 (2020).

[40]J. Tucker, R. S. Barnetson, and O. B. Eden, "Atopy after bone marrow transplantation.," BMJ **290**, 116–117 (1985).

[41]S. A. Walker, P. G. Riches, R. G. Wild, A. M. Ward, P. J. Shaw, S. Desai, and J. R. Hobbs, "Total and allergen-specific IgE in relation to allergic response pattern following bone marrow transplantation," Clinical and Experimental Immunology **66**, 633–639 (1986).

[42]J. Storek, H. Vliagoftis, A. Grizel, A. W. Lyon, A. Daly, F. Khan, T. Bowen, M. Game, L. Larratt, R. Turner, and L. Huebsch, "Allergy transfer with hematopoietic cell transplantation from an unrelated donor," Bone Marrow Transplantation **46**, 605–606 (2011).

[43]D. Charpin, J. Birnbaum, A. Lanteaume, and D. Vervloet, "Prevalence of allergy to hymenoptera stings in different samples of the general population," The Journal of Allergy and Clinical Immunology **90**, 331–334 (1992).

[44]C. Incorvaia, M. Mauro, and E. A. Pastorello, "Hymenoptera stings in conscripts," Allergy: European Journal of Allergy and Clinical Immunology **52**, 680–681 (1997).

[45]A. F. Kalyoncu, A. Uğur Demir, Ü. Özcan, C. Özkuyumcu, A. Altay Şahin, and Y. Izzettin Bariş, "Bee and wasp venom allergy in Turkey," Annals of Allergy, Asthma and Immunology **78**, 408–412 (1997).

[46]S. Blank, S. Haemmerle, T. Jaeger, D. Russkamp, J. Ring, C. B. Schmidt-Weber, and M. Ollert, "Prevalence of Hymenoptera venom allergy and sensitization in the population-representative German KORA cohort," Allergo Journal International **28**, 183–191 (2019).

[47]D. B. Golden, D. G. Marsh, A. Kagey-Sobotka, L. Freidhoff, M. Szklo, M. D. Valentine, and L. M. Lichtenstein, "Epidemiology of Insect Venom Sensitivity," JAMA: The Journal of the American Medical Association **262**, 240–244 (1989).

[48]C. Grigoreas, I. D. Galatas, C. Kiamouris, and D. Papaioannou, "Insect-venom allergy in Greek adults," Allergy: European Journal of Allergy and Clinical Immunology **52**, 51–57 (1997).

[49]J. Fernandez, M. Blanca, V. Soriano, J. Sanchez, and C. Juarez, "Epidemiological study of the prevalence of allergic reactions to Hymenoptera in a rural population in the Mediterranean area," Clinical and Experimental Allergy **29**, 1069–1074 (1999).

[50]T. Schäfer and B. Przybilla, "IgE antibodies to hymenoptera venoms in the serum are common in the general population and are related to indications of atopy," Allergy: European Journal of Allergy and Clinical Immunology **51**, 372–377 (1996).

[51]E. Novembre, A. Cianferoni, R. Bernardini, M. Veltroni, A. Ingargiola, E. Lombardi, and A. Vierucci, "Epidemiology of insect venom sensitivity in children and its correlation to clinical and atopic features," Clinical and Experimental Allergy **28**, 834–838 (1998).

[52]M. Worm, A. Moneret-Vautrin, K. Scherer, R. Lang, M. Fernandez-Rivas, V. Cardona, M. L. Kowalski, M. Jutel, I. Poziomkowska-Gesicka, N. G. Papadopoulos, K. Beyer, T. Mustakov, G. Christoff, M. B. Bilò, A. Muraro, J. O. Hourihane, and L. B. Grabenhenrich, "First European data from the network of severe allergic reactions (NORA)," Allergy: European Journal of Allergy and Clinical Immunology **69**, 1397–1404 (2014).

[53]G. J. Sturm, E. M. Varga, G. Roberts, H. Mosbech, M. B. Bilò, C. A. Akdis, D. Antolín-Amérigo, E. Cichocka-Jarosz, R. Gawlik, T. Jakob, M. Kosnik, J. Lange, E. Mingomataj, D. I. Mitsias, M. Ollert, J. N. Oude Elberink, O. Pfaar, C. Pitsios, V. Pravettoni, F. Ruëff, B. A. Sin, I. Agache, E. Angier, S. Arasi, M. A. Calderón, M. Fernandez-Rivas, S. Halken, M. Jutel, S. Lau, G. B. Pajno,

R. van Ree, D. Ryan, O. Spranger, R. G. van Wijk, S. Dhami, H. Zaman, A. Sheikh, and A. Muraro, "EAACI guidelines on allergen immunotherapy: Hymenoptera venom allergy," Allergy: European Journal of Allergy and Clinical Immunology **73**, 744–764 (2018).

[54]C. A. Akdis and M. Akdis, "Mechanisms of allergen-specific immunotherapy and immune tolerance to allergens," World Allergy Organization Journal **8**, 1–12 (2015).

[55]W. van de Veen, B. Stanic, O. F. Wirz, K. Jansen, A. Globinska, and M. Akdis, "Role of regulatory B cells in immune tolerance to allergens and beyond," Journal of Allergy and Clinical Immunology **138**, 654–665 (2016).

[56]A. Kessel, T. Haj, R. Peri, A. Snir, D. Melamed, E. Sabo, and E. Toubi, "Human CD19+CD25high B regulatory cells suppress proliferation of CD4+ T cells and enhance Foxp3 and CTLA-4 expression in T-regulatory cells," Autoimmunity Reviews **11**, 670–677 (2012).

[57]K. M. Lee, R. T. Stott, G. Zhao, J. Soohoo, W. Xiong, M. M. Lian, L. Fitzgerald, S. Shi, E. Akrawi, J. Lei, S. Deng, H. Yeh, J. F. Markmann, and J. I. Kim, "TGF-β-producing regulatory B cells induce regulatory T cells and promote transplantation tolerance," European Journal of Immunology **44**, 1728–1736 (2014).

[58]C. Möbs, H. Ipsen, L. Mayer, C. Slotosch, A. Petersen, P. A. Würtzen, M. Hertl, and W. Pfützner, "Birch pollen immunotherapy results in long-term loss of Bet v 1-specific TH2 responses, transient TR1 activation, and synthesis of IgE-blocking antibodies," Journal of Allergy and Clinical Immunology **130**, 10.1016/j.jaci.2012.07.056 (2012).

[59]F. Bonifazi, M. Jutel, B. M. Biló, J. Birnbaum, and U. Muller, "Prevention and treatment of hymenoptera venom allergy: Guidelines for clinical practice," Allergy: European Journal of Allergy and Clinical Immunology **60**, 1459–1470 (2005).

[60]A. Goldberg and R. Confino-Cohen, "Bee venom immunotherapy - How early is it effective?" Allergy: European Journal of Allergy and Clinical Immunology **65**, 391–395 (2010).

[61]A. Goldberg, A. Yogev, and R. Confino-Cohen, "Three days rush venom immunotherapy in bee allergy: Safe, inexpensive and instantaneously effective," International Archives of Allergy and Immunology **156**, 90–98 (2011).

[62]R. E. Reisman, "Duration of venom immunotherapy: Relationship to the severity of symptoms of initial insect sting anaphylaxis," The Journal of Allergy and Clinical Immunology **92**, 831–836 (1993).

[63]D. B. Golden, "Discontinuing venom immunotherapy.," Current opinion in allergy and clinical immunology **1**, 353–356 (2001).

[64]D. B. Golden, K. A. Kwiterovich, A. Kagey-Sobotka, M. D. Valentine, and L. M. Lichtenstein, "Discontinuing venom immunotherapy: Outcome after five years," Journal of Allergy and Clinical Immunology **97**, 579–587 (1996).

[65]E. Lerch and U. R. Müller, "Long-term protection after stopping venom immunotherapy: Results of re-stings in 200 patients," Journal of Allergy and Clinical Immunology **101**, 606–612 (1998).

[66]U. Müller, A. Helbling, and E. Bercthold, "Immunotherapy with honeybee venom and yellow jacket venom is different regarding efficacy and safety," Journal of Allergy and Clinical Immunology **89**, 529–535 (1992).

[67]F. Ruëff, B. Vos, J. Oude Elberink, A. Bender, R. Chatelain, S. Dugas-Breit, H. P. Horny, H. Küchenhoff, A. Linhardt, S. Mastnik, K. Sotlar, E. Stretz, R. Vollrath, B. Przybilla, and M. Flaig, "Predictors of clinical effectiveness of Hymenoptera venom immunotherapy," Clinical and Experimental Allergy **44**, 736–746 (2014).

[68]J. R. A. dos Santos Pinto, E. G. P. Fox, D. M. Saidemberg, L. D. Santos, R. Anally, S. Menegasso, E. A. Machado, and O. C. Bueno, "Proteomic View of the Venom from the Fire Ant Solenopsis invicta Buren," `10.1021/pr300451g` (2012).

[69]M. Van Vaerenbergh, G. Debyser, B. Devreese, and D. C. de Graaf, "Exploring the hidden honeybee (Apis mellifera) venom proteome by integrating a combinatorial peptide ligand library approach with FTMS," Journal of Proteomics **99**, 169–178 (2014).

[70]C. L. de Souza, J. R. A. dos Santos-Pinto, F. G. Esteves, A. Perez-Riverol, L. G. R. Fernandes, R. de Lima Zollner, and M. S. Palma, "Revisiting Polybia paulista wasp venom using shotgun proteomics – Insights into the N-linked glycosylated venom proteins," Journal of Proteomics **200**, 60–73 (2019).

[71]C. S. Hughes, S. Foehr, D. A. Garfield, E. E. Furlong, L. M. Steinmetz, and J. Krijgsveld, "Ultrasensitive proteome analysis using paramagnetic bead technology," Molecular Systems Biology **10**, 757 (2014).

[72]A. Dobin, C. A. Davis, F. Schlesinger, J. Drenkow, C. Zaleski, S. Jha, P. Batut, M. Chaisson, and T. R. Gingeras, "STAR: Ultrafast universal RNA-seq aligner," Bioinformatics **29**, 15–21 (2013).

[73]A. T. Lun, S. Riesenfeld, T. Andrews, T. P. Dao, T. Gomes, and J. C. Marioni, "Distinguishing cells from empty droplets in droplet-based single-cell RNA sequencing data," bioRxiv, 1–9 (2018).

[74]Y. Hao, S. Hao, E. Andersen-Nissen, W. M. Mauck, S. Zheng, A. Butler, M. J. Lee, A. J. Wilk, C. Darby, M. Zager, P. Hoffman, M. Stoeckius, E. Papalexi, E. P. Mimitou, J. Jain, A. Srivastava, T. Stuart, L. M. Fleming, B. Yeung, A. J. Rogers, J. M. McElrath, C. A. Blish, R. Gottardo, P. Smibert, and R. Satija, "Integrated analysis of multimodal single-cell data," Cell **184**, 3573–3587.e29 (2021).

[75]S. F. Altschul, W. Gish, W. Miller, E. W. Myers, and D. J. Lipman, "Basic local alignment search tool.," Journal of molecular biology **215**, 403–10 (1990).

[76]M. A. Larkin, G. Blackshields, N. P. Brown, R. Chenna, P. A. Mcgettigan, H. McWilliam, F. Valentin, I. M. Wallace, A. Wilm, R. Lopez, J. D. Thompson, T. J. Gibson, and D. G. Higgins, "Clustal W and Clustal X version 2.0," Bioinformatics **23**, 2947–2948 (2007).

[77]P. Jones, D. Binns, H. Y. Chang, M. Fraser, W. Li, C. McAnulla, H. McWilliam, J. Maslen, A. Mitchell, G. Nuka, S. Pesseat, A. F. Quinn, A. Sangrador-Vegas, M. Scheremetjew, S. Y. Yong, R. Lopez, and S. Hunter, "InterProScan 5: Genome-scale protein function classification," Bioinformatics **30**, 1236–1240 (2014).

[78]E. Gasteiger, C. Hoogland, A. Gattiker, S. Duvaud, M. R. Wilkins, R. D. Appel, and A. Bairoch, "Protein Identification and Analysis Tools on the ExPASy Server," The Proteomics Protocols Handbook, 571–607 (2005).

[79]J. J. Almagro Armenteros, K. D. Tsirigos, C. K. Sønderby, T. N. Petersen, O. Winther, S. Brunak, G. von Heijne, and H. Nielsen, "SignalP 5.0 improves signal peptide predictions using deep neural networks," Nature Biotechnology **37**, 420–423 (2019).

[80]J. Grosch, C. Hilger, M. B. Bilò, S. Kler, M. Schiener, G. Dittmar, F. Bernardin, A. Lesur, M. Ollert, C. B. Schmidt-Weber, and S. Blank, "Shedding Light on the Venom Proteomes of the Allergy-Relevant Hymenoptera Polistes dominula (European Paper Wasp) and Vespula spp. (Yellow Jacket)," Toxins **12**, 323 (2020).

[81]J. Grosch, B. Eberlein, S. Waldherr, M. Pascal, C. San Bartolomé, F. De La Roca Pinzón, M. Dittmar, C. Hilger, M. Ollert, T. Biedermann, U. Darsow, M. B. Bilò, C. B. Schmidt-Weber, and S. Blank, "Characterization of New Allergens from the Venom of the European Paper Wasp Polistes dominula," Toxins **13**, 559 (2021).

[82]C. Radauer, A. Nandy, F. Ferreira, R. E. Goodman, J. N. Larsen, J. Lidholm, A. Pomés, M. Raulf-Heimsoth, P. Rozynek, W. R. Thomas, and H. Breiteneder, "Update of the WHO/IUIS Allergen Nomenclature Database based on analysis of allergen sequences," Allergy: European Journal of Allergy and Clinical Immunology **69**, 413–419 (2014).

[83]T. P. King, G. Lu, M. Gonzalez, N. Qian, and L. Soldatova, "Yellow jacket venom allergens, hyaluronidase and phospholipase: Sequence similarity and antigenic cross-reactivity with their hornet and wasp homologs and possible implications for clinical allergy," Journal of Allergy and Clinical Immunology **98**, 588–600 (1996).

[84]L. D. Santos, K. S. Santos, B. M. de Souza, H. A. Arcuri, E. Cunha-Neto, F. M. Castro, J. E. Kalil, and M. S. Palma, "Purification, sequencing and structural characterization of the phospholipase A1from the venom of the social wasp Polybia paulista (Hymenoptera, Vespidae)," Toxicon **50**, 923–937 (2007).

[85]H. Yang, X. Xu, D. Ma, K. Zhang, and R. Lai, "A phospholipase A1 platelet activator from the wasp venom of Vespa magnifica (Smith)," Toxicon **51**, 289–296 (2008).

[86]R. I. Monsalve, A. Vega, L. Marqués, A. Miranda, J. Fernández, V. Soriano, S. Cruz, C. Domínguez-Noche, L. Sánchez-Morillas, M. Armisen-Gil, R. Guspí, and D. Barber, "Component-resolved diagnosis of vespid venom-allergic individuals: Phospholipases and antigen 5s are necessary to identify Vespula or Polistes sensitization," Allergy: European Journal of Allergy and Clinical Immunology **67**, 528–536 (2012).

[87]E. Habermann, "Bee and wasp venoms," Science **177**, 314–322 (1972).

[88]K. Aertgeerts, "Crystal structure of human dipeptidyl peptidase IV in complex with a decapeptide reveals details on substrate specificity and tetrahedral intermediate formation," Protein Science **13**, 412–421 (2004).

[89]S. Blank, H. Seismann, B. Bockisch, I. Braren, L. Cifuentes, M. McIntyre, D. Rühl, J. Ring, R. Bredehorst, M. W. Ollert, T. Grunwald, and E. Spillner, "Identification, Recombinant Expression, and Characterization of the 100 kDa

High Molecular Weight Hymenoptera Venom Allergens Api m 5 and Ves v 3," The Journal of Immunology **184**, 5403–5413 (2010).

[90]G. Kreil, L. Haiml, and G. Suchanek, "Stepwise Cleavage of the Pro Part of Promelittin by Dipeptidylpeptidase IV: Evidence for a New Type of Precursor—Product Conversion," European Journal of Biochemistry **111**, 49–58 (1980).

[91]V. S. Lee, W. C. Tu, T. R. Jinn, C. C. Peng, L. J. Lin, and J. T. Tzen, "Molecular cloning of the precursor polypeptide of mastoparan B and its putative processing enzyme, dipeptidyl peptidase IV, from the black-bellied hornet, Vespa basalis," Insect Molecular Biology **16**, 231–237 (2007).

[92]M. Schiener, C. Hilger, B. Eberlein, M. Pascal, A. Kuehn, D. Revets, S. Planchon, G. Pietsch, P. Serrano, C. Moreno-Aguilar, F. De La Roca, T. Biedermann, U. Darsow, C. B. Schmidt-Weber, M. Ollert, and S. Blank, "The high molecular weight dipeptidyl peptidase IV Pol d 3 is a major allergen of Polistes dominula venom," Scientific Reports **8**, 1–10 (2018).

[93]B. Pantera, D. R. Hoffman, L. Carresi, G. Cappugi, S. Turillazzi, G. Manao, M. Severino, I. Spadolini, G. Orsomando, G. Moneti, and L. Pazzagli, "Characterization of the major allergens purified from the venom of the paper wasp Polistes gallicus," Biochimica et Biophysica Acta - General Subjects **1623**, 72–81 (2003).

[94]K. M. Winningham, C. D. Fitch, M. Schmidt, and D. R. Hoffman, "Hymenoptera venom protease allergens," Journal of Allergy and Clinical Immunology **114**, 928–933 (2004).

[95]S. Vaiyapuri, S. C. Wagstaff, R. A. Harrison, J. M. Gibbins, and E. G. Hutchinson, "Evolutionary analysis of novel serine proteases in the Venom Gland transcriptome of Bitis gabonica rhinoceros," PLoS ONE **6**, `10.1371/journal.pone.0021532` (2011).

[96]G. M. Gibbs, K. Roelants, and M. K. O'Bryan, "The CAP superfamily: Cysteine-rich secretory proteins, antigen 5, and pathogenesis-related 1 proteins - Roles in reproduction, cancer, and immune defense," Endocrine Reviews **29**, 865–897 (2008).

[97]M. Nobile, V. Magnelli, L. Lagostena, J. Mochca-Morales, L. D. Possani, and G. Prestipino, "The toxin helothermine affects potassium currents in newborn rat cerebellar granule cells," The Journal of Membrane Biology **139**, 49–55 (1994).

[98]J. Morrissette, J. Krätzschmar, B. Haendler, R. El-Hayek, J. Mochca-Morales, B. M. Martin, J. R. Patel, R. L. Moss, W. D. Schleuning, and R. Coronado, "Primary structure and properties of helothermine, a peptide toxin that blocks ryanodine receptors," Biophysical Journal **68**, 2280–2288 (1995).

[99]M. Nobile, F. Noceti, G. Prestipino, and L. D. Possani, "Helothermine, a lizard venom toxin, inhibits calcium current in cerebellar granules," Experimental Brain Research **110**, 15–20 (1996).

[100]T. C. Assumpção, D. Ma, A. Schwarz, K. Reiter, Jaime M Santana, J. F. Andersen, J. M. Ribeiro, G. Nardone, L. L. Yu, and I. M. Francischetti, "Salivary antigen-5/CAP Family members are Cu2+-dependent antioxidant enzymes that scavenge O2.- and inhibit collagen-induced platelet aggregation and neutrophil oxidative burst," Journal of Biological Chemistry **288**, 14341–14361 (2013).

[101]S. Blank, Y. Michel, H. Seismann, M. Plum, K. Greunke, T. Grunwald, R. Bredehorst, M. Ollert, I. Braren, and E. Spillner, "Evaluation of Different Glycoforms of Honeybee Venom Major Allergen Phospholipase A2 (Api m 1) Produced in Insect Cells," **2**, 415–422 (2011).

[102]N. Peiren, D. C. de Graaf, M. Brunain, C. H. Bridts, D. G. Ebo, W. J. Stevens, and F. J. Jacobs, "Molecular cloning and expression of icarapin, a novel IgE-binding bee venom protein," FEBS Letters **580**, 4895–4899 (2006).

[103]S. Blank, M. B. Bilò, and M. Ollert, "Component-resolved diagnostics to direct in venom immunotherapy: Important steps towards precision medicine," Clinical and Experimental Allergy **48**, 354–364 (2018).

[104]M. Frick, S. Müller, F. Bantleon, J. Huss-Marp, J. Lidholm, E. Spillner, and T. Jakob, "RApi m 3 and rApi m 10 improve detection of honey bee sensitization in Hymenoptera venom-allergic patients with double sensitization to honey bee and yellow jacket venom," Allergy: European Journal of Allergy and Clinical Immunology **70**, 1665–1668 (2015).

[105]M. Feindor, M. D. Heath, S. J. Hewings, T. L. Carreno Velazquez, S. Blank, J. Grosch, T. Jakob, P. Schmid-Grendelmeier, L. Klimek, D. B. Golden, M. A. Skinner, and M. F. Kramer, "Venom immunotherapy: From proteins to product to patient protection," Toxins **13**, 1–17 (2021).

[106]J. B. Harris and T. Scott-Davey, "Secreted phospholipases A2 of snake venoms: Effects on the peripheral neuromuscular system with comments on the role of phospholipases A2 in disorders of the CNS and their uses in industry," Toxins **5**, 2533–2571 (2013).

[107]B. U. Atakuziev, F. Nuritova, and P. B. Usmanov, "Phospholipase A2 from the venom of the spider Eresus niger," Chemistry of Natural Compounds **27**, 487–489 (1991).

[108]J. Köhler, S. Blank, S. Müller, F. Bantleon, M. Frick, J. Huss-Marp, J. Lidholm, E. Spillner, and T. Jakob, "Component resolution reveals additional major allergens in patients with honeybee venom allergy," Journal of Allergy and Clinical Immunology **133**, 10.1016/j.jaci.2013.10.060 (2014).

[109]N. Peiren, F. Vanrobaeys, D. C. D. Graaf, B. Devreese, J. V. Beeumen, and F. J. Jacobs, "The protein composition of honeybee venom reconsidered by a proteomic approach," **1752**, 1–5 (2005).

[110]Y. Yamazaki, K. Takani, H. Atoda, and T. Morita, "Snake Venom Vascular Endothelial Growth Factors (VEGFs) Exhibit Potent Activity through Their Specific Recognition of KDR (VEGF Receptor 2)," Journal of Biological Chemistry **278**, 51985–51988 (2003).

[111]D. Russkamp, M. Van Vaerenbergh, S. Etzold, B. Eberlein, U. Darsow, M. Schiener, L. De Smet, M. Absmaier, T. Biedermann, E. Spillner, M. Ollert, T. Jakob, C. B. Schmidt-Weber, D. C. de Graaf, and S. Blank, "Characterization of the honeybee venom proteins C1q-like protein and PVF1 and their allergenic potential," Toxicon **150**, 198–206 (2018).

[112]V. Joukov, A. Kaipainen, M. Jeltsch, K. Pajusola, B. Olofsson, V. Kumar, U. Eriksson, and K. Alitalo, "Vascular Endothelial Growth Factors VEGF-B and VEGF-C," Journal of Cellular Physiology **173**, 211–215 (1997).

[113]A. Anisimov, A. Alitalo, P. Korpisalo, J. Soronen, S. Kaijalainen, V. M. Leppänen, M. Jeltsch, S. Ylä-Herttuala, and K. Alitalo, "Activated forms of VEGF-C and VEGF-D provide improved vascular function in skeletal muscle," Circulation Research **104**, 1302–1312 (2009).

[114]S. K. Jha, K. Rauniyar, T. Karpanen, V. M. Leppänen, P. Brouillard, M. Vikkula, K. Alitalo, and M. Jeltsch, "Efficient activation of the lymphangiogenic growth factor VEGF-C requires the C-terminal domain of VEGF-C and the N-terminal domain of CCBE1," Scientific Reports **7**, 1–13 (2017).

[115]V. Joukov, T. Sorsa, V. Kumar, M. Jeltsch, L. Claesson-Welsh, Y. Cao, O. Saksela, N. Kalkkinen, and K. Alitalo, "Proteolytic processing regulates receptor specificity and activity of VEGF-C," EMBO Journal **16**, 3898–3911 (1997).

[116]S. Turillazzi, G. Mastrobuoni, F. R. Dani, G. Moneti, G. Pieraccini, G. La Marca, G. Bartolucci, B. Perito, D. Lambardi, V. Cavallini, and L. Dapporto,

"Dominulin A and B: Two new antibacterial peptides identified on the cuticle and in the venom of the social paper wasp Polistes dominulus using MALDI-TOF, MALDI-TOF/TOF, and ESI-ion trap," Journal of the American Society for Mass Spectrometry **17**, 376–383 (2006).

[117]N. G. Park, Y. Yamato, S. Lee, and G. Sugihara, "Interaction of mastoparan-B from venom of a hornet in taiwan with phospholipid bilayers and its antimicrobial activity," Biopolymers **36**, 793–801 (1995).

[118]H. Yoshida, R. G. Geller, and J. J. Pisano, "Vespulakinins: New Carbohydrate-Containing Bradykinin Derivatives," Biochemistry **15**, 61–64 (1976).

[119]M. Franz and S. Mense, "Muscle receptors with group IV afferent fibres responding to application of bradykinin," Brain Research **92**, 369–383 (1975).

[120]S. B. Sindher, A. Long, S. Acharya, V. Sampath, and K. C. Nadeau, "The Use of Biomarkers to Predict Aero-Allergen and Food Immunotherapy Responses," Clinical Reviews in Allergy and Immunology **55**, 190–204 (2018).

[121]H. Breiteneder, Y. Q. Peng, I. Agache, Z. Diamant, T. Eiwegger, W. J. Fokkens, C. Traidl-Hoffmann, K. Nadeau, R. E. O'Hehir, L. O'Mahony, O. Pfaar, M. J. Torres, D. Y. Wang, L. Zhang, and C. A. Akdis, "Biomarkers for diagnosis and prediction of therapy responses in allergic diseases and asthma," Allergy: European Journal of Allergy and Clinical Immunology **75**, 3039–3068 (2020).

[122]U. M. Zissler and C. B. Schmidt-Weber, "Predicting Success of Allergen-Specific Immunotherapy," Frontiers in Immunology **11**, 1–6 (2020).

[123]C. Pitsios, "Allergen immunotherapy: Biomarkers and clinical outcome measures," Journal of Asthma and Allergy **14**, 141–148 (2021).

[124]L. Zhu, P. Yang, Y. Zhao, Z. Zhuang, Z. Wang, R. Song, J. Zhang, C. Liu, Q. Gao, Q. Xu, X. Wei, H. X. Sun, B. Ye, Y. Wu, N. Zhang, G. Lei, L. Yu, J. Yan, G. Diao, F. Meng, C. Bai, P. Mao, Y. Yu, M. Wang, Y. Yuan, Q. Deng, Z. Li, Y. Huang, G. Hu, Y. Liu, X. Wang, Z. Xu, P. Liu, Y. Bi, Y. Shi, S. Zhang, Z. Chen, J. Wang, X. Xu, G. Wu, F. S. Wang, G. F. Gao, L. Liu, and W. J. Liu, "Single-Cell Sequencing of Peripheral Mononuclear Cells Reveals Distinct Immune Response Landscapes of COVID-19 and Influenza Patients," Immunity **53**, 685–696.e3 (2020).

[125]S. Chen, L. Yang, X. Lu, B. Li, J. Y.-H. Chan, D. Cai, and Y. Li, "Gene expression profiling of CD3γ, δ, , and ζ chains in CD4 + and CD8 + T cells from human umbilical cord blood," Hematology **15**, 230–235 (2010).

[126]B. Franz, K. F. May, G. Dranoff, and K. Wucherpfennig, "Ex vivo characterization and isolation of rare memory B cells with antigen tetramers," Blood **118**, 348–357 (2011).

[127]P. A. Szabo, H. M. Levitin, M. Miron, M. E. Snyder, T. Senda, J. Yuan, Y. L. Cheng, E. C. Bush, P. Dogra, P. Thapa, D. L. Farber, and P. A. Sims, "Single-cell transcriptomics of human T cells reveals tissue and activation signatures in health and disease," Nature Communications **10**, 10.1038/s41467-019-12464-3 (2019).

[128]E. Cano-Gamez, B. Soskic, T. I. Roumeliotis, E. So, D. J. Smyth, M. Baldrighi, D. Willé, N. Nakic, J. Esparza-Gordillo, C. G. Larminie, P. G. Bronson, D. F. Tough, W. C. Rowan, J. S. Choudhary, and G. Trynka, "Single-cell transcriptomics identifies an effectorness gradient shaping the response of CD4+ T cells to cytokines," Nature Communications **11**, 1–15 (2020).

[129]F. Sallusto, D. Lenig, R. Förster, M. Lipp, and A. Lanzavecchia, "Two subsets of memory T lymphocytes with distinct homing potentials and effector functions," Nature **401**, 708–712 (1999).

[130]E. Machura, B. Mazur, W. Pieniażek, and K. Karczewska, "Expression of naive/memory (CD45RA/CD45RO) markers by peripheral blood CD4 + and CD8 + T cells in children with asthma," Archivum Immunologiae et Therapiae Experimentalis **56**, 55–62 (2008).

[131]S. R. Hall, B. M. Heffernan, N. T. Thompson, and W. C. Rowan, "CD4+CD45RA+ and CD4+CD45RO+ T cells differ in their TCR-associated signaling responses," European Journal of Immunology **29**, 2098–2106 (1999).

[132]E. Sebzda, Z. Zou, J. S. Lee, T. Wang, and M. L. Kahn, "Transcription factor KLF2 regulates the migration of naive T cells by restricting chemokine receptor expression patterns," Nature Immunology **9**, 292–300 (2008).

[133]M. A. Weinreich, K. Takada, C. Skon, S. L. Reiner, S. C. Jameson, and K. A. Hogquist, "KLF2 Transcription-Factor Deficiency in T Cells Results in Unrestrained Cytokine Production and Upregulation of Bystander Chemokine Receptors," Immunity **31**, 122–130 (2009).

[134]D. E. Starkie, J. E. Compson, S. Rapecki, and D. J. Lightwood, "Generation of recombinant monoclonal antibodies from immunised mice and rabbits via flow cytometry and sorting of antigen-specific IgG+ memory B cells," PLoS ONE **11**, 1–26 (2016).

[135]D. Croote, S. Darmanis, K. C. Nadeau, and S. R. Quake, "Antibodies Cloned From Single," Science **1309**, 1306–1309 (2018).

[136]L. Lei, K. Tran, Y. Wang, J. J. Steinhardt, Y. Xiao, C.-I. Chiang, R. T. Wyatt, and Y. Li, "Antigen-Specific Single B Cell Sorting and Monoclonal Antibody Cloning in Guinea Pigs," Frontiers in Microbiology **10**, 1–19 (2019).

[137]I. Setliff, A. R. Shiakolas, K. A. Pilewski, P. Acharya, L. Morris, and I. S. Georgiev, "High-Throughput Mapping of B Cell Receptor Sequences to Antigen Specificity Resource High-Throughput Mapping of B Cell Receptor Sequences to Antigen Specificity," Cell **179**, 1–11 (2019).

[138]M. Binder, G. Fierlbeck, T. P. King, P. Valent, and H. J. Bühring, "Individual hymenoptera venom compounds induce upregulation of the basophil activation marker ectonucleotide pyrophosphatase/phosphodiesterase 3 (CD203c) in sensitized patients," International Archives of Allergy and Immunology **129**, 160–168 (2002).

[139]T. Hanke, P. Szawlowski, and R. E. Randall, "Construction of solid matrix-antibody-antigen complexes containing simian immunodeficiency virus p27 using tag-specific monoclonal antibody and tag-linked antigen," Journal of General Virology **73**, 653–660 (1992).

[140]L. Molday and R. Molday, "1D4 – A Versatile Epitope Tag for the Purification and Characterization of Expressed Membrane and Soluble Proteins," Methods in Molecular Biology **1177**, 193–209 (2014).

[141]A. Einhauer and A. Jungbauer, "Affinity of the monoclonal antibody M1 directed against the FLAG peptide," Journal of Chromatography A **921**, 25–30 (2001).

[142]T. P. Hopp, K. S. Prickett, V. L. Price, R. T. Libby, C. J. March, D. P. Cerretti, D. L. Urdal, and P. J. Conlon, "A short polypeptide marker sequence useful for recombinant protein identification and purification," Bio/Technology **6**, 1204–1210 (1988).

[143]A. Skerra and T. G. Schmidt, "Use of the Strep-tag and streptavidin for detection and purification of recombinant proteins," Methods in Enzymology **326**, 271–304 (2000).

[144]M. B. Bilò, M. Ollert, and S. Blank, "The role of component-resolved diagnosis in Hymenoptera venom allergy," Current Opinion in Allergy and Clinical Immunology **19**, 614–622 (2019).

[145]M. Schiener, B. Eberlein, C. Moreno-Aguilar, G. Pietsch, P. Serrano, M. McIntyre, L. Schwarze, D. Russkamp, T. Biedermann, E. Spillner, U. Darsow, M. Ollert, C. B. Schmidt-Weber, and S. Blank, "Application of recombinant antigen 5 allergens from seven allergy-relevant Hymenoptera species in diagnostics," Allergy **72**, 98–108 (2017).

[146]P. A. Galindo-Bonilla, A. Galán-Nieto, T. Alfaya-Arias, C. García-Rodríguez, F. de la Roca-Pinzón, and F. Feo-Brito, "Component-resolved diagnosis in vespid venom-allergic individuals," Allergologia et Immunopathologia **43**, 398–402 (2015).

[147]N. Novak, "Targeting Dendritic Cells in Allergen Immunotherapy," Immunology and Allergy Clinics of North America **26**, 307–319 (2006).

[148]K. Lundberg, F. Rydnert, S. Broos, M. Andersson, L. Greiff, and M. Lindstedt, "Allergen-specific immunotherapy alters the frequency, as well as the FcR and CLR expression profiles of human dendritic cell subsets," PLoS ONE **11**, 1–13 (2016).

[149]N. Novak, T. Bieber, and N. Katoh, "Engagement of FcϵRI on Human Monocytes Induces the Production of IL-10 and Prevents Their Differentiation in Dendritic Cells," The Journal of Immunology **167**, 797–804 (2001).

[150]T. Brckalo, F. Calzetti, B. Pérez-Cabezas, F. E. Borràs, M. A. Cassatella, and M. López-Botet, "Functional analysis of the CD300e receptor in human monocytes and myeloid dendritic cells," European Journal of Immunology **40**, 722–732 (2010).

[151]F. Borrego, "The CD300 molecules: An emerging family of regulators of the immune system," Blood **121**, 1951–1960 (2013).

[152]S. Coletta, V. Salvi, C. Della Bella, A. Bertocco, S. Lonardi, E. Trevellin, M. Fassan, M. M. D'Elios, W. Vermi, R. Vettor, S. Cagnin, S. Sozzani, G. Codolo, and M. de Bernard, "The immune receptor CD300e negatively regulates T cell activation by impairing the STAT1-dependent antigen presentation," Scientific Reports **10**, 16501 (2020).

[153]S. H. Pulugulla, T. A. Packard, N. L. Galloway, Z. W. Grimmett, G. Doitsh, J. Adamik, D. L. Galson, W. C. Greene, and P. E. Auron, "Distinct mechanisms regulate IL1B gene transcription in lymphoid CD4 T cells and monocytes," Cytokine **111**, 373–381 (2018).

[154]C. E. Sutton, S. J. Lalor, C. M. Sweeney, C. F. Brereton, E. C. Lavelle, and K. H. Mills, "Interleukin-1 and IL-23 Induce Innate IL-17 Production from

$\gamma\delta$ T Cells, Amplifying Th17 Responses and Autoimmunity," Immunity **31**, 331–341 (2009).

[155]M. Schenk, M. Fabri, S. R. Krutzik, D. J. Lee, D. M. Vu, P. A. Sieling, D. Montoya, P. T. Liu, and R. L. Modlin, "Interleukin-1β triggers the differentiation of macrophages with enhanced capacity to present mycobacterial antigen to T cells," Immunology **141**, 174–180 (2014).

[156]S. Z. Ben-Sasson, K. Wang, J. Cohen, and W. E. Paul, "IL-1β strikingly enhances antigen-driven CD4 and CD8 T-cell responses," Cold Spring Harbor Symposia on Quantitative Biology **78**, 117–124 (2013).

[157]H. L. Hutton, J. D. Ooi, S. R. Holdsworth, and A. R. Kitching, "The NLRP3 inflammasome in kidney disease and autoimmunity," Nephrology **21**, 736–744 (2016).

[158]J. M. LaSalle and D. A. Hafler, "The coexpression of CD45RA and CD45RO isoforms on T cells during the S/G2/M stages of cell cycle," Cellular Immunology **138**, 197–206 (1991).

[159]S. M. Henson, N. E. Riddell, and A. N. Akbar, "Properties of end-stage human T cells defined by CD45RA re-expression," Current Opinion in Immunology **24**, 476–481 (2012).

[160]N. D. Pennock, J. T. White, E. W. Cross, E. E. Cheney, B. A. Tamburini, and R. M. Kedl, "T cell responses: naïve to memory and everything in between," Advances in Physiology Education **37**, 273–283 (2013).

[161]S. M. Kaech, E. J. Wherry, and R. Ahmed, "Effector and memory T-cell differentiation: Implications for vaccine development," Nature Reviews Immunology **2**, 251–262 (2002).

[162]P. E. Chappell, L. I. Garner, J. Yan, C. Metcalfe, D. Hatherley, S. Johnson, C. V. Robinson, S. M. Lea, and M. H. Brown, "Structures of CD6 and Its Ligand CD166 Give Insight into Their Interaction," Structure **23**, 1426–1436 (2015).

[163]G. Enyindah-Asonye, Y. Li, J. H. Ruth, D. S. Spassov, K. E. Hebron, A. Zijlstra, M. M. Moasser, B. Wang, N. G. Singer, H. Cui, R. A. Ohara, S. M. Rasmussen, D. A. Fox, and F. Lin, "CD318 is a ligand for CD6," Proceedings of the National Academy of Sciences of the United States of America **114**, E6912–E6921 (2017).

[164]A. W. Zimmerman, B. Joosten, R. Torensma, J. R. Parnes, F. N. Van Leeuwen, and C. G. Figdor, "Long-term engagement of CD6 and ALCAM is essential for T-cell proliferation induced by dendritic cells," Blood **107**, 3212–3220 (2006).

[165]M. I. Oliveira, C. M. Gonçalves, M. Pinto, S. Fabre, A. M. Santos, S. F. Lee, M. A. Castro, R. J. Nunes, R. R. Barbosa, J. R. Parnes, C. Yu, S. J. Davis, A. Moreira, G. Bismuth, and A. M. Carmo, "CD6 attenuates early and late signaling events, setting thresholds for T-cell activation," European Journal of Immunology **42**, 195–205 (2012).

[166]C. M. Gonçalves, S. N. Henriques, R. F. Santos, and A. M. Carmo, "CD6, a rheostat-type signalosome that tunes T cell activation," Frontiers in Immunology **9**, 1–9 (2018).

[167]M. B. Meddens, S. F. Mennens, F. B. Celikkol, J. Te Riet, J. S. Kanger, B. Joosten, J. J. Witsenburg, R. Brock, C. G. Figdor, and A. Cambi, "Biophysical characterization of CD6 - TCR/CD3 Interplay in T Cells," Frontiers in Immunology **9**, 1–15 (2018).

[168]D. Mori, C. Grégoire, G. Voisinne, J. Celis-Gutierrez, R. Aussel, L. Girard, M. Camus, M. Marcellin, J. Argenty, O. Burlet-Schiltz, F. Fiore, A. G. de Peredo, M. Malissen, R. Roncagalli, and B. Malissen, "The T cell CD6 receptor operates a multitask signalosome with opposite functions in T cell activation," Journal of Experimental Medicine **218**, `10.1084/JEM.20201011` (2021).

[169]J. W. Schoggins and C. M. Rice, "Interferon-stimulated genes and their antiviral effector functions," Current Opinion in Virology **1**, 519–525 (2011).

[170]M. B. Malterer, S. J. Glass, and J. P. Newman, "Interferon-stimulated genes: A complex web of host defenses," Annual Review of Immunology **44**, 735–745 (2014).

[171]C. J. Fox, P. S. Hammerman, and C. B. Thompson, "The Pim kinases control rapamycin-resistant T cell survival and activation," Journal of Experimental Medicine **201**, 259–266 (2005).

[172]B. A. Linowes, D. L. Ligons, A. S. Nam, C. Hong, H. R. Keller, X. Tai, M. A. Luckey, and J.-h. Park, "Pim1 permits generation and survival of CD4 + T cells in the absence of γc cytokine receptor signaling," European Journal of Immunology **43**, 2283–2294 (2013).

[173]W. J. Leonard, J. X. Lin, and J. J. O'Shea, "The γ c Family of Cytokines: Basic Biology to Therapeutic Ramifications," Immunity **50**, 832–850 (2019).

[174]K. Ciminski, G. P. Chase, M. Beer, and M. Schwemmle, "Influenza A Viruses: Understanding Human Host Determinants," Trends in Molecular Medicine **27**, 104–112 (2021).

[175]A. Mozzi, C. Pontremoli, D. Forni, M. Clerici, U. Pozzoli, N. Bresolin, R. Cagliani, and M. Sironi, "OASes and STING: Adaptive Evolution in Concert," Genome Biology and Evolution **7**, 1016–1032 (2015).

[176]V. K. Vachon, B. M. Calderon, and G. L. Conn, "A novel RNA molecular signature for activation of 2-5 oligoadenylate synthetase-1," Nucleic Acids Research **43**, 544–552 (2015).

[177]K. F. Zoccal, C. D. S. Bitencourt, F. W. G. Paula-Silva, C. A. Sorgi, K. de Castro Figueiredo Bordon, E. C. Arantes, and L. H. Faccioli, "TLR2, TLR4 and CD14 Recognize Venom-Associated Molecular Patterns from Tityus serrulatus to Induce Macrophage-Derived Inflammatory Mediators," PLoS ONE **9**, edited by P. Talamas-Rohana, e88174 (2014).

[178]V. Moreira, C. Teixeira, H. Borges da Silva, M. R. D'Império Lima, and M. C. Dos-Santos, "The role of TLR2 in the acute inflammatory response induced by Bothrops atrox snake venom," Toxicon **118**, 121–128 (2016).

[179]U. H. von Andrian and C. R. Mackay, "T-Cell Function and Migration — Two Sides of the Same Coin," New England Journal of Medicine **343**, edited by I. R. Mackay and F. S. Rosen, 1020–1034 (2000).

[180]D. Masopust and J. M. Schenkel, "The integration of T cell migration, differentiation and function," Nature Reviews Immunology **13**, 309–320 (2013).

[181]J. M. Reynolds and C. Dong, "Toll-like receptor regulation of effector T lymphocyte function," Trends in Immunology **34**, 511–519 (2013).

[182]H.-G. Lee, M.-Z. Cho, and J.-M. Choi, "Bystander CD4+ T cells: crossroads between innate and adaptive immunity," Experimental & Molecular Medicine **52**, 1255–1263 (2020).

[183]V. Sobek, N. Birkner, I. Falk, A. Würch, C. J. Kirschning, H. Wagner, R. Wallich, M. C. Lamers, and M. M. Simon, "Direct Toll-like receptor 2 mediated co-stimulation of T cells in the mouse system as a basis for chronic inflammatory joint disease.," Arthritis research & therapy **6**, `10.1186/ar1212` (2004).

[184]T. Imanishi, H. Hara, S. Suzuki, N. Suzuki, S. Akira, and T. Saito, "Cutting Edge: TLR2 Directly Triggers Th1 Effector Functions," The Journal of Immunology **178**, 6715–6719 (2007).

[185]J. M. Reynolds, B. P. Pappu, J. Peng, G. J. Martinez, Y. Zhang, Y. Chung, L. Ma, X. O. Yang, R. I. Nurieva, Q. Tian, and C. Dong, "Toll-like receptor 2 signaling in CD4+ T lymphocytes promotes T helper 17 responses and regulates the pathogenesis of autoimmune disease," Immunity **32**, 692–702 (2010).

[186]H. Chakir, D. K. Y. Lam, A.-M. Lemay, and J. R. Webb, "'Bystander polarization' of CD4+ T cells: activation with high-dose IL-2 renders naive T cells responsive to IL-12 and/or IL-18 in the absence of TCR ligation," European Journal of Immunology **33**, 1788–1798 (2003).

[187]R. B. Munk, K. Sugiyama, P. Ghosh, C. Y. Sasaki, L. Rezanka, K. Banerjee, H. Takahashi, R. Sen, and D. L. Longo, "Antigen-Independent IFN-γ Production by Human Naïve CD4+ T Cells Activated by IL-12 Plus IL-18," PLoS ONE **6**, edited by D. Klinman, e18553 (2011).

[188]A. V. Villarino, E. Gallo, and A. K. Abbas, "STAT1-Activating Cytokines Limit Th17 Responses through Both T-bet–Dependent and –Independent Mechanisms," The Journal of Immunology **185**, 6461–6471 (2010).

[189]K. Hirahara, K. Ghoreschi, X.-p. Yang, H. Takahashi, A. Laurence, G. Vahedi, G. Sciumè, A. O. Hall, C. D. Dupont, L. M. Francisco, Q. Chen, M. Tanaka, Y. Kanno, H.-w. Sun, A. H. Sharpe, C. A. Hunter, and J. J. O'Shea, "Interleukin-27 Priming of T Cells Controls IL-17 Production In trans via Induction of the Ligand PD-L1," Immunity **36**, 1017–1030 (2012).

[190]C. Sun, R. Mezzadra, and T. N. Schumacher, "Regulation and Function of the PD-L1 Checkpoint," Immunity **48**, 434–452 (2018).

[191]A. Visekruna, M. Huber, A. Hellhund, E. Bothur, K. Reinhard, N. Bollig, N. Schmidt, T. Joeris, M. Lohoff, and U. Steinhoff, "c-Rel is crucial for the induction of Foxp3 + regulatory CD4 + T cells but not T H 17 cells," European Journal of Immunology **40**, 671–676 (2010).

[192]A. Visekruna, A. Volkov, and U. Steinhoff, "A Key Role for NF- κ B Transcription Factor c-Rel in T-Lymphocyte-Differentiation and Effector Functions," Clinical and Developmental Immunology **2012**, 1–9 (2012).

[193]E. Ronin, M. Lubrano di Ricco, R. Vallion, J. Divoux, H.-K. Kwon, S. Grégoire, D. Collares, A. Rouers, V. Baud, C. Benoist, and B. L. Salomon, "The NF-κB RelA Transcription Factor Is Critical for Regulatory T Cell Activation and Stability," Frontiers in Immunology **10**, 1–15 (2019).

[194]M. Li-Weber, M. Giaisi, S. Baumann, K. Pálfi, and P. H. Krammer, "NF-κB synergizes with NF-AT and NF-IL6 in activation of the IL-4 gene in T cells," European Journal of Immunology **34**, 1111–1118 (2004).

[195]A. Balasubramani, Y. Shibata, G. E. Crawford, A. S. Baldwin, R. D. Hatton, and C. T. Weaver, "Modular utilization of distal cis-regulatory elements controls

Ifng gene expression in T cells activated by distinct stimuli," Immunity **33**, 35–47 (2010).

[196]Q. Ruan, V. Kameswaran, Y. Zhang, S. Zheng, J. Sun, J. Wang, J. DeVirgiliis, H.-C. Liou, A. A. Beg, and Y. H. Chen, "The Th17 immune response is controlled by the Rel–RORγ–RORγT transcriptional axis," Journal of Experimental Medicine **208**, 2321–2333 (2011).

[197]C. E. Egwuagu, C.-R. Yu, M. Zhang, R. M. Mahdi, S. J. Kim, and I. Gery, "Suppressors of Cytokine Signaling Proteins Are Differentially Expressed in Th1 and Th2 Cells: Implications for Th Cell Lineage Commitment and Maintenance," The Journal of Immunology **168**, 3181–3187 (2002).

[198]Y. I. Seki, H. Inoue, N. Nagata, K. Hayashi, S. Fukuyama, K. Matsumoto, O. Komine, S. Hamano, K. Himeno, K. Inagaki-Ohara, N. Cacalano, A. O'Garra, T. Oshida, H. Saito, J. A. Johnston, A. Yoshimura, and M. Kubo, "SOCS-3 regulates onset and maintenance of TH2-mediated allergic responses," Nature Medicine **9**, 1047–1054 (2003).

[199]I. Kinjyo, H. Inoue, S. Hamano, S. Fukuyama, T. Yoshimura, K. Koga, H. Takaki, K. Himeno, G. Takaesu, T. Kobayashi, and A. Yoshimura, "Loss of SOCS3 in T helper cells resulted in reduced immune responses and hyperproduction of interleukin 10 and transforming growth factor–β1," Journal of Experimental Medicine **203**, 1021–1031 (2006).

[200]U. M. Zissler, C. A. Jakwerth, F. M. Guerth, L. Pechtold, J. A. Aguilar-Pimentel, K. Dietz, K. Suttner, G. Piontek, B. Haller, Z. Hajdu, M. Schiemann, C. B. Schmidt-Weber, and A. M. Chaker, "Early IL-10 producing B-cells and coinciding Th/Tr17 shifts during three year grass-pollen AIT," EBioMedicine **36**, 475–488 (2018).

[201]D. Calzada, S. Baos, L. Cremades-Jimeno, and B. Cárdaba, "Immunological mechanisms in allergic diseases and allergen tolerance: The role of Treg cells," Journal of Immunology Research **2018**, 10.1155/2018/6012053 (2018).

[202]J. Wang, L. Qiu, Y. Chen, and M. Chen, "Sublingual immunotherapy increases Treg/Th17 ratio in allergic rhinitis," Open Medicine (Poland) **16**, 826–832 (2021).

[203]F. Perez, C. N. Ruera, E. Miculan, P. Carasi, K. Dubois-Camacho, L. Garbi, L. Guzman, M. A. Hermoso, and F. G. Chirdo, "IL-33 Alarmin and Its Active Proinflammatory Fragments Are Released in Small Intestine in Celiac Disease," Frontiers in Immunology **11**, 1–15 (2020).

[204]C. Cayrol, A. Duval, P. Schmitt, S. Roga, M. Camus, A. Stella, O. Burlet-Schiltz, A. Gonzalez-De-Peredo, and J. P. Girard, "Environmental allergens induce allergic inflammation through proteolytic maturation of IL-33," Nature Immunology **19**, 375–385 (2018).

[205]B. C. Chan, C. W. Lam, L. S. Tam, and C. K. Wong, "IL33: Roles in allergic inflammation and therapeutic perspectives," Frontiers in Immunology **10**, 1–11 (2019).

[206]C. L. Hsu, K. D. Chhiba, R. Krier-Burris, S. Hosakoppal, S. Berdnikovs, M. L. Miller, and P. J. Bryce, "Allergic inflammation is initiated by IL-33–dependent crosstalk between mast cells and basophils," PLoS ONE **15**, 1–21 (2020).

[207]A. Holgado, H. Braun, E. Van Nuffel, S. Detry, M. J. Schuijs, K. Deswarte, K. Vergote, M. Haegman, G. Baudelet, J. Haustraete, H. Hammad, B. N. Lambrecht, S. N. Savvides, I. S. Afonina, and R. Beyaert, "IL-33trap is a novel IL-33–neutralizing biologic that inhibits allergic airway inflammation," Journal of Allergy and Clinical Immunology **144**, 204–215 (2019).

[208]S. Chinthrajah, S. Cao, C. Liu, S.-C. Lyu, S. B. Sindher, A. Long, V. Sampath, D. Petroni, M. Londei, and K. C. Nadeau, "Phase 2a randomized, placebo-controlled study of anti–IL-33 in peanut allergy," JCI Insight **4**, 10.1172/jci.insight.131347 (2019).

[209]E. Pastille, M. H. Wasmer, A. Adamczyk, V. P. Vu, L. F. Mager, N. N. T. Phuong, V. Palmieri, C. Simillion, W. Hansen, S. Kasper, M. Schuler, B. Muggli, K. D. McCoy, J. Buer, I. Zlobec, A. M. Westendorf, and P. Krebs, "The IL-33/ST2 pathway shapes the regulatory T cell phenotype to promote intestinal cancer," Mucosal Immunology **12**, 990–1003 (2019).

[210]C. Schiering, T. Krausgruber, A. Chomka, A. Fröhlich, K. Adelmann, E. A. Wohlfert, J. Pott, T. Griseri, J. Bollrath, A. N. Hegazy, O. J. Harrison, B. M. Owens, M. Löhning, Y. Belkaid, P. G. Fallon, and F. Powrie, "The alarmin IL-33 promotes regulatory T-cell function in the intestine," Nature **513**, 564–568 (2014).

[211]A. Yu, L. Zhu, N. H. Altman, and T. R. Malek, "A Low Interleukin-2 Receptor Signaling Threshold Supports the Development and Homeostasis of T Regulatory Cells," Immunity **30**, 204–217 (2009).

[212]A. K. Abbas, E. Trotta, D. R. Simeonov, A. Marson, and J. A. Bluestone, "Revisiting IL-2: Biology and therapeutic prospects," Science Immunology **3**, 10.1126/sciimmunol.aat1482 (2018).

[213]T. Kretzschmar, L. Aoustin, O. Zingel, M. Marangi, B. Vonach, H. Towbin, and M. Geiser, "High-level expression in insect cells and purification of secreted monomeric single-chain Fv antibodies," Journal of Immunological Methods **195**, 93–101 (1996).

[214]B. Reavy, A. Ziegler, J. Diplexcito, S. M. Macintosh, L. Torrance, and M. Mayo, "Expression of functional recombinant antibody molecules in insect cell expression systems," Protein Expression and Purification **18**, 221–228 (2000).

[215]Y. Zhang, H. Q. Yang, F. Fang, L. L. Song, Y. Y. Jiao, H. Wang, X. L. Peng, Y. P. Zheng, J. Wang, J. S. He, and T. Hung, "Single chain variable fragment against Aβ expressed in baculovirus inhibits Abeta fibril elongation and promotes its disaggregation," PLoS ONE **10**, 1–16 (2015).

[216]F. Monteiro, N. Carinhas, M. J. Carrondo, V. Bernal, and P. M. Alves, "Toward system-level understanding of baculovirus-host cell interactions: From molecular fundamental studies to large-scale proteomics approaches," Frontiers in Microbiology **3**, 1–16 (2012).

[217]S. Sakamoto, F. Taura, R. Tsuchihashi, W. Putalun, J. Kinjo, H. Tanaka, and S. Morimoto, "Expression, Purification, and Characterization of Anti-Plumbagin Single-Chain Variable Fragment Antibody in Sf9 Insect Cell," Hybridoma **29**, 481–488 (2010).

[218]J. S. Huston, M. Mudgett-Hunter, M.-s. Tai, J. McCartney, F. Warren, E. Haber, and H. Oppermann, "Protein Engineering of Single-Chain Fv Analogs and Fusion Proteins," Methods Enzymol **178** (1991).